THE UPR IN CHRONIC KIDNEY DISEASE DEVELOPMENT

THE CONTRIBUTION OF THE UNFOLDED PROTEIN RESPONSE (UPR) TO CHRONIC KIDNEY DISEASE DEVELOPMENT IN A MOUSE MODEL

By

ZAHRAA MOHAMMED-ALI, Hon. B.Sc.

A Thesis

Submitted to the School of Graduate Studies

In Partial Fulfillment of the Requirements

For the Degree

Doctor of Philosophy

McMaster University

DOCTOR OF PHILOSOPHY (2016) McMaster University
Department of Medical Sciences Hamilton, Ontario, Canada

TITLE: The contribution of the unfolded protein response (UPR) to chronic kidney kidney disease development in a mouse model.

AUTHOR: Zahraa Mohammed-Ali, Hon. B.Sc. in Biology (McMaster University)

SUPERVISOR: Dr. Jeffrey G. Dickhout

NUMBER OF PAGES: xv,184

ABSTRACT

Presently, there is a significant need to develop therapeutics to combat chronic kidney disease (CKD) due to the rise in its prevalence along with the burden of disease it conveys to the patients that suffer from CKD. Further, it's association with comorbities including hypertension and cardiovascular disease contribute to CKD's adverse effects on human health. Experimental and clinical evidence points to a role for endoplasmic reticulum (ER) stress in pathogenesis of CKD, however, the mechanism by which ER stress components ameliorate CKD in animal studies have not been fully elucidated. The research presented in this thesis has explored the impact of modulating the ER stress responses on CKD development. A central focus in this thesis involved investigating the pathways regulated during ER stress inhibition and the identification of therapeutic targets that could be used to treat CKD.

Firstly, a model of CKD in the C57BL/6 mouse was established (Chapter 2). This model involved a uninephrectomy combined with Angiotensin (Ang) II and deoxycorticosterone acetate (DOCA) infusion and high salt diet. This model overcame the resistance of C57BL/6 mice against CKD development and allowed the use of genetic knockout mice that are commonly available on the C57BL/6 background. Moreover, the Ang II/DOCA salt model exhibited key features of human CKD within 21 days including proteinuria, glomerulosclerosis, renal interstitial fibrosis, inflammation and apoptosis.

A time point analysis of the Ang II/DOCA salt model showed that ER stress was upregulated in the kidneys within 7 days along with the occurrence of proteinuria, fibrosis and inflammation (Chapter 3). Treatment with 4-phenyl butyric acid (4-PBA), a small molecular weight chaperone, used to alleviate ER stress, resulted in attenuated hypertension, proteinuria, glomerulosclerosis, fibrosis and inflammation. Further investigation showed that 4-PBA halted CKD progression through its effect on 1) the glomeruli, where 4-PBA treated mice had lower glomerulosclerosis and 2) the tubules, where 4-PBA resulted in an increased level

of cubilin available on the membranes for the reabsorption of hyperfiltered albumin in CKD (Chapter 3). When the Ang II/DOCA salt model was applied to mice deficient in CHOP, a pro-apoptotic gene upregulated by ER stress, glomerulosclerosis, proteinuria, fibrosis and inflammation were significantly reduced compared to wildtype (WT) mice. CHOP deficient mice were shown to have higher levels of nephrin, an important component of the renal filtration barrier and thus greater glomerular structure integrity than WT mice and improved CKD.

Chapter 4 of this thesis describes the effects of heterozygosity in GRP78, the key regulator of the unfolded protein response (UPR) on Ang II/DOCA salt-induced CKD. $GRP78^{+/-}$ mice showed lower proteinuria, fibrosis and macrophage infiltration than WT mice.

Collectively, the data discussed in this thesis presents potential therapeutic targets within the UPR and demonstrates pharmacological ER stress inhibition as a strategy to ameliorate CKD.

ACKNOWLEDGEMENTS

I would like to acknowledge all the wonderful people I have met during my graduate years that were my source of strength and support in completing my PhD thesis.

First, I am extremely grateful to my supervisor Dr. Jeffrey G. Dickhout for giving me the opportunity to engage in meaningful and creative work contributing to a PhD thesis. Thank you for providing me with several opportunities to develop as a scientist through conferences, presentations and publications. I would also like to acknowledge the extensive contributions of my mentors and committee members, Dr. Suleiman Igdoura who I have had the pleasure to know since my undergraduate years and who has greatly pushed me to grow as a scientist ever since, Dr. Martin Stampfli who in addition to being on my committee member was also my comprehensive examination advisor, thank you for your intense efforts in creating a thinker out of me throughout and always being there to bounce ideas or have interesting conversations. A massive thank you goes to Dr. Richard C. Austin for being very thorough in appraising my data during presentations, for always welcoming collaborations on several of my projects and for organizing events to introduce students to new science and help us network. I would also like to acknowledge the Austin lab for their friendship and tremendous support and guidance to me in my research projects, Drs. Ali Al-hashimi, Edward Lynn, Gabriel Guylay, Elizabeth Crane, Sarka Lhotak and Sudesh Sood.

Special thanks to Dr. Kjetil Ask who has collaborated with us in many of my thesis experiments and has always been a source of guidance and support. I greatly enjoyed our chats on various pathways common to lung and renal fibrosis and for introducing me to opportunities that furthered my career growth. Many thanks go to Ehab Ayaub, Dr. Asks's PhD student for his friendship and for being an amazing person to work with. I would also like to thank Dr. Joan Krepinsky for her interest, collaboration and invaluable feedback on my second first author paper.

Throughout my five years I have made some lasting friendships. A big thank you goes to our laboratory superstar Dr. Chao Lu who has given me invaluable technical guidance in all my experiments. I am very lucky to have known fellow graduate students Victoria Yum and Celeste Collins who have made my graduate experience infinitely more enjoyable and who I have greatly missed in the lab after their graduation. Current lab members Victor Tat, Safa Naeil and Rachel Carlisle thank you for your friendship and always being there to exchange ideas and work together on experiments. Past and present undergraduate students Gaile Cruz and Mandeep Marway, thank you for approaching lab work with so much enthusiasm, I am sure you two have a very bright future ahead of you. To my friends in other research areas a big thank you goes to Anaam Ali, Dr. Manali Mukherjee, Dr. Shaima Salman who have remarkably influenced my personal growth and inspired me to explore my full potential as a career woman.

Last but not the least, I would like to thank my family. Mama, Baba, I made it!!! My parents Khadija and Naji who strived hard so I can realize my dreams and who never stopped believing in me. I would not be the person I am today without your love, patience and devotion to my goals and personal growth. My siblings Hiba, Noor and Ahmed for constantly cheering me on and always being there. My husband, Al-harith, for his endless love and support specially in the past year, for relentlessly listening to the mix of my science, career goals and the dilemmas that go with them.

TABLE OF CONTENTS

LIST OF ABBREVIATIONS

4-PBA	4-phenyl butyric acid
ACE	angiotensin converting enzyme
Acta 2	smooth muscle alpha (α)-2 actin
ACTB	actin, beta
AKI	acute kidney injury
Ang II	angiotensin II
ANP	atrial natriuretic peptide
AP-1	activator protein-1
ARB	angiotensin II receptor blocker
Ask1	apoptosis signal-regulating kinase 1
ATF4	activating transcription factor 4
ATF6	activating transcription factor 6
Bad	bcl2-associated death promoter
Bak	bcl2-antagonist/killer 1
Bax	bcl2-associated X protein
BBC3/PUMA	bcl2 binding component 3/p53 upregulated modulator of apoptosis
Bcl2	b-cell CLL/Lymphoma2
Bif-1	bax-Interacting Factor 1
BNP	brain natriuretic peptide
Ccl20	C-C Motif Chemokine Ligand 20
CCR5	C-C Motif Chemokine Receptor 5
CHOP	CCAAT/enhancer-binding protein homologous protein
CKD	chronic kidney disease
Col	collagen

CsA	Cyclosporin A
Dahl S	Dahl salt sensitive (rat)
DOCA	deoxycorticosterone acetate
ECM	extracellular matrix
eIF2α	eukaryotic initiation factor 2α
EMT	epithelial to mesenchymal transition
ER	endoplasmic reticulum
FKBP13	FK506-Binding Protein 2 (13kD)
FKBP65	FK506 Binding Protein 10 (65 KDa)
FN1	Fibronectin
Foxp3	Forkhead Box P3
FSGS	focal segmental glomerular sclerosis
GADD34	growth arrest and DNA damage inducible protein 34
GAPDH	glyceraldehyde 3-phosphate dehydrogenase
GFR	glomerular filtration rate
ESRD	end stage renal disease
GRP78	glucose regulated protein 78 kDa
GRP94	glucose regulated protein 94 kDa
GUSB	glucuronidase beta
H & E	hematoxylin and eosin
Hmox-1	heme oxygenase 1
Hsp47	heat shock protein 47
IKK	IKK IκB Kinase
IL	interleukin
ILK	integrin-linked kinase
IP-10	Interferon gamma-induced protein 10

IPO8	Importin8
IRE1α	inositol requiring enzyme 1α
IκB	inhibitor of NF-κB
JNK	JUN N-terminal kinase
Lgals3	lectin, galactoside binding soluble 3
LOXL2	lysyl oxidase like 2
MEFs	mouse embryonic fibroblasts
Mmp	matrix metallopeptidase
NF-κB	Nuclear factor kappa B
PAS	Periodic acid-Schiff
Pcsk9	Proprotein Convertase Subtilisin/Kexin Type 9
PDI	protein disulfide isomerase
PERK	double-stranded RNA-activated protein kinase (PKR)-like ER kinase
PHLDA1	pleckstrin homology-like domain family member A1
RAAS	renin angiotensin aldosterone system
RHR	Rel homoly region
Ror2	receptor tyrosine kinase like orphan receptor 2
RPLP2	ribosomal protein lateral stalk subunit p2
SHR	spontaneously hypertensive rat
SREBP-1	sterol regulatory element binding protein-1
TBP	TATA-binding protein
TG	Thapsigargin
TGF-β	transforming growth factor beta
Timp-1	tissue inhibitor of metalloproteinases 1
TLR	toll-like receptor
TM	Tunicamycin

TRAF2	TNFα receptor-associated factor 2
TRP53	transformation related protein 53
TUNEL	Terminal deoxynucleotidyl transferase dUTP nick end labeling
UPR	unfolded protein response
UUO	unilateral ureteral obstruction
WKY	Wistar-Kyoto (rat)
Wnt	Wingless-type MMTV integration site family
XBP1	X-box binding protein 1
YWHAZ	Tyrosine 3-Monooxygenase/Tryptophan 5-Monooxygenase Activation Protein Zeta

PREFACE

This thesis is structured in the “sandwich” format as per the instructions explained in the “Guide for the Preparation of Master’s and Doctoral Theses” provided by the School of Graduate Studies at McMaster University. Chapter 1 consists of a general introduction composed of sections adapted from a review article and a book chapter that I wrote during my doctoral studies. The body of this thesis is comprised of 3 chapters (Chapter 2-4), each of which represent an independent study. Chapter 2 has already been published in Biomed Research International, Chapter 3 has been submitted to Nature Scientific Reports (under review, minor revisions) at the time of the thesis submission and Chapter 4 has been prepared to be submitted to American Journal of Physiology- Renal Physiology. Since the research conducted in each study was a collaborative effort, the manuscripts produced are muti-authored. In this section I will elaborate on different author contributions to the review, book chapter and manuscripts I have generated during my doctoral studies.

Chapter 1: This chapter is an introduction to my PhD thesis and will consist of material adapted from a review article and a book chapter which I wrote during my graduate studies.

Publication 1 (Review Article): Crosstalk between the unfolded protein response and NF-κB-mediated inflammation in the progression of chronic kidney disease. *Journal of Immunology Research.*

2015. doi: 10.1155/2015/428508. **Authors:** Zahraa Mohammed-Ali, Gaile L.

Cruz and Jeffrey G. Dickhout. My contribution to this work involved conducting the literature review, summarizing relevant research on the role of inflammation in the development of kidney disease in humans as well as in animal models. My thesis supervisor, Dr. Jeffrey G. Dickhout provided intellectual feedback and acted as the corresponding author. Gaile L. Cruz (undergraduate student) contributed to this review by assisting in in-vitro experiments on the tools used to study ER stress.

Publication 2 (Book Chapter): Animal Models of Kidney Disease (submitted). Authors: Zahraa Mohammed-Ali, Rachel E. Carlisle, Samera Nademi and Jeffrey G. Dickhout. In "Animal Models for the Study of Human Disease 2nd Edition" to be published in June 2017 (Elsevier publishing group, Academic Press). For this book chapter, I wrote the section entitled "Animal models of chronic kidney disease". My role involved conducting a literature review and writing this section in its entirety. My thesis supervisor, Dr. Jeffrey G. Dickhout provided intellectual feedback and acted as the corresponding author.

Chapter 2: **Development of a Model of Chronic Kidney Disease in the C57BL/6 Mouse with Properties of Progressive Human CKD.** *BioMed Research International.* 2015. http://dx.doi.org/10.1155/2015/172302. **Authors:** Zahraa Mohammed-Ali, Gaile L. Cruz, Rachel E. Carlisle, Kaitlyn E. Werner, Kjetil Ask and Jeffrey G. Dickhout.

Establishing a mouse model of chronic kidney disease set the foundation for my doctoral thesis work and so the experiments in this study were conducted

between 2011-2013. As a primary author, I designed and performed all the experiments, analyzed all the data and wrote the manuscript. Gaile L. Cruz (undergraduate student), Rachel E. Carlisle (graduate student) and Katie Werner (undergraduate student) provided me with experimental assistance. Dr. Kjetil Ask (McMaster University collaborator) provided me with feedback on pulmonary edema in the CKD model.

Chapter 3: **ER stress inhibition attenuates chronic kidney disease progression by preserving glomerular filtration barrier integrity and endocytic receptor-mediated albumin scavenging.** *Nature Scientific Reports,* 2016 (under review, minor revisions). **Authors:** Zahraa Mohammed-Ali, Chao Lu, Mandeep K. Marway, Rachel E. Carlisle, Kjetil Ask, Dusan Lukic, Joan K. Krepinsky, Jeffrey G. Dickhout.

This study constitutes the main portion of my doctoral thesis and includes a time point analysis of chronic kidney disease progression in an Angiotensin II/DOCA salt mouse model, a drug intervention and gene knockdown experiments to explore CKD progression. I designed and performed all of the experiments and analysis in this study between 2013-2016. I was assisted by Dr. Chao Lu (technologist) in all the mouse experiments. Mandeep K. Marway joined our laboratory in January (2016) as an undergraduate research assistant and has helped me investigate the effect of our model and 4-PBA treatment on the levels of endocytic receptors, megalin and cubilin and the impact of CHOP deficiency on nephrin protein levels. Rachel E Carlisle, a fellow graduate student, provided

me with renal tissue from 3 mice treated with AngII/DOCA and 4-PBA to add to my Ang II/DOCA+4-PBA group and helped review the manuscript before submission. Our collaborator, Dr. Joan Krepinsky (McMaster University) has provided us with human tissue (via pathologist Dr. Dusan Lukic) to validate and translate our work to human CKD. Dr. Kjetil Ask (McMaster University collaborator) has kindly provided us with CHOP deficient mice. Drs. Krepinsky and Ask also reviewed and critically appraised the manuscript.

Chapter 4: **GRP78 heterozygosity imparts protection against Angiotensin II/DOCA salt-induced CKD in the C57BL/6 mouse. Authors:** Zahraa Mohammed-Ali, Chao Lu, Mandeep Marway, Edward G. Lynn, Richard C. Austin, Jeffrey G. Dickhout.

The research in this study is focused on the effect of GRP78 heterozygosity on chronic kidney disease development in a mouse model. I designed and performed all the experiments with technical assistance provided by Dr. Chao Lu between 2012-2016. Mandeep Marway (undergraduate student), assisted in evaluating GRP78 expression in different groups. GRP78 heterozygous mice were kindly provided by Dr. Richard C. Austin's group where Dr. Edward G. Lynn managed the breeding colony.

Finally, Chapter 5 involves a discussion of my doctoral thesis, summarizing conclusions and expressing the overall significance of our studies in the context of the field of nephrology as well as future directions.

Chapter 1

INTRODUCTION

Chronic Kidney disease: Definition, Prevalence and Treatments

Chronic kidney disease (CKD) is defined as abnormalities of kidney structure or function, present for > 3months with implications for health according to the Kidney Disease: Improving Global Outcomes (KDIGO) organization (Stevens, Levin, & Kidney Disease: Improving Global Outcomes Chronic Kidney Disease Guideline Development Work Group, 2013). The criteria for CKD diagnosis includes a glomerular filtration rate (GFR) threshold of less than 60 ml/min per 1.73 m^2 and an albumin-creatinine ratio of 30 mg/g or greater. CKD is classified in stages based on cause and severity of abnormal kidney measures, however, identifying the cause has been emphasized in the guidelines due to its importance in predicting outcome and determining cause-specific treatments. Severity is expressed by the level of albuminuria and decrease in GFR (Stevens et al., 2013).

The global prevalence of CKD is high (8-16%) and presents a major health burden due to its associated risk of progression to end-stage renal disease (ESRD), cardiovascular disease and premature death (Jha et al., 2013). Worldwide, an estimated 1.9 million ESRD patients were on renal replacement therapy in 2010 and the prevalence of CKD has experienced an increase of 134.6% from 1990 (Anand, Bitton, & Gaziano, 2013; Mortality & Causes of Death, 2015). In addition to the increase in CKD prevalence, the rise of its concordant comorbidities including hypertension and diabetes represents a considerable financial burden to the economy and deteriorates quality of life for a significant segment of society (Jha et al., 2013).

Presently, there is no cure for CKD and therapies available are focused on preventing disease progression and preserving organ function. According to the KDIGO guidelines, management of CKD involves blood pressure lowering and reduction in proteinuria through Renin-Angiotensin-Aldosterone System (RAAS) blockade. Additionally, lifestyle interventions include glycemic control in diabetic nephropathy (target hemoglobin A1C level of 7%), achieving a healthy BMI of 20-25 kg/m2, smoking cessation and exercise (Stevens et al., 2013).

ER Stress in Kidney Disease[1]

Endoplasmic reticulum (ER) stress is cellular pathology that occurs due to an imbalance between protein folding capacity and protein folding demand (J. G. Dickhout & Krepinsky, 2009; Remuzzi & Bertani, 1998). The accumulation of misfolded proteins in the ER results from disturbances in ER homeostasis making conditions unfavourable for protein folding or mutations in proteins that impair their proper folding (J. G. Dickhout & Krepinsky, 2009). These disturbances in ER homeostasis include hypoxia, glucose depletion and oxidative stress (Inagi, 2009). ER stress plays an important role in the pathogenesis of chronic diseases associated with the accumulation of misfolded proteins. These include neurodegenerative diseases such as Alzheimer's and Parkinson's diseases, atherosclerosis, diabetes mellitus and chronic kidney disease (Xu, Bailly-Maitre, &

[1] This section has been adapted from Mohammed-Ali, Z et al. (2015) **Crosstalk between the unfolded protein response and NF-κB-mediated inflammation in the progression of chronic kidney disease.** *Journal of Immunology Research.* 2015. doi: 10.1155/2015/428508.

Reed, 2005; Yoshida, 2007; Zhang & Kaufman, 2006). ER stress results in the activation of the unfolded protein response (UPR), an evolutionarily conserved cellular response regulated primarily by glucose regulated protein 78-KD (GRP78). The UPR involves the activation of processes such as apoptosis and inflammation that determine the fate of cell survival and tissue scarring (J. G. Dickhout & Krepinsky, 2009; Garg et al., 2012; Xu et al., 2005). Therefore, ER stress is an important factor in the development of renal diseases and the study of the UPR pathways is likely to reveal molecular targets that influence disease progression.

The UPR includes the dissociation of GRP78 from three known ER transmembrane proteins: PKR (double-stranded RNA-dependent protein kinase)-like ER protein kinase (PERK), inositol-requiring enzyme 1 (IRE1) and activating transcription factor 6 (ATF6) (Cybulsky, 2010; J. G. Dickhout & Krepinsky, 2009; Inagi, 2010). UPR activation causes the release of ATF6 leading to its cleavage in the Golgi by site 1 and site 2 proteases (Ye et al., 2000; Zhang et al., 2006). The cytosolic, DNA-binding fragment of ATF6 travels to the nucleus where it activates the transcription of ER chaperones, enzymes that aid in protein folding and secretion as well as components of ER-associated degradation (Inagi, 2010). PERK is a Ser/Thr protein kinase and is activated through homodimerization and transphosphorylation during the UPR. PERK activation leads to the phosphorylation and inhibition of eIF2α, a component of the translation initiation complex (Kaufman, 2004; S. Wang & Kaufman, 2012). This pathway reduces the recognition of initiation AUG codon thereby attenuating translation to decrease

protein load on the ER. Certain mRNAs with short open reading frames in the 5'-untranslated region are preferentially translated in this pathway including activating transcription factor (ATF4) (Kaufman, 2004; S. Wang & Kaufman, 2012). ATF4 is a transcription factor that induces the expression of ER stress target genes, notably CCAAT/enhancer-binding protein homologous protein (CHOP) resulting in apoptosis (J. G. Dickhout & Krepinsky, 2009; Inagi, 2010). CHOP is a transcription factor that upregulates expression of pro-apoptotic factors and decreases anti-apoptotic genes such as Bcl2 (J. G. Dickhout & Krepinsky, 2009; Inagi, 2010). IRE1α activation results in X-box-binding protein-1 (XBP1) mRNA splicing. This step causes a change in the reading frame allowing the translation of a transcription factor that induces expression of genes with an ER stress response element including ER chaperons such as GRP78 (Chen & Brandizzi, 2013; Hetz, Martinon, Rodriguez, & Glimcher, 2011; Inagi, 2010; Jager, Bertrand, Gorman, Vandenabeele, & Samali, 2012).

Kidney biopsies from patients at different stages of glomerulonephritis showed upregulation of GRP78 and CHOP highlighting the significance of ER stress responses in renal disease progression (Markan et al., 2009). As well, the upregulation of ER stress markers has also been shown in nephrotic syndrome patients (Wu, He, Jing, Li, & Zhang, 2010). ER stress pathways may be targeted pharmacologically to attempt to modify the outcome of renal disease (Inagi, 2010). The use of 4-phenylbutyric acid (4-PBA), a low molecular weight chemical chaperone which prevented ER stress, in a rat model of streptozotocin-induced

diabetic nephropathy significantly reduced urinary protein excretion (Luo et al., 2010). Treatment with 4-PBA in this model also reduced basement membrane thickening, mesangial cell proliferation and mesangial matrix accumulation in rats with diabetic nephropathy (Luo et al., 2010). In a model of acute kidney injury, 4-PBA treatment prevented damage to the outer medullary stripe of the kidney and reduced ER stress upregulation and CHOP-induced apoptosis (Carlisle et al., 2014). Further, the deletion of the GRP78 ER retention sequence, KDEL, has been show to exacerbate renal injury by increased urinary protein excretion and tubular damage in an in-vivo model of albumin overload (K. Kimura, Jin, Ogawa, & Aoe, 2008). Therefore, the manipulation of the UPR has a significant impact on CKD progression.

ER stress Pathways[2]

ER stress-induced inflammation

All three arms of the UPR, IRE1-α, PERK and ATF6, result in transcriptional activation of pro-inflammatory genes by primarily activating NF-κB (Hasnain, Lourie, Das, Chen, & McGuckin, 2012; Hotamisligil, 2010; Zhang & Kaufman, 2008). In mammals, the NF-κB family consists of five members: p65/RelA, cRel, RelB, p100/p52, and p105/p50 (Sanz et al., 2010). These proteins can

[2] This section has been adapted from Mohammed-Ali, Z et al. (2015) **Crosstalk between the unfolded protein response and NF-κB-mediated inflammation in the progression of chronic kidney disease.** *Journal of Immunology Research.* 2015. doi: 10.1155/2015/428508.

homodimerize and form heterodimers with each other and share a highly conserved domain, Rel homology region (RHR) (Baldwin, 1996; Oeckinghaus, Hayden, & Ghosh, 2011; Sanz et al., 2010). NF-κB dimers are bound to inhibitory IκB proteins in the cytoplasm and are inactive since IκB interferes with the function of nuclear localization sequence present on the RHR domain (Beg et al., 1992). Phosphorylation and subsequent degradation of IκB is required for NF-κB translocation to the nucleus (Oeckinghaus et al., 2011).

Figure 1 shows an overview of the pathways involved in ER stress-mediated activation of inflammatory gene transcription. During prolonged ER stress, the dissociation of GRP78 results in autophosphorylation of IRE1α causing a conformational change in its cytosolic domain. The cytosolic domain of activated IRE1α then binds to adaptor protein TNFα receptor-associated factor 2 (TRAF2) (Urano et al., 2000). The IRE1α-TRAF2 complex recruits IκB Kinase (IKK), phosphorylating IκB resulting in its degradation and NF-κB activation (Hu, Han, Couvillon, Kaufman, & Exton, 2006; Kaneko, Niinuma, & Nomura, 2003). IRE1α-TRAF2 complex can also recruit Jun-amino-terminal kinase (JNK) leading to phosphorylation of transcription factor AP-1, linking ER stress to other pro-inflammatory pathways (Davis, 2000). UPR activation of PERK results in translation attenuation via phosphorylation of eIF2α, a component of the translation initiation complex. This process causes decreased translation of IκB, freeing more NF-κB to translocate to the nucleus (J. Deng et al., 2004; Jiang et al., 2003). ATF6 leaves the ER upon activation and undergoes cleavage by site 1 and site 2

proteases in the Golgi complex. These activated ATF6 fragments form homodimers and induce transcription of acute-phase response genes (Ye et al., 2000; Zhang & Kaufman, 2008; Zhang et al., 2006). Although the ATF6 pathway can also result in NF-κB activation via phosphorylation of AKT (Yamazaki et al., 2009), the PERK and IRE1α arms of the UPR have been demonstrated as crucial for ER-stress induced NF-κB activation. In a study by Kaneko et al. (Kaneko et al., 2003), human embryonic kidney 293T cells treated with thapsigargin showed phosphorylation and degradation of IκB and upregulation of NF-κB. This effect was suppressed with transfection of dominant negative mutant of IRE1α or a dominant-negative mutant of TRAF2 (Kaneko et al., 2003). ER stress-induced activation of NF-κB using thapsigargin and tunicamycin was impaired with IRE1α knockdown and IRE1α$^{-/-}$ in mouse embryonic fibroblasts (MEFs) (Hu et al., 2006). Reconstitution of IRE1α$^{-/-}$ MEFs with IRE1α resulted in the recovery of ER stress-induced NF-κB activation (Hu et al., 2006). Similarly, studies have shown eIF2α phosphorylation results in NF-κB activation through translation attenuation as it occurs independently of IκB phosphorylation or degradation (J. Deng et al., 2004; Jiang et al., 2003). Moreover, PERK$^{-/-}$ and eIF2α mutant MEFs inhibited NF-κB activation in response to treatment with ER stress agents indicating PERK-induced eIF2α phosphorylation is essential in NF-κB activation (Jiang et al., 2003). The analysis performed in Chapter 3 and 4 of this thesis involves the study of the effect of UPR modulation on NF-κB-mediated inflammatory pathways, innate immune response genes and macrophage and T cell infiltration.

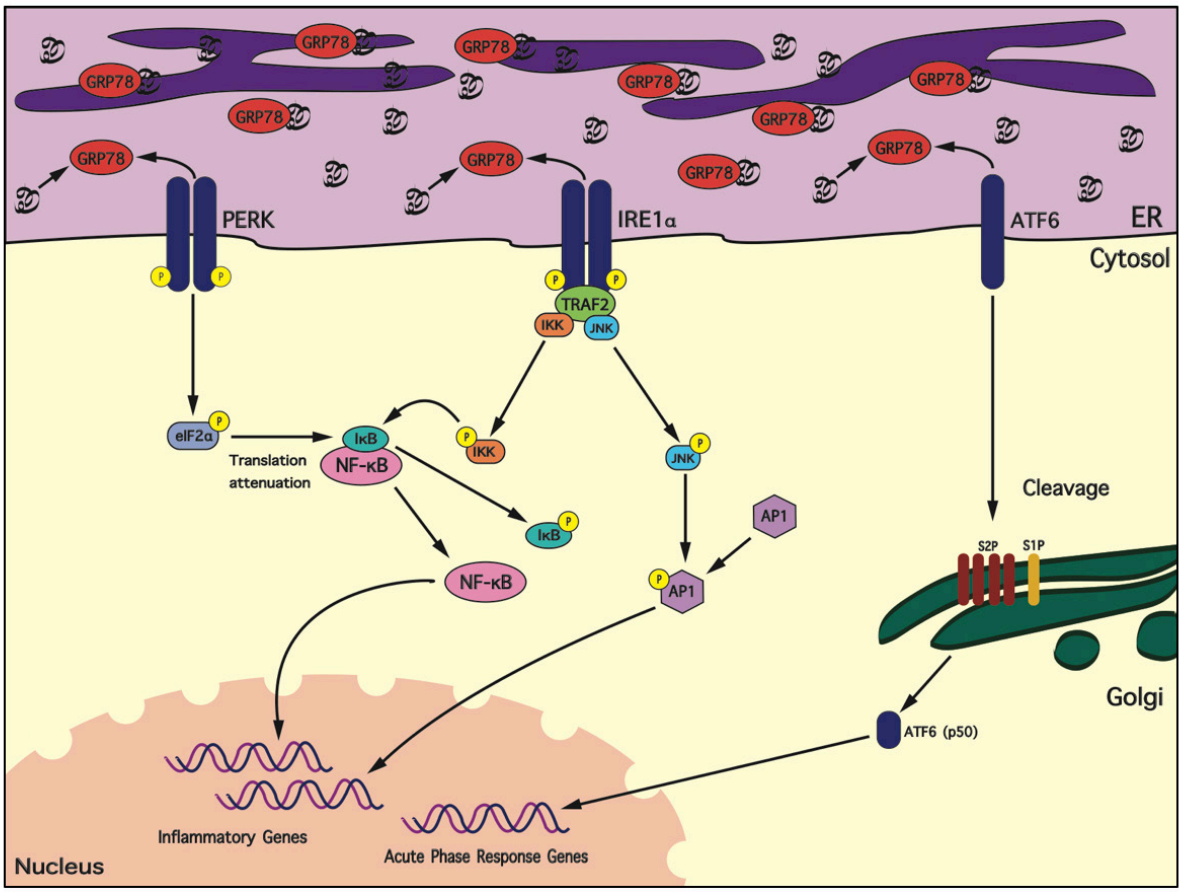

Figure 1: Overview of UPR-induced inflammatory gene transcription

Figure 1. Overview of UPR-induced inflammatory gene transcription. The dissociation of GRP78 from the transmembrane transducers, PERK, IRE1α or ATF6 leads to their activation. PERK activation brought about by autophosphorylation results in the phosphorylation of eIF2α and general translation attenuation reducing the binding of NF-κB to its inhibitory subunit IκB due to IκB's shorter half-life. This steps allows NF-κB to enter the nucleus and activate transcription of inflammatory genes. Autophosphorylation of IRE1α causes the cytosolic domain to associate with TRAF2. The IRE1α-TRAF2 complex recruits IKK which phosphorylates IκB resulting in NF-κB activation. As well, this complex recruits protein kinase JNK leading to phosphorylation of transcription factor AP-1. Upon activation, ATF6 leaves the ER and undergoes cleavage by site 1 and site 2 proteases in the Golgi complex. The 50-kilodalton cleavage product (p50) acts as a transcription factor in the nucleus and results in the transcriptional initiation of acute phase inflammatory response genes

ER stress-induced apoptosis

Apoptosis is triggered through multiple pro-apoptotic pathways of the UPR during prolonged ER stress (Inagi, 2010). The loss of renal tubular epithelial cells through apoptosis occurs in both acute and chronic kidney diseases. An increase in apoptosis has been demonstrated using TUNEL staining on kidney sections from diabetic nephropathy patients (Kumar, Robertson, & Burns, 2004) and from rats in the streptozotocin-induced diabetic nephropathy model (G. Liu et al., 2008). As well, apoptotic nuclei have been observed in polycystic human kidneys and kidney sections from mouse models of the disease (Woo, 1995). The absence of apoptosis in the normal human and mouse kidneys implies that apoptosis may contribute to the progressive loss of renal tissue in polycystic kidney disease (Woo, 1995). Cyclosporine A (CsA), an immunosuppressive drug used to improve graft survival rates following organ transplantation has been shown to induce acute and chronic nephropathy (Yoon & Yang, 2009). CsA nephropathy has been showed to cause an increase in apoptosis combined with the upregulation of ER stress in both human disease (Lhotak et al., 2012; Yoon & Yang, 2009) and animal models (Han et al., 2008; Lhotak et al., 2012). Therefore, apoptosis is a common feature of most renal pathologies and is strongly associated with ER stress. Apoptotic cell loss from nephron segments leads to tubular atrophy and their loss eventually leads to a decline in GFR. Therefore, characterizing the molecular pathways activated in apoptotic responses and their time frames during disease progression would allow

the development of therapeutic strategies (Sanz, Santamaria, Ruiz-Ortega, Egido, & Ortiz, 2008).

During prolonged ER stress, the activation of IRE1α and CHOP can result in apoptosis and under normal physiological conditions is useful in eliminating stressed cells. Damaged but non-apoptotic cells can induce inflammation, however, apoptosis is generally accompanied by phagocytic clearance that induces an anti-inflammatory response (Tabas & Ron, 2011). The activation of JNK downstream of the IRE1α-TRAF2 complex that forms upon IRE1α phosphorylation allows JNK to phosphorylate pro-survival protein Bcl-2 inhibiting its activity. Bcl-2 mediates survival cell survival by sequestering BH3-only proteins such as Bad, Bim and BBC3/PUMA, which are necessary for Bax/Bak-mediated apoptosis. CHOP also blocks Bcl2 expression (Szegezdi, Logue, Gorman, & Samali, 2006). These changes allow the activation of Bax and Bak, which olidomerize to form pores in the mitochondrial outer membrane causing the release of cytochrome c. Cytosolic cytochrome c results in caspase activation and subsequent cell death (Westphal, Dewson, Czabotar, & Kluck, 2011). Chapter 3 and 4 of this thesis involves an analysis of the effect of manipulating the UPR on ER stress-induced apoptotic genes in a CKD mouse model.

ER stress and fibrosis

Renal fibrosis is characterized by extracellular matrix (ECM) deposition and is an inevitable outcome of progressive CKD. The mechanisms underlying renal fibrosis

involve multiple players, however, cellular differentiation into myofibroblasts has been implicated as a key component in this process (Baum & Duffy, 2011). Myofibroblasts can be defined by the presence of ruffled membranes, α-smooth muscle actin staining and a highly active ER and are considered to be the dominant collagen-producing cells in many pathologies, including wound healing, organ fibrosis, and cancer (Baum & Duffy, 2011; LeBleu et al., 2013). Sources of myfibroblasts in the kidney include resident fibroblast expansion and renal epithelial cells that acquire a myofibroblast phenotype through a process referred to as epithelial to mesenchymal transition (EMT) (Y. Liu, 2010). This change is characterized by the loss of epithelial proteins such as E-cadherin, zonula occludens-1 and cytokeratin and the acquisition of new mesenchymal markers including vimentin, α-smooth muscle actin, fibronectin and collagen (Y. Liu, 2010). The alteration in protein markers is also accompanied by a change in cell morphology where reorganization of the cortical actin cytoskeleton occurs thus enabling dynamic cell elongation and increased contractility and motility (Nelson, Khauv, Bissell, & Radisky, 2008). EMT is thought to be an adaptive response of renal epithelial cells to chronic injury and is induced by three interconnected signaling pathways: TGF-β/Smad, integrin/integrin-linked kinase (ILK) and wnt/β-catenin. In addition to EMT induction, these pathways stimulate the transcription of ECM components and inhibitors of matrix metalloproteinases, which degrade the ECM (M. K. Kim et al., 2013).

The direct involvement of UPR components in the development of renal interstitial fibrosis has yet to be established, however, studies have shown a relationship between ER stress activation and EMT in the kidney. For instance, ER stress induction by the sarcoplasmic/endoplasmic reticulum Ca^{2+}ATPase inhibitor, TG, and the calcineurin inhibitor CsA results in loss of renal epithelial cell junctions thus allowing myofibroblast differentiation (Carlisle et al., 2012; Pallet et al., 2008b). In fact, recent work in our laboratory has shown that UPR inducers drive myofibroblast differentiation from renal proximal tubular epithelial cells through a process of endothelial to mesenchymal transformation (EMT) to myofibroblasts (Carlisle et al., 2012). Additionally, the use of ER stress inhibitor 4-PBA caused a significant decrease in fibrosis as shown by marked reduction in collagen type I, fibronectin and α-SMA in rats undergoing the unilateral ureteral obstruction (UUO) model (Chiang et al., 2011). Thus, the UPR may be a central mediating mechanism of renal fibrosis through its influence on myofibroblast differentiation. Chapter 3 and 4 of this thesis involves an analysis of the effect of manipulating the UPR on key fibrotic genes in the TGF-β and Wnt pathways and ECM deposition in a CKD mouse model.

Studying ER stress in-vivo and in-vitro[3]

Since ER stress pathways and inflammatory responses have been demonstrated in human CKD as well as animal models of the disease, the use of pharmacological tools in vitro and in vivo may help elucidate molecular targets essential to disease progression. **Table 1** summarizes drugs that could be used to manipulate the UPR.

[3] This section has been adapted from Mohammed-Ali, Z et al. (2015) **Crosstalk between the unfolded protein response and NF-κB-mediated inflammation in the progression of chronic kidney disease.** *Journal of Immunology Research.* 2015. doi: 10.1155/2015/428508.

Table 1. Pharmacological manipulation of the UPR.

UPR Gene	Pharmacological Manipulation	Description
PERK	Salubrinal	Phosphatase Inhibitor, prevents dephosphorylation of eIF2α
	GSK2606414	Potent and selective PERK inhibitor
IRE1α	STF083010	Specifically inhibits IRE1α endonuclease activity during ER stress without affecting its kinase activity
	Irestatin	Specific inhibitor of IRE1α
ATF6	4-(2-aminoethyl) benzenesulfonyl fluoride (AEBSF)	Serine protease inhibitor, inhibits site 1 and site 2 proteases preventing ATF6 cleavage and inhibits transcription of ATF6 target genes
Small chemical protein folding chaperones	4-phenylbutyrate (4-PBA)	4-PBA and TUDCA aid in protein folding reducing their accumulation in the ER
	Tauroursodeoxycholic acid (TUDCA)	
UPR activating agents	Tunicamycin	Inhibitor of N-linked protein glycosylation, hinders a process required for proper protein folding
	Thapsigargin	Inhibitor of sarcoplasmic/endoplasmic reticulum calcium ATPase (SERCA) pump, causing ER stress
	Indoxyl Sulfate	Uremic toxin that causes ER stress via oxidative stress

Table 1. Pharmacological manipulation of the UPR. To study the various pathways of the UPR, pharmacological manipulations to the specific pathways can be utilized. To examine the PERK pathway, salubrinal is an inhibitor of the dephosphorylation of eIF2α. To investigate the IRE1 pathway, STF-083010 and Irestatin are inhibitors of IRE1 endonuclease activity. The ATF6 pathway can be inhibited with 4-(2-aminoetheryl) benzenesulfonyl fluoride (AEBSF) to prevent cleavage of ATF6. The role of protein folding chaperones can be determined by utilizing artificial chaperones including 4-phenylbutyrate (4-PBA) and tauroursodeoxycholic acid (TUDCA), which aid in the folding of proteins. Further, to investigate sustained activation of the unfolded protein response, classic ER stress inducers, tunicamycin and thapsigargin, can be used as well as disease-related inducers including indoxyl sulfate.

Salubrinal (Sal) is a small molecule identified through high-throughput screening for its ability to enable cells to withstand ER stress. This drug acts as a phosphatase inhibitor specific in preventing the activation of eIF2α, a key component of the PERK pathway (Boyce et al., 2005). *In vivo*, Sal has been shown to protect against cyclosporine A-induced nephrotoxicity (Pallet et al., 2008a), which has been associated with ER stress (Bouvier et al., 2009). GSK2606414 is a potent and selective PERK inhibitor shown to inhibit PERK activation in response to ER stress in A549, a human lung adenocarcinoma cell line and inhibits the growth of human tumor xenografts in mice (Axten et al., 2012). Since it penetrates the blood-brain barrier, GSK2606414 administration has been shown to impart neuroprotective effects and prevent clinical disease in prion-infected mice (Moreno et al., 2013). Therefore, Sal and GSK2606414 provide pharmacological interventions that could be used to study the effect of the PERK pathway on ER stress-induced inflammation.

STF 083010 is a novel molecule, first identified though high-throughput screening. This reagent was able to inhibit IRE1α endonuclease activity during ER stress both in vitro and in vivo. Pre-treatment of RPMI 8226 human multiple myeloma cells with STF 083010 blocked XBP1 splicing activated by both tunicamycin- and thapsigargin-induced ER stress. Additionally, treatment of XBP1-luciferase reporter mice with STF 083010, reduced XBP1 splicing in an in vivo model of ER stress induced by bortezomib (Papandreou et al., 2011).

Irestatin, is another molecule that is able inhibit IRE1α endonuclease activity and has been reported to disrupt the growth of malignant myeloma cells (Feldman & Koong, 2007). Therefore, STF 083010 as well as Irestatin could be used as pharmacological tools to study the effect of inhibiting the IRE-1α pathway on ER stress-induced inflammation.

4-(2-aminoethyl) benzenesulfonyl fluoride (AEBSF) has been shown to prevent ER stress-induced cleavage of ATF6α and ATF6β, resulting in inhibition of transcriptional induction of ATF6-target genes (Okada et al., 2003). This compound has been used been used as a serine protease inhibitor in both *in vitro* (Colgan, Tang, Werstuck, & Austin, 2007; Lhotak et al., 2012) and *in vivo* studies (Buitrago-Rey, Olarte, & Gomez-Marin, 2002; Zen et al., 2011). Therefore, AEBSF could be used as a pharmacological tool to study the effect of inhibiting the ATF6 pathway on ER stress-induced inflammation.

4-PBA is a chemical chaperone that has been shown to stabilize protein conformation and improve protein folding in the ER by inhibiting ER stress. This drug has been used clinically for the treatment of urea cycle disorders in children, sickle cell disease, thalassemia, and cystic fibrosis (Perlmutter, 2002). In particular, in vitro studies have shown that 4-PBA administration results in a reduction in GRP78 levels in response to ER stress (Basseri, Lhotak, Sharma, & Austin, 2009; X. L. Liu et al., 2004). In a mouse model of brain ischemia, pre-treatment or post-treatment of 4-PBA at therapeutic doses was able attenuate disease progression possibly as a result of a decrease in protein load retained by the ER (Qi, Hosoi,

Okuma, Kaneko, & Nomura, 2004). Due to its efficacy in ER stress inhibition and the ease of its use where it can be administered to mice in the drinking water, 4-PBA was used as a pharmacological intervention to inhibit ER stress in a mouse model of CKD in Chapter 3 of this thesis.

Tauroursodeoxycholate (TUDCA), a derivative of an endogenous bile acid, is another chaperone that has been shown to resolve ER stress in liver and adipose tissue thereby normalizing hyperglycemia and restoring systemic insulin sensitivity in obese and diabetic mice (Ozcan et al., 2006). TUDCA has also been shown to inhibit the expression of ER stress markers in intestinal epithelial cells (Berger & Haller, 2011) and attenuate intestinal inflammation in a rodent model of inflammatory bowel disease (Uchida, Yamada, Hayakawa, & Hoshino, 1997). Therefore, both 4-PBA and TUDCA could be used to manipulate ER stress responses.

ER stress-inducing agents Tunicamycin (TM), Thapsigargin (TG) and Indoxyl sulfate (IS) could be used to evaluate the effects of ER stress induction in vitro and in vivo. TM is a nucleoside antibiotic, which inhibits N-linked protein glycosylation and is used to model acute kidney injury (AKI) in vivo (Carlisle et al., 2014). TG is a plant-derived sesquiterpene lactone and induces ER stress by inhibiting the sarcoplamsic/endoplasmic reticulum calcium ATPase (SERCA) pump and altering Ca homeostasis (Lytton, Westlin, & Hanley, 1991). Both TG and TM result in upregulation of ER stress markers GRP78, GRP94, CHOP and phosphorylated eIF2α in human proximal tubule cells (Carlisle et al., 2014; Carlisle et al., 2012; J.

G. Dickhout et al., 2012). IS is a uremic toxin that has been reported to accumulate in the serum of CKD patients and contribute to disease progression (Barreto et al., 2009; Namba, Okuda, Morimoto, Kojima, & Morita, 2010). IS interacts with organic anion transporter types 1 and 3 and is therefore able to incorporate into the basolateral membrane of renal proximal tubular cells (Enomoto et al., 2002). IS was shown to induce ER stress via oxidative stress in human proximal tubular cells and inhibits cell proliferation through the upregulation of CHOP and ATF4 in these cells (Kawakami et al., 2010).

Animal models of CKD[4]

In the studies included in my PhD thesis, a model of hypertensive CKD was used. Models of hypertensive CKD are important since hypertension has been reported to occur in 85% to 95% of patients with CKD (stages 3-5) (Rao, Qiu, Wang, & Bakris, 2008). Hypertension has been considered a cause for CKD development and is an independent risk factor for CKD progression to ESRD as well as cardiovascular events in CKD patients such as myocardial infarction and stroke (Barri, 2008). In the RENAAL study, every 10-mmHg rise in systolic blood pressure increased the risk for ESRD or death by 11% (Bakris et al., 2003). Further, anti-hypertensive drugs including β-blockers and dihydropiridine calcium channel

[4] This section has been adapted from Mohammed-Ali, Z et al. (submitted) **Animal Models of Kidney Disease.** In "Animal Models for the Study of Human Disease 2nd Edition" (Elsevier publishing group, Academic Press).

blockers are widely used in the treatment of CKD patients. Along with increased blood pressure, hypertensive CKD in humans is characterized by proteinuria and glomerulosclerosis resulting in declining GFR (Rao et al., 2008). Renal histological analysis shows interstitial fibrosis and associated renal inflammation where T cells and macrophages have been implicated in the pathogenesis and progression of CKD (Silverstein, 2009). The upregulation of the UPR has been reported in human CKD (Wu et al., 2010) and plays an important role in determining the fate of renal glomerular and tubular cells during CKD. Animal models of hypertensive CKD discussed here display most of the features of human hypertensive CKD and its associated comorbidities, particularly cardiovascular disease.

Spontaneously Hypertensive Rat (SHR)

The spontaneously hypertensive rat (SHR) is the most commonly used model of hypertension and cardiovascular disease. The SHR strain was produced by Okamoto et al. in the 1960s by selective inbreeding of Wistar-Kyoto (WKY) rats with high blood pressure (Okamoto & Aoki, 1963). Therefore, normotensive WKY rats are employed as normotensive controls in studies on SHRs. Hypertension starts to develop in these rats at 5-6 weeks of age, and systolic blood pressure plateaus at approximately 200 mmHg at about 15 weeks (Tanase, Yamori, Hansen, & Lovenberg, 1982). In the early stages of hypertension, SHRs experience increased cardiac output and normal total peripheral resistance, however, as the hypertensive state stabilizes, cardiac output returns to normal and

hypertrophied blood vessels produce a higher total peripheral resistance (J.G. Dickhout & Lee, 1997; Smith & Hutchins, 1979). Proteinuria, glomerulosclerosis and interstitial fibrosis along with characteristics of cardiovascular disease such as cardiac hypertrophy begin to develop between the initiation of hypertension and its plateau phase at 40 weeks (Conrad et al., 1995; Feld, Van Liew, Brentjens, & Boylan, 1981; Ofstad & Iversen, 2005). Between 14 and 15 weeks renal pathology begins to appear and may be exacerbated by high salt diet, however, this animal model is mostly salt resistant. Between 30 and 32 weeks, male SHRs exhibit a 20% to 30% decrease in GFR (Reckelhoff, Zhang, & Granger, 1997) as renal pathology progresses. Age-related GFR decrease is absent in female SHRs. Female SHRs also have approximately six-fold lower proteinuria (Reckelhoff et al., 1997). Some level of protein cast formation can be seen at 40 weeks and these increase with time (Ofstad & Iversen, 2005). Inflammation in the form of lymphocyte and macrophage infiltrates as well as the increased expression of cytokines and chemokines has been observed at the pre-hypertensive stage (3 weeks) in renal tissue of SHRs (Biswas & de Faria, 2007; Rodriguez-Iturbe, Quiroz, Ferrebuz, Parra, & Vaziri, 2004). Treatment with anti-inflammatory agents has shown a reduction in blood pressure and inflammation in adult SHRs (Rodriguez-Iturbe et al., 2005; Rodriguez-Iturbe et al., 2002). Oxidative stress precedes inflammation (occurs at 2 weeks) in SHR kidneys (Biswas & de Faria, 2007). Inflammatory and ER stress marker expression have been reported in the blood vessels and cardiac tissue of SHRs (Carlisle et al., 2016; Guo & Yang, 2015; Miguel-Carrasco,

Zambrano, Blanca, Mate, & Vazquez, 2010; Sanz-Rosa et al., 2005; Spitler, Matsumoto, & Webb, 2013; Sun, Zhang, Li, & Wang, 2015). Compared to other models of hypertensive CKD such as the Dahl S model, SHR rats develop a much lower level of renal injury. The absence of progressive renal damage has been attributed to enhanced preglomerular vasoconstriction which prevents systemic hypertension from being transmitted to the glomeruli (Arendshorst & Beierwaltes, 1979; G. Kimura & Brenner, 1997). Combining uninephrectomy with the SHR model intensifies and accelerates glomerulosclerosis, urinary protein excretion and fibrosis (Dworkin & Feiner, 1986; Kinuno, Tomoda, Koike, Takata, & Inoue, 2005). These changes have been reported due to inhibition of vascular narrowing of the preglomerular resistance vessels by uninephrectomy. Adaptations to uninephrectomy such as glomerular enlargement are also impaired in the SHR (Kinuno et al., 2005). Alternatively, placing SHRs on high salt accelerates the development of hypertension and cardiac remodeling (H. C. Yu et al., 1998). As well, high salt-fed SHR rats have higher urinary protein excretion and glomerular damage than those fed low salt diets (Blizard, Peterson, Iskandar, Shihabi, & Adams, 1991). The SHR has become the model of choice to test anti-hypertensive drugs. Another valuable contribution of the SHR, is in mapping and identification of genes responsible for the development of hypertension. Although, just like humans, the SHR model experiences a progression starting with a pre-hypertensive, developing and sustained hypertensive phase, the lifespans of SHRs (1.5-2.5 years) and their normotensive controls (2.5-3 years) are short. This makes

the SHR convenient for the study of hypertension and ageing. As well, SHR is also suited for the study of gender in hypertension. As well, SHR has been crossed with other strains to create new models such as the SHR heart failure (SHHF) rat to model congestive heart failure secondary to essential hypertension and the stroke-prone SHR (SHRSP), a unique model of severe hypertension and hemorrhagic stroke.

Dahl Salt Sensitive rat

The Dahl Salt Sensitive rat is another model of hypertensive CKD and develops hypertension when fed a high salt diet (Dahl, Heine, & Tassinari, 1962, 1963). In experiments with this strain, low-salt diet generally involves 0.1-0.4% NaCl whereas high salt refers to 4%- 8% NaCl diet (De Miguel, Das, Lund, & Mattson, 2010; Hayakawa, Coffee, & Raij, 1997; Rapp & Dene, 1985; H. C. Yu et al., 1998). Upon high salt-feeding these rats rapidly develop significant hypertension, mesangial expansion and glomerulosclerosis (Raij, Azar, & Keane, 1984). Salt-resistant Brown-Norway (BN) and consomic rats (SS. BN13) in which chromosome 13 from the BN has been introgressed into the Dahl S genetic background are included as salt-resistant controls in experiments with the Dahl S (Cowley et al., 2001; Hoagland et al., 2004). The increase in mean arterial pressure is attributed to sodium retention and can be prevented through the use of diuretics (Greene, Yu, Roman, & Cowley, 1990; Tobian et al., 1979). Along with hypertension, Dahl S rats experience endothelial dysfunction and cardiac hypertrophy and fibrosis

(Hayakawa et al., 1997; M. Yu et al., 2003). Cardiac hypertrophy is comparable to that seen in the SHR but cardiac failure occurs much earlier in the Dahl S than in the SHR (Hasenfuss, 1998). Urinary excretion of protein, albumin and nephrin has been shown in Dahl S rats on high salt (Hye Khan et al., 2013). Protein cast formation has been reported in the medulla (Hye Khan et al., 2013; Rapp & Dene, 1985; M. Yu et al., 2003) and can also be observed in the cortex. Renal interstitial fibrosis and inflammation in the form of T cell and macrophage infiltrates has been documented in the cortex and medulla associated with renal damage in this model (De Miguel et al., 2010; Hye Khan et al., 2013; Mattson, James, Berdan, & Meister, 2006). High salt Dahl S rats also show an increased renal expression of ER stress genes (Hye Khan et al., 2013). As with most rat models, the Dahl salt sensitive model is cost effective and easily- manageable, time efficient and non-invasive. Salt sensitivity makes the Dahl S clinically relevant. Renal injury in this model is similar to that seen in patients with diabetic nephropathy (O'Bryan & Hostetter, 1997; Ritz & Orth, 1999) and in hypertensive African Americans (Campese, 1994; Cowley & Roman, 1996), a population five times more likely to progress to ESRD (Hsu, Lin, Vittinghoff, & Shlipak, 2003; Norris et al., 2006).

Renal Mass Reduction

The 5/6 nephrectomy model entails reducing the total mass of the kidney by 5/6th. The most common technique involves a two-step procedure. A full uninephrectomy is performed on one kidney. Two-third of the remnant kidney is then ablated either

by anterior (Al Banchaabouchi et al., 1998) or posterior (Ma & Fogo, 2003) renal artery branch ligation or by kidney pole resection (Kren & Hostetter, 1999; Leelahavanichkul et al., 2010). The ligation method is not feasible in the mouse due to limited artery branching however, the polar excision method can be used in both rats and mice (Yang, Zuo, & Fogo, 2010). Various mouse and rat strains are differentially responsive to renal mass reduction in terms of CKD progression (Fleck et al., 2006; Ortiz et al., 2015). Both mice and rats experience hypertension, glomerular and tubulointerstitial damage and proteinuria as a result of this model but CKD progression is accelerated in some strains. The CD-1 strain of mice has shown progressive increase in albuminuria, severe glomerulosclerosis, hypertension and renal interstitial and cardiac fibrosis by 4 weeks on the model (Leelahavanichkul et al., 2010). Swiss-webster mice, the 129/Sv strain and its inbred substrain (129S3) develop disease in 9-12 weeks (Leelahavanichkul et al., 2010; Ma & Fogo, 2003). The C57BL/6 strain, however, is the most resistant strain to this model showing increased albuminuria at 16 weeks without the development of hypertension, progressive CKD or cardiac fibrosis (Leelahavanichkul et al., 2010; Ortiz et al., 2015; Yang et al., 2010). Rats generally show more susceptibility to CKD induced by renal mass reduction. However, a report by Fleck *et al*. showed that Sprague-Dawley rats were less susceptible than Wistar rats (Fleck et al., 2006). Rats show the development of hypertension and proteinuria at 4 weeks and glomerulosclerosis, renal fibrosis and mesangial expansion by 8 weeks (Fleck et al., 2006; Ma et al., 2005; Zhao et al., 2012). Progressive CKD is also denoted by

tubular protein cast formation (Li et al., 2012; Zhao et al., 2012), as well as renal inflammation, and oxidative stress (Ghosh et al., 2009; H. J. Kim & Vaziri, 2010; Romero et al., 1999). ER stress inhibition has been shown to ameliorate renal injury, heart dysfunction, myocardial fibrosis and apoptosis (Ding, Wang, Zhang, & Gu, 2016). Immune suppression has also been shown to significantly reduce fibrosis and inflammation in this model (Romero et al., 1999). Renal mass reduction is a reliable model for the induction of CKD in rodents as it provides robust readouts in terms of glomerulosclerosis, proteinuria and hypertension. It is ideal to model decline in renal function in humans through loss of nephron number. The main limitation of the 5/6 nephrectomy is the need for two surgical interventions requiring technical expertise to perform the surgeries successfully. Additionally, the remnant kidney is small and, especially in the mouse, provides very little renal tissue for analysis. Another disadvantage is the variability in responses from different strains and the variability, which may be created in the model itself. Since the surgery is technically demanding, and there is a direct correlation between disease severity and the amount of renal mass removed or infracted, variation in surgical technique or renal anatomy between animals will cause wide variability in disease severity requiring large sample size to adequately power statistical tests.

DOCA-salt

This model entails the administration of deoxycorticosterone acetate (DOCA), an aldosterone precursor, combined with a unilateral uninephrectomy and high salt

diet. DOCA is administered through subcutaneous injection or implanted as a pellet while salt loading involves 1% NaCl in drinking water (Dobrzynski, Wang, Chao, & Chao, 2000; Hartner, Cordasic, Klanke, Veelken, & Hilgers, 2003; Jadhav, Torlakovic, & Ndisang, 2009; Xia, Bledsoe, Chao, & Chao, 2005). This model exhibits a suppressed renin-angiotensin system with decreased plasma renin concentrations. The increased aldosterone results in increased sodium and water reabsorption from epithelial cells in the distal nephron of the kidney thereby increasing blood pressures. Clinically, primary aldosteronism or a decrease in renin to aldosterone ratio is an important cause of hypertension (Drenjancevic-Peric et al., 2011; Iyer, Chan, & Brown, 2010; Tomaschitz, Pilz, Ritz, Obermayer-Pietsch, & Pieber, 2010). This model has been performed in both mice and rats and hypertension and renal damage is more severe in males than in females (Bubb, Khambata, & Ahluwalia, 2012; Karatas et al., 2008). The response to DOCA-salt is strain-dependent in mice where the 129/Sv strain has shown more susceptibility to progressive renal damage and hypertension than C57BL/6 mice (Hartner et al., 2003). This model produces hypertension, proteinuria, luminal protein cast formation and glomerulosclerosis (Hartner et al., 2003; Jadhav et al., 2009; Xia et al., 2005). Renal interstitial fibrosis and inflammation are indicated by the increase in TGF-β and collagen deposition as well as the upregulation of pro-inflammatory transcription factors NF-κB and AP-1 and immune cell infiltrates (Jadhav et al., 2009) (Elmarakby, Quigley, Imig, Pollock, & Pollock, 2008). DOCA-salt administration also results in oxidative stress through superoxide formation in the

vasculature and the kidney. The mineralcorticoid receptor that aldosterone binds to is not only present on renal epithelia but is also found on vascular smooth muscle cells, cardiac fibroblasts and the brain. Therefore, the DOCA-salt model also manifests chronic cardiovascular remodeling including cardiac hypertrophy and fibrosis in both the left and right ventricles resulting in inflammatory cell infiltration into the cardiac tissue and upregulation of hypertrophy markers ANP and BNP (Dobrzynski et al., 2000; Karatas et al., 2008). Morphological changes are accompanied by function changes that include an increase in action potential duration at 20%, 50% and 90% of repolarization (Loch, Hoey, & Brown, 2006). This model is known to cause smooth muscle and endothelial dysfunction and vascular hypertrophy in small and large arteries (Cordellini, 1999; L. Y. Deng & Schiffrin, 1992; Iyer et al., 2010). The DOCA-salt model is a model of human primary aldosteronism and volume-dependent hypertension. The technical requirements of this model are somewhat invasive and two surgeries would be required if a DOCA pellet is implanted subcutaneously instead of injections. However, this model has a lower risk of mortality due to procedures alone in comparison to the 5/6 nephrectomy model. This model generally lasts for no more than 8-12 weeks and is therefore not a good model to study the effects of ageing on aldosterone-induced hypertension. However, the DOCA-salt model is a popular choice in the study of the effect of high dietary salt intake on CKD progression.

Angiotensin II infusion

Chronic Angiotensin (Ang) II infusion, usually through the implantation of Ang II osmotic minipumps, has been used as a model of progressive CKD in mice and rats. Sustained elevations in circulating levels of Ang II result in renal dysfunction, proteinuria, focal tubulointerstitial and vascular damage (Ortiz et al., 2015). The pleiotropic actions of Ang II encompass Ang-II vasoconstriction and hypertension as well as stimulating aldosterone secretion, superoxide production, TGF-β-mediated fibrosis and inflammation via NF-κB activation (Agarwal, Campbell, & Warnock, 2004; Muller et al., 2000; Ozawa, Kobori, Suzaki, & Navar, 2007; Ruiz-Ortega et al., 2006). As well, ER stress genes have been reported to be upregulated in the kidney and cardiac tissue with Ang II infusion in mice (Kassan et al., 2012; T. N. Wang et al., 2015). In fact, ER stress inhibition has been shown to attenuate cardiac hypertrophy, cell death and fibrosis (Kassan et al., 2012). Ang II infusion has also been combined with models of reduced renal mass and with the DOCA-salt model. Ang II administration has been shown to overcome the resistance of C57BL/6 mice to CKD induction and results in hypertension, albuminuria and severe glomerulosclerosis by 4 weeks instead of 16 weeks (Leelahavanichkul et al., 2010). The Ang II/DOCA salt model which involves a uninephrectomy following by Angiotensin II infusion through an osmotic minipump, a DOCA pellet implantation and high salt was also designed to overcome the resistance of C57BL/6 mice to CKD development (Kirchhoff et al., 2008; Z Mohammed-Ali, 2015). Female mice experience less severe CKD due to this

model compared to male mice (Z Mohammed-Ali, 2015). Increase in systolic blood pressure and proteinuria is seen after the first week on the Ang II/DOCA salt model (Kirchhoff et al., 2008; Z Mohammed-Ali, 2015). Renal damage involved protein cast formation, glomerulosclerosis, apoptosis and renal interstitial fibrosis and inflammation. Inflammation resulted in both T cell and macrophage infiltration and upregulation of inflammatory mediators MCP-1 and IP-10 (Kirchhoff et al., 2008; Z Mohammed-Ali, 2015). Cardiac hypertrophy and fibrosis as well as pulmonary edema also manifest in this model (Kirchhoff et al., 2008; Z Mohammed-Ali, 2015). The intrarenal renin-angiotensin system is important in the pathophysiology of hypertension and hypertensive nephropathy. CKD management guidelines emphasize angiotensin-converting enzyme inhibitors or Angiotension II type 1 receptor blockers as antiproteinuric and renoprotective therapy regardless of their effect on hypertension (Griffin & Bidani, 2009). Therefore, models of Ang II-driven CKD are clinically relevant. Consequently, the Ang II/DOCA salt model is the one that will be used for all *in vivo* experiments in this thesis and is characterized in Chapter 2. The C57BL/6 mouse serves as a genetic background for several transgenic and gene knockout models. However, this strain is highly resistant to CKD development. Therefore, the development of a model with stable CKD development in this strain would widen the scope of experiments focused on CKD progression.

Central Aim and Thesis Objectives

Overall, the central hypothesis of this PhD thesis is as follows: UPR modulation impacts CKD development. To test this hypothesis, I pursued the following thesis objectives:

(1) To establish and characterize a model of CKD in the C57BL/6 mouse (Chapter 2).

(2) To study the progression of CKD and the pattern of UPR, inflammatory and fibrotic pathways activated during CKD development through a time point analysis of our CKD mouse model (Chapter 3)

(3) To investigate the impact of manipulating the UPR on CKD development by inhibiting ER stress pharmacologically using 4-PBA and by using genetic knockouts of the key UPR gene CHOP (Chapter 3).

(4) To propose mechanisms by which ER stress inhibition ameliorates proteinuria and alleviates CKD (Chapter 3).

(5) To describe the effects of heterozygosity in GRP78, the key regulator of the UPR, on CKD development (Chapter 4).

Chapter 2

Development of a model of chronic kidney disease (CKD) in the C57BL/6 mouse with properties of progressive human CKD.

Summary and Significance:

This article involved the characterization of a mouse model of CKD in the C57BL/6 mouse. The model described combines a uninephrectomy with Ang II and DOCA infusion and high dietary salt intake (Ang II/DOCA salt). Mice exposed to this model experienced a significant increase in systolic and diastolic blood pressure, proteinuria and albuminuria. Kidneys from mice exposed to Ang II/DOCA salt showed an increase in protein cast formation, glomerulosclerosis, TUNEL-positive cells, fibrosis and macrophage infiltration compared to SHAM-operated controls. The pathology observed in this model was influenced by gender as female mice developed less severe disease. This model is clinically-relevant since it exhibits key features of CKD seen in humans and is based on Ang II activity. Increased Ang II activity is an established factor contributing to CKD progression and its pharmacological inhibition is the primary therapeutic strategy used to treat CKD presently. C57BL/6 mice are the background strain for several gene knockouts but are resistant to CKD induction by methods such as renal mass reduction or protein overload. Therefore, developing a CKD model in this strain is useful in diversifying gene knockout experiments in the context of CKD.

Development of a model of chronic kidney disease (CKD) in the C57BL/6 mouse with properties of progressive human CKD.

Zahraa Mohammed-Ali[1], Gaile L. Cruz[1], Chao Lu[1], Rachel E. Carlisle[1], Kaitlyn E. Werner[1], Kjetil Ask[2] and Jeffrey G. Dickhout[1].

[1]Department of Medicine, Division of Nephrology, McMaster University and St. Joseph's Healthcare Hamilton, Hamilton, Ontario, Canada

[2]Department of Medicine, Division of Respirology, McMaster University and St. Joseph's Healthcare Hamilton, Hamilton, Ontario, Canada

SOURCES OF FUNDING:

This work was supported by research grants to Jeffrey G. Dickhout from the Canadian Institutes of Health Research (OSO-115895 and MOP-133484). Financial support from St. Joseph's Healthcare Hamilton is also acknowledged. Jeffrey G. Dickhout also acknowledges salary support from St. Joseph's Healthcare Hamilton and holds a McMaster University, Department of Medicine Internal Career Research Award. Support from the division of Nephrology in the Department of Medicine at McMaster University is also acknowledged. Dr. Dickhout also holds a Kidney foundation of Canada, Krescent New Investigator award.

Conflict of Interest Statement: The authors declare that there is no conflict of interest regarding publication of this manuscript.

Address Correspondence to:
Jeffrey G. Dickhout, PhD
Department of Medicine, Division of Nephrology
McMaster University and St. Joseph's Healthcare Hamilton
50 Charlton Avenue East
Hamilton, ON, Canada, L8N 4A6
Email: jdickhou@stjosham.on.ca

Abstract

Chronic kidney disease (CKD) is a major healthcare problem with increasing prevalence in the population. CKD leads to end stage renal disease and increases the risk of cardiovascular disease. As such, it is important to study the mechanisms underlying CKD progression. To this end, an animal model was developed to allow the testing of new treatment strategies or molecular targets for CKD prevention. Many underlying risk factors result in CKD but the disease itself has common features, including renal interstitial fibrosis, tubular epithelial cell loss through apoptosis, glomerular damage and renal inflammation. Further, CKD shows differences in prevalence between the genders with premenopausal women being relatively resistant to CKD. We sought to develop and characterize an animal model with these common features of human CKD in the C57BL/6 mouse. Mice of this genetic background have been used to produce many transgenic strains that are commercially available. Thus, a CKD model in this strain would allow the testing of the effects of numerous genes on the severity or progression of CKD with minimal cost. This paper describes such a mouse model of CKD utilizing angiotensin II and deoxycorticosterone acetate as inducers.

Introduction

Although various models of chronic kidney disease (CKD) have been established in the rat [1], the ability to transgenically manipulate the rat is not nearly as well established as in the mouse. Further, many genetic knockout mouse strains, including tissue specific and conditionally inducible knockouts, are available on the C57BL/6 background [2]. However, this mouse has proven to be resistant to the development of CKD. C57BL/6 mice have shown resistance to the induction of CKD by standard techniques such as streptozotocin-induced diabetes [3], bovine serum albumin-overload proteinuria [4] and reduced renal mass [5]. Thus, developing a mouse model of CKD on the C57BL/6 background, that shares salient pathological features of human CKD, allows the use of pre-existing knockout stains. Experiments on these knockout strains would determine the effect of these genes on the development of renal interstitial fibrosis, proteinuria and the chronic inflammatory response in CKD.

A model has been developed in the C57BL/6 that shows features of progressive human CKD, including proteinuria and inflammation [6]. In this model, mice are uninephrectomized, given Angiotensin (Ang) II infusion and deoxycorticosterone acetate (DOCA) with 1% salt in the drinking water. This model can be referred to as the Ang II/DOCA salt mouse. The use of Ang II and DOCA with a high salt diet in this model results in sodium retention and volume expansion and therefore hypertension [7]. As well, the reduction in renal mass promotes hyperfiltration, which contributes to proteinuria [8]. The dysregulation of

the Renin-Angiotensin-Aldosterone system that is stimulated in this model plays a central role in cardiorenal syndrome [9]. This fact is well-supported by the success of Angiotensin Converting Ezyme (ACE) inhibitors and Angiotensin Receptor blockers (ARBs) as first line therapies in the treatment of hypertension and kidney disease patients [9, 10]. As previously demonstrated by Kirchhoff et al. (2008), this mouse model of CKD induces proteinuria, renal injury and increased systolic blood pressure [6]. In this paper, we will further characterize this model by quantifying the apoptotic responses in renal tubular epithelium, as well as renal interstitial fibrosis and the inflammatory response. Further, we sought to determine whether gender alters the severity of the development of these features of CKD in this model.

Methods and Materials

Model of CKD in C57BL/6 mice

Ten-week-old mice (gender-balanced groups) underwent uninephrectomy (Unx) or a sham uninephrectomy under isofluorane/oxygen anaesthetisa 2-weeks before the start of the experiment and were allowed to recover (Figure 1). The Unx mice were then given 1% sodium chloride in the drinking water and received DOCA pellet implants and Ang II infusion using osmotic mini pumps. Model 1004 Alzet osmotic infusion pumps (Durect) containing Ang II in sterile water were subcutaneously implanted in the back of the necks of mice under isofluorane/oxygen anaesthetisa to deliver a dose of 1.5 ng Ang II (Sigma) per

minute per gram body weight. At this time, a 50 mg 21-day release DOCA pellet (Innovative research of America, M-121) was also implanted subcutaneously. Mice that underwent the sham Unx were also treated with a sham procedure for subcutaneous implantation. All mice were sacrificed on day 21 post-implantation. This animal utilization and the described procedures were approved by the McMaster University Research Ethics Board.

Blood pressure measurements in animal model of CKD

Blood pressure measurements were obtained with tail cuff plethysmography using a CODA (Kent Scientific) blood pressure analyzer before Ang II/DOCA implantation and also before sacrifice (Figure 1). Briefly, animals were placed in restraint and positioned on a heating pad with a tail cuff attached to the machine. The cuff then measured the systolic blood pressure, diastolic blood pressure and heart rate.

Urinalysis, metabolic cages, microalbumuria ELISA

Before the surgical procedure and after 3 weeks on treatment with AngII/DOCA salt, mice were placed in metabolic cages for 24h urine collection (Figure 1). Urine samples were sent to our in-house laboratory to evaluate total protein concentrations and an ELISA was used to measure mouse urine albumin concentration (BETHYL Laboratories) to determine hypertension-induced proteinuria.

Tissue preparation for histological assessment and immunohistochemical analysis of protein cast formation, renal interstitial fibrosis, apoptosis and glomerular sclerosis

Renal tissue was prepared for histological analysis. The tissue was fixed in 4% paraformaldehyde upon sacrificing the animal. The tissue was then embedded in paraffin blocks and sectioned (4 μm) using a microtome. To assess protein cast formation and glomerular injury score, these tissues were stained with Periodic Acid Schiff (PAS) stain and imaged using a light microscope (Olympus).

Collagen deposition indicating extracellular matrix accumulation and renal interstitial fibrosis was evaluated using Masson's Trichrome stain (Sigma-Aldrich).

To assess apoptosis, kidney sections were stained using the protocol and reagents provided by the TACS 2 TdT-Fluor *In Situ* Apoptosis Detection Kit (Trevigen, Cat # 4812-30-K). This method is based on specific binding of TdT to 3'-OH ends of DNA and the incorporation of biotinylated deoxyuridine at sites of DNA breaks. This signal is then amplified by avidin-peroxidase, allowing apoptotic cells where DNA fragmentation has occurred to be visualized with light microscopy [11].

The sections were analyzed using an Olympus BX41 microscope. Immunohistochemistry sections were imaged with a 20X and a 40X objective lens. For the quantification of protein cast formation, apoptosis and F4/80 staining, ten microscopic fields were sampled in each of the cortex and the

medulla. To score glomeruli, ten microscopic fields were sampled from the cortex allowing the scoring of approximately 50 glomeruli per animal. Images were analyzed for protein cast formation using the Metamorph program to select and quantify PAS-stained areas as a percentage of the total area of each image. The average of protein cast areas density was then calculated for each animal. TUNEL-stained sections were processed using the cell count tool in Image J software. Glomerular sclerosis was assessed based on the scale and method used in a previous study [12].

Lungs from AngII/DOCA salt and sham mice were extracted without performing a broncheoalveolar lavage procedure, fixed in 4% paraformaldehyde for 24 hours. After standard paraffin embedding, 4μM thick specimens were sectioned and stained with H&E stain to visualize lung damage. Mouse hearts were weighed upon sacrifice and this parameter was normalized to body weight in grams to provide a measure of increase in cardiac mass. The hearts were then fixed in 4% paraformaldehyde for 24 hours, embedded in paraffin, sectioned and stained with PAS to evaluate areas of hypertrophy.

Statistical Analysis

Statistical Analysis was performed using GraphPad Prism software. T-tests were used to compare data between groups and significance is denoted by $P<0.05$. Bar graphs show group averages and standard error of the mean as error bars.

Results

Development of hypertensive proteinuria in Ang II/DOCA salt model

Blood pressure measurements were taken using tail cuff measurements before the subcutaneous implantation of the osmotic pump containing Ang II and the DOCA pellet as well as at the end of the model before sacrificing the mice. Ang II/DOCA salt mice experienced a significant increase in systolic (Figure 2A; $P<0.001$, $N=14$) and diastolic blood pressure (Figure 2B; $P<0.001$, $N=14$) 21-days after implantation. Ang II/DOCA salt mice also had significantly higher systolic ($P<0.001$, $N=14$) and diastolic ($P<0.001$, $N=14$) blood pressure compared to sham operated controls 21-days after implantation. This hypertensive response was accompanied by an increase in total protein (Figure 2C) and albumin (Figure 2D) excreted in the urine over 24h. Ang II/DOCA salt mice experienced significantly higher total protein ($P=0.009$, $N=14$) and total albumin ($p<0.001$, $N=14$) in 24h urine compared to measurements obtained before implantation. Total 24h urine protein ($p=0.006$, $N=14$) and albumin ($P<0.001$, $N=14$) were also significantly higher with Ang II/DOCA salt treatment compared to sham controls. In order to assess CKD progression in this model, the time course of the evolution of proteinuria was followed at days 0, 7, 14, 18 and 21after Ang II/DOCA salt treatment. Proteinuria was significantly elevated at days 18 and 21 (Figure 2 E).

Characteristics of renal tissue damage in response to Ang II/DOCA salt treatment

The proteinuria data was consistent with the immunohistological analysis of PAS-stained kidney sections showing percentage of protein cast formation as compared to sham controls (Figure 3A). Kidneys from Ang II/DOCA salt mice showed a significantly higher percentage of protein cast formation as compared to sham controls. PAS staining images show increased protein cast formation in renal tubules of the cortex (P=0.003, N=14) and Medulla (p=0.01, N=14) in Ang /II/DOCA salt mice compared to sham controls (Figure 3B). Higher magnification images of PAS staining showed increased glomerular sclerosis in the cortex of Ang II/DOCA salt mice compared to sham mice as indicated by the arrows (Figure 3C). Quantification of glomerular sclerosis by two independent assessors utilizing the method of Raij et al. [12] indicated that the Ang II/DOCA salt mice displayed significantly elevated glomerular sclerosis scores (P<0.001, N=10) compared to age-matched sham operated controls (Figure 3D).

In order to assess renal cell loss, we performed TUNEL staining. TUNEL staining images demonstrated increased apoptosis (Figure 3E; arrows) in kidney micrographs of Ang II/DOCA salt mice compared to sham animals (Figure 3F; P<0.001, N=10). Immunohistochemical staining for F4/80, a highly specific macrophage cell surface marker [13], demonstrated a significant increase in macrophage infiltration density (Figure 3G) in response to Ang II/DOCA salt treatment compared to sham controls (Figure 3H; P=0.02, N=5). To examine

renal interstitial fibrosis, we stained kidney sections with Masson's Trichrome stain. Indeed, in our Ang II/DOCA salt model, we saw increased collagen deposition as indicated by blue-stained fibres in the renal interstitium of areas showing kidney damage in the Ang II/DOCA salt mice compared to sham controls (Figure 3I).

Impact of CKD on cardiac and lung function and morphology

Microscope images of heart cross-section portrayed right and left ventricle hypertrophy in response to Ang II/DOCA salt treatment (Figure 4A). Cardiac muscle hypertrophy is an adaption to fluid retention and hypervolemia resulting from the model. This phenomenon is confirmed by the increase in heart weights (mg/g of body weight) ($P<0.001$, $N=14$) observed in mice treated with Ang II/DOCA salt compared to sham controls (Figure 4B). Lung sections derived from Ang II/DOCA salt mice showed features of pulmonary edema, inflammatory infiltrates and thickening of the alveoli. Signs of increased vessel thickness and capillaries congested with red blood cells are also observed (Figure 4C). Although further characterization is required, it is likely that that the observed pulmonary changes are driven by sodium retention and the severe hypervolemic changes observed in this model.

Impact of Gender on renal tissue damage induced by Ang II/DOCA salt model

Both male (P=0.02, N=7) and female (P=0.04, N=7) Ang II/DOCA salt mice developed proteinuria compared to their respective sham controls as a result of the CKD model. However, male Ang II/DOCA salt mice showed significantly higher total protein in 24h urine (P= 0.04, N=7) compared to female Ang II/DOCA salt mice (Figure 5A). Total 24h urine albumin measurements showed a similar trend where male Ang II/DOCA salt mice (P<0.001, N=6) experience a higher level of albumin in the urine compared to their sham controls and compared to female Ang II/DOCA salt mice (P=0.03, N=6). Although female Ang II/DOCA salt mice had a higher albumin level in 24h urine (P=0.11, N=6) than their sham controls, this increase was not significant (Figure 5B). Protein cast formation was significantly higher in the cortex (P=0.02, N=7) and medulla (p=0.04, N=7) of Ang II/DOCA salt male mice and in the cortex (p=0.004, N=7) and medulla (P=0.01, N=7) of Ang II/DOCA salt female mice compared to their respective sham controls. The percentage of PAS-stained area was higher in the cortex (P=0.048, N=7) and medulla (P=0.145, N=7) of male mice treated with Ang II/DOCA salt compared to female mice treated with Ang II/DOCA salt (Figure 5C). TUNEL staining was used to assess the influence of gender on kidney cell death and, ultimately, nephron loss. Although female Ang II/DOCA salt mice experienced an increase in apoptosis (P=0.03, N=5) compared to female sham controls, the apoptosis observed in male mice treated with Ang II/DOCA salt was significantly

higher (P=0.002, N=5) compared to Ang II/DOCA salt treated females (Figure 5D). In addition, Masson's Trichrome staining showed a higher level of collagen deposition and renal interstitial fibrosis (indicated by blue staining) in male Ang II/DOCA salt mice compared to female Ang II/DOCA salt mice (Figure 5E).

Discussion

CKD is characterized by reduction in glomerular filtration rate (GFR), albuminuria, and structural or functional abnormalities of the kidney [14]. CKD is increasing in prevalence globally and its comorbidities include cardiovascular disease, increased all-cause and cardiovascular mortality, kidney-disease progression to ESRD and acute kidney injury [15, 16]. The financial impact of CKD places a large burden on health care systems with high costs associated with renal replacement therapy, dialysis, and cardiovascular complications [15]. The C57BL/6 mouse has been the most preferred strain for the generation of transgenic and knockout animal models and will be utilized to develop a genome-wide panel of knockout animals to characterize gene function [2]. The Ang II/DOCA salt model described here shows a robust CKD response that closely mimics human CKD. Developing this model allows the use of genetically modified mice in order to identify gene targets that play a role in CKD development and progression.

Similar to the description of the model provided by Kirchhoff *et al*. [6], we found systolic blood pressure to be elevated; additionally, we determined that diastolic

blood pressure was also elevated. We present data for the total 24-h excretion of both protein and albumin, demonstrating that the Ang II/DOCA salt model induced significant proteinuria and albuminuria. This finding is similar to the increase in albuminuria/creatinine ratio described by Kirchhoff *et al.* [6]. Further, we show the evolution of proteinuria in the model at days 0, 7, 14, 18 and 21 where we observe a statistically significant increase in proteinuria at day 18 and day 21. We also demonstrate that protein cast formation and glomerular sclerosis were significantly increased in the model, similar to findings by Kirchhoff *et al.* [6]. We further investigated renal injury by examining apoptosis through TUNEL staining and found it to be significantly elevated. Additionally, the kidneys were found to have a significant infiltration of macrophages and showed renal interstitial fibrosis through trichrome staining. Similar to Kirchhoff *et al.* [6], we found end-organ damage in the heart characterized by cardiac hypertrophy. We extended these findings to examine the lung, where we noted an edematous effusion in airspaces. Further, we characterized the model for gender differences and found that the female gender imparted protection from proteinuria, albuminuria, protein cast formation, apoptosis and renal interstitial fibrosis.

Hypertensive proteinuria is a common feature of CKD. Therefore, animal models that display this feature have been used to investigate disease-specific mechanisms, molecular pathogenesis and potential therapies [1]. The increased glomerular permeability during hypertensive CKD allows protein hyperfiltration into the proximal tubules causing renal tissue damage. Filtered albumin and other

proteins that accumulate within intracellular compartments of proximal tubular cells perturb cell function by several mechanisms [17]. Hypertension is an important contributor to ESRD [18]. Proteinuria is associated with glomerular damage and podocyte depletion [19] and can be used in the classification of different stages of CKD clinically [20]. The Ang II/DOCA salt model displays hypertensive proteinuria that mirrors human CKD, as demonstrated by a significant increase in systolic and diastolic blood pressure, as well as proteinuria and albuminuria. Overt proteinuria evolved later in this model at days 18 and 21, indicating disease progression in response to glomerular injury. The glomerulosclerosis seen in our model involves inflammation and fibrosis around the area of the damaged glomeruli and could potentially result in tubular atrophy and degeneration [19]. Tubulointerstitial injury caused by proteinuria includes the formation of protein casts that may block the tubular lumen [19] and this phenomenon has been shown in our model.

As CKD progresses tubular cell atrophy results primarily due to apoptosis. An increase in apoptosis has been demonstrated using TUNEL staining on kidney sections from diabetic nephropathy patients [21] and from rats in the streptozotocin-induced diabetic nephropathy model [22]. In addition, apoptotic nuclei have been observed in polycystic human kidneys and kidney sections from mouse models of the disease [23]. The loss of renal tubular epithelial cells through apoptosis occurs in both acute and chronic kidney diseases [24]. Apoptotic cell loss from nephron segments leads to tubular atrophy and their loss

eventually leads to a decline in GFR. Since the Ang II/DOCA salt model displays a robust apoptotic response, it could be used in identifying therapeutic targets against apoptosis that are able to halt CKD progression [24].

Macrophage infiltration has been studied as a universal feature of tubulointerstitial damage regardless of disease origin [25, 26], and is a key feature of experimental and human kidney disease models [26, 27]. Macrophages have been shown to release cytotoxic moieties such as proteolytic enzymes, reactive oxygen and nitrogen species, as well as proinflammatory cytokines and chemokines [28]. By expressing cytokines such as TGF-β and connective tissue growth factor, macrophages are able to induce myofibroblast differentiation and extra cellular matrix deposition, key processes in renal interstitial fibrosis [29, 30]. Increased macrophage infiltration is associated with glomerulosclerosis and tubulointerstitial fibrosis [27, 31, 32]. Both macrophage infiltration and renal interstitial fibrosis have been demonstrated in the Ang II/DOCA salt model of CKD. Further studies would be focused on the time course of the development of these phenomena in order to establish pathways that lead to CKD progression.

CKD, through its effects on volume overload plays an important pathophysiological role in multiple organ failure. The effect of volume overload on the heart is to develop cardiac hypertrophy through myocardial stretch. This effect is reflected in our model. As hypertrophy progresses from compensation to

decompensated heart failure, volume overload affects the lungs and results in pulmonary edema [33]. This phenomenon is also reflected in our model.

The findings that Ang II/DOCA salt mice show a gender-based difference in severity of CKD are consistent with findings in the human population [34] and in agreement with previous clinical and experimental studies on the protective effect of female gender on the development of renal diseases [35-38]. Female mice, subjected to this model, show significantly lower levels of proteinuria. Ang II/DOCA salt female mice also experienced a trend for decreased protein cast formation and collagen deposition thereby indicating lower level of renal tissue damage compared to Ang II/DOCA salt male mice. A recent study identified gender difference as a modifier of susceptibility to ER stress-induced injury in tunicamycin-treated mice, a model of acute kidney injury, showing reduced renal pathology in female mice [39]. The reduced induction of apoptosis in female Ang II/DOCA salt mice in our CKD model is therefore in agreement with *in vivo* experiments of endoplasmic reticulum stress-induced acute kidney injury in the tunicamycin mouse models [39].

Clinical studies have demonstrated an association between male gender and a faster rate of CKD progression [36]. Interestingly, the impact of gender is restricted to premenopausal women and is, therefore, thought to be an estradiol-mediated protective effect [35]. This finding is supported by experimental studies. Aged male rats have been shown to develop decreased GFR, increased glomerular injury and increased proteinuria earlier than female rats [37]. In

addition, estradiol treatment caused a reduction in glomerulosclerosis, expression of adhesion and extracellular matrix molecules and prevented tubular damage in animal models of unilateral nephrectomy and chronic renal allograft rejection [38, 40]. These studies indicate a renoprotective role for estradiol and although our experiments show that female gender imparts a protective effect on CKD development, the potential role of estradiol is still to be determined.

In conclusion, the Ang II/DOCA salt model produces a significant degree of CKD that mimics progressive human CKD in the C57BL/6 mouse. This pathology includes proteinuria, intertubular protein casts, renal interstitial fibrosis, and tubular epithelial cell apoptosis. As this model recapitulates many of the aspects of pathology found in human CKD [41], it will be of great utility to determine the specific effect of various candidates genes on CKD severity and progression. Further, a gender effect was observed where female mice showed lower proteinuria and apoptosis in kidney tissue. Future work in this model may allow the precise molecular nature of the protective effect of the female gender to be determined.

Figure Captions

Figure 1. Ang II/DOCA salt model of chronic kidney disease in the C57BL/6 mouse.

Graph describing time course development of CKD.

Figure 2. Development of hypertensive proteinuria in Ang II/DOCA salt model of CKD in the C57BL/6 mouse. For all graphs, * indicates a significant difference between two groups where P<0.05. For **A- D**, □ signifies pre-treatment whereas ■ signifies 21-days post-treatment with Ang II/DOCA. **A, B.** Changes in systolic and diastolic blood pressure in response to Ang II/DOCA. **C, D.** Total 24h urinary protein and albumin excretion with Ang II/DOCA treatment. **E.** Time-course development of proteinuria, expressed as total 24h protein excretion at days 7, 14, 18 and 21 post-treatment with Ang II/DOCA.

Figure 3. Renal tissue damage in response to Ang II/DOCA salt CKD mouse model. For all graphs, * indicates a significant difference between two groups where P<0.05. Effect of Ang II/DOCA salt model on **A, B.** protein cast formation in the cortex and medulla, **C, D.** Glomerulosclerosis, **E, F.** Apoptosis, **G, H.** Macrophage (F4/80+ cells) infiltration, **I.** Interstitial Fibrosis (Masson's Trichome staining).

Figure 4. Effect of Ang II/DOCA salt model on cardiac and lung tissue. A. Images of heart cross-section cardiac hypertrophy in Ang II/DOCA salt model. **B.** Graph showing increase in heart weights (mg/g of body weight) in response to Ang II/DOCA where * indicates a significant difference between two groups where ($P<0.05$). **C.** Lung damage (20X, 40X) in response to Ang II/DOCA compared to SHAM controls.

Figure 5. Impact of gender on CKD induced by Ang II/DOCA salt model. For all graphs, * indicates a significant difference between two groups where $P<0.05$. Ang II/ DOCA salt is denoted by ■, whereas □ denotes SHAM operated controls. 'M' and 'F' indicate sections from male and female mouse kidneys respectively. Influence of gender on the development of **A.** Proteinuria **B.** Albuminuria **C.** Protein cast formation **D.** Apoptosis **E.** Interstitial Fibrosis.

FIGURE 1

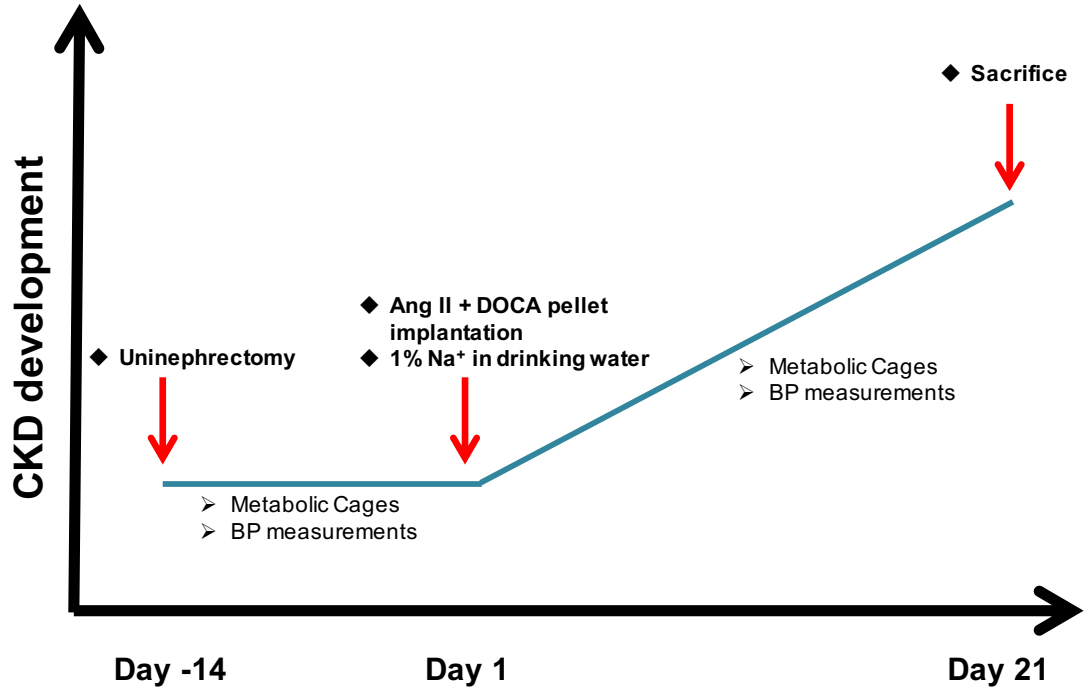
CKD development
◆ Uninephrectomy
◆ Ang II + DOCA pellet implantation
◆ 1% Na+ in drinking water
◆ Sacrifice
➢ Metabolic Cages
➢ BP measurements
➢ Metabolic Cages
➢ BP measurements
Day -14
Day 1
Day 21

FIGURE 2

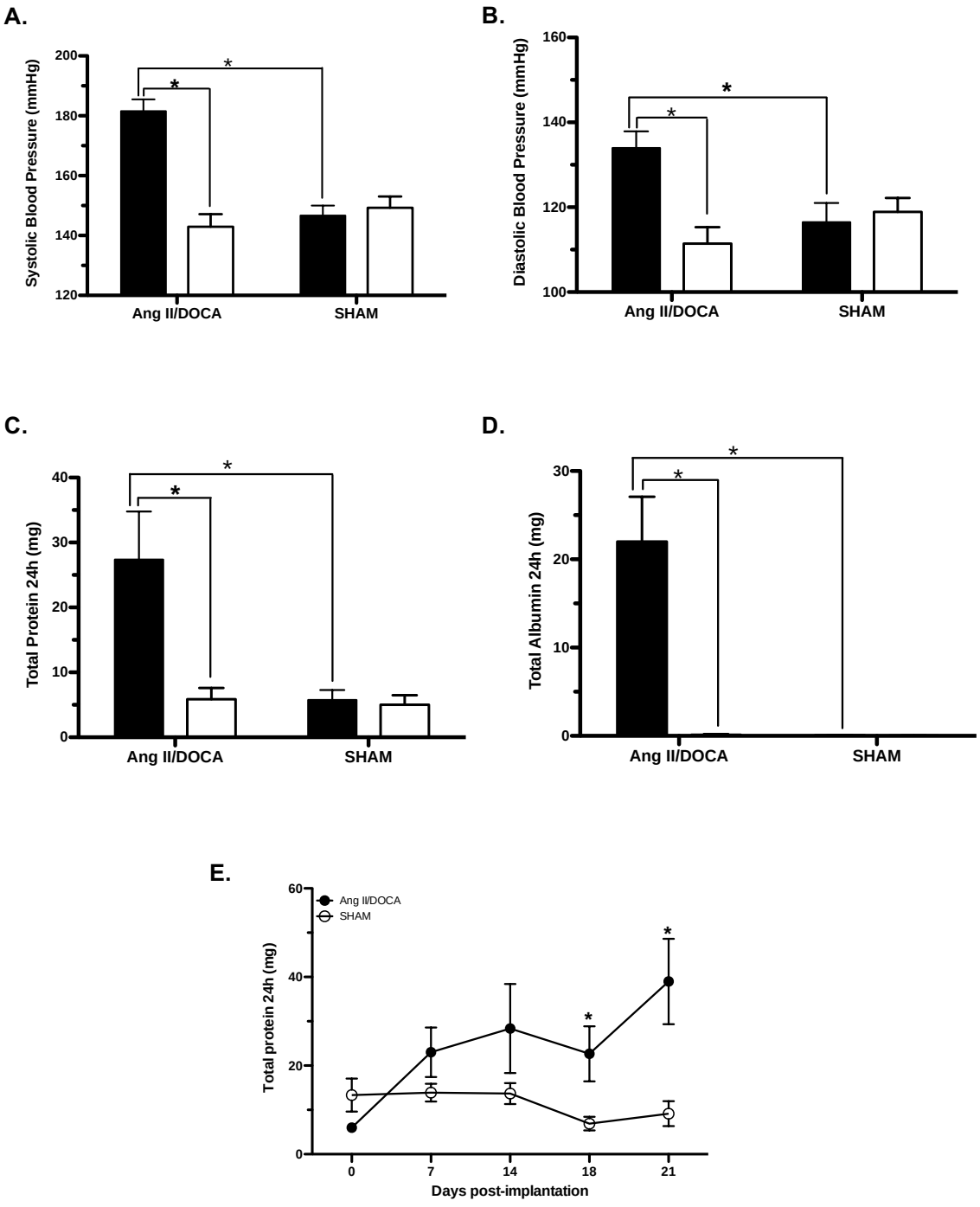
A.
Systolic Blood Pressure (mmHg)
200
180
160
140
120
*
*
Ang II/DOCA
SHAM
B.
Diastolic Blood Pressure (mmHg)
160
140
120
100
*
*
Ang II/DOCA
SHAM
C.
Total Protein 24h (mg)
40
30
20
10
0
*
*
Ang II/DOCA
SHAM
D.
Total Albumin 24h (mg)
30
20
10
0
*
*
Ang II/DOCA
SHAM
E.
Total protein 24h (mg)
60
40
20
0
Ang II/DOCA
SHAM
*
*
0
7
14
18
21
Days post-implantation

FIGURE 3

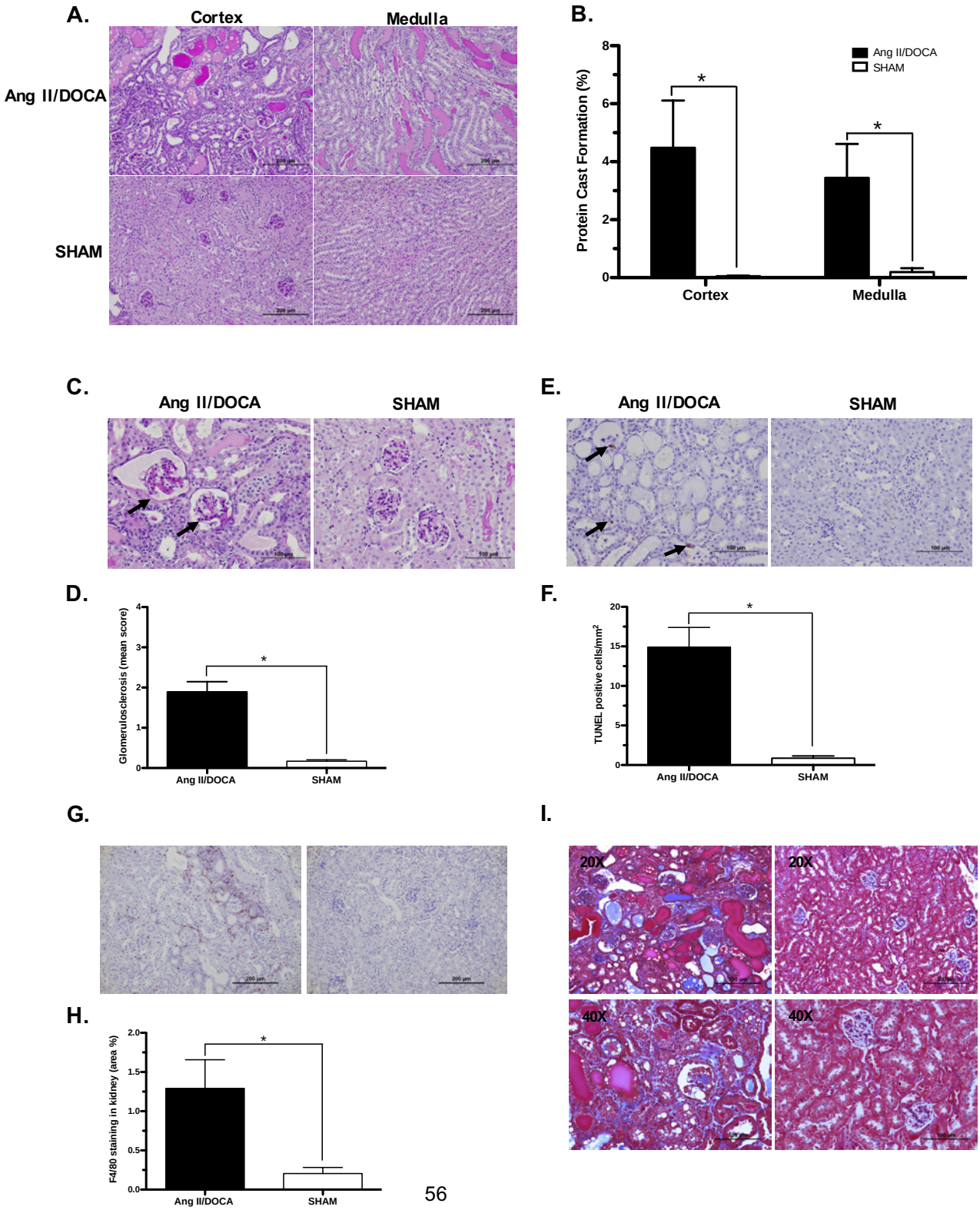
A.
Cortex
Medulla
Ang II/DOCA
SHAM
B.
Ang II/DOCA
SHAM
Protein Cast Formation (%)
Cortex
Medulla
C.
Ang II/DOCA
SHAM
E.
Ang II/DOCA
SHAM
D.
Glomerulosclerosis (mean score)
Ang II/DOCA
SHAM
F.
TUNEL positive cells/mm²
Ang II/DOCA
SHAM
G.
H.
F4/80 staining in kidney (area %)
Ang II/DOCA
SHAM
I.
20X
20X
40X
40X

FIGURE 4

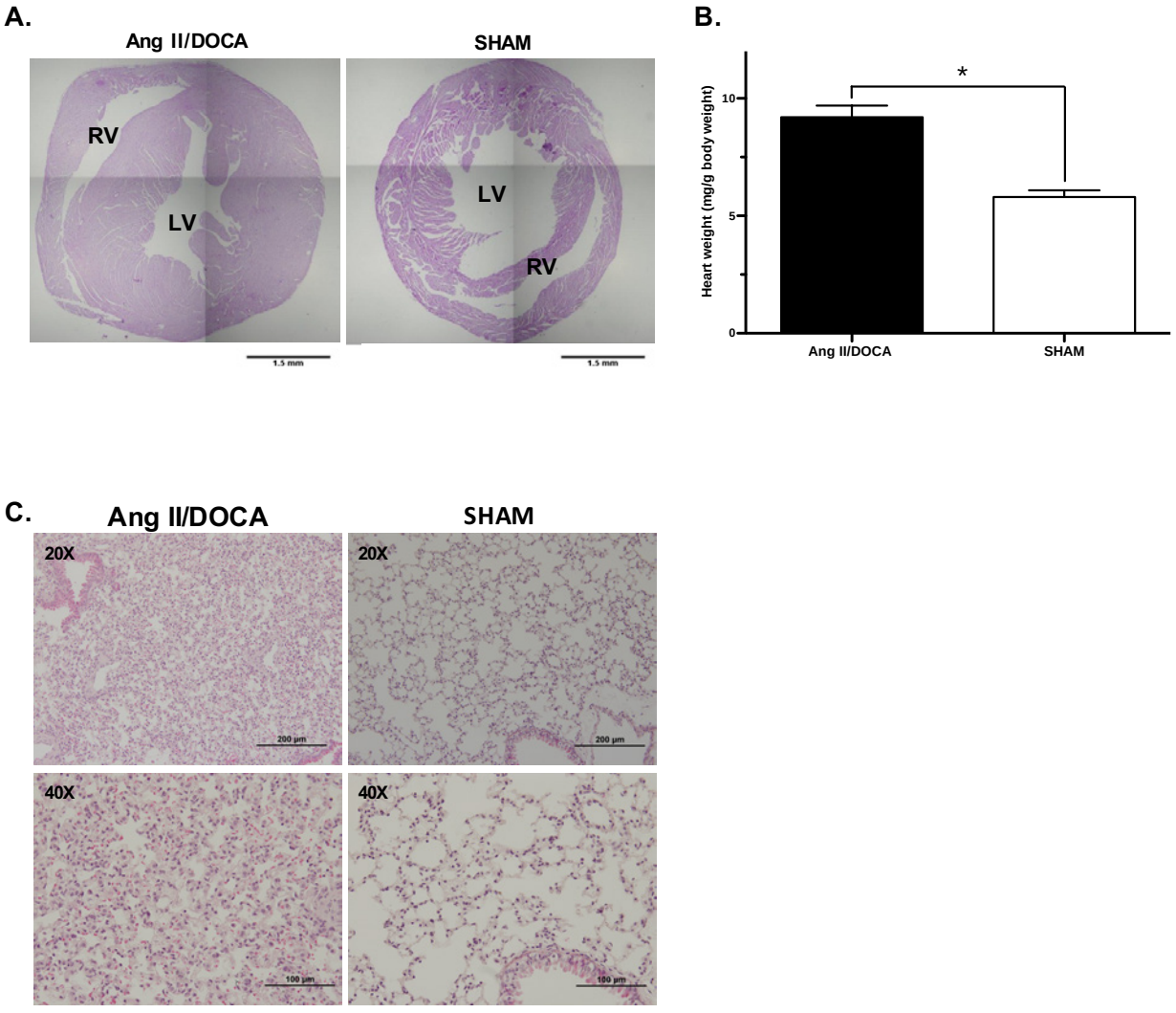
A.
Ang II/DOCA
SHAM
RV
LV
LV
RV
1.5 mm
1.5 mm
B.
*
Heart weight (mg/g body weight)
10
5
0
Ang II/DOCA
SHAM
C.
Ang II/DOCA
SHAM
20X
20X
200 µm
200 µm
40X
40X
100 µm
100 µm

FIGURE 5

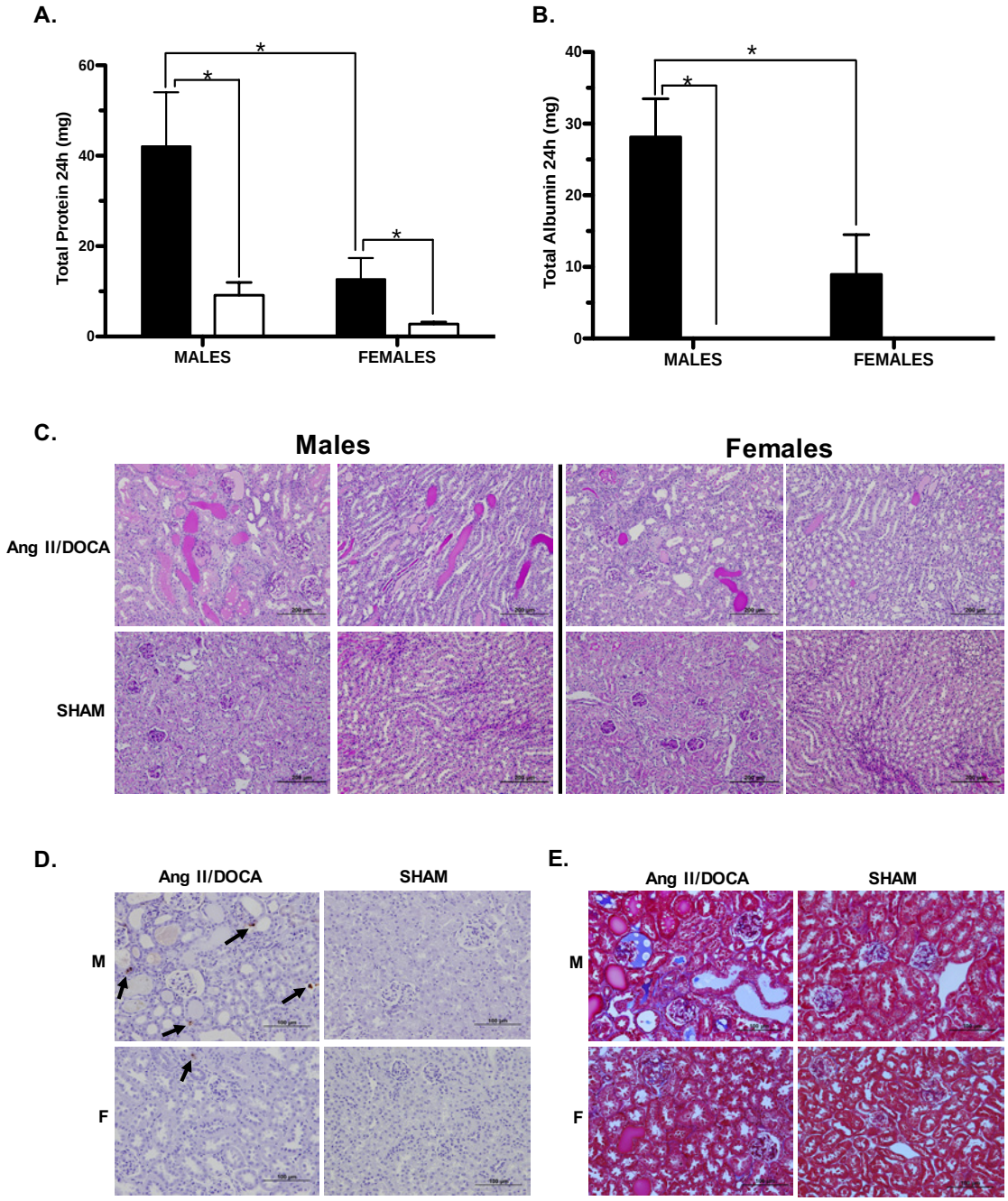
A.
Total Protein 24h (mg)
60
40
20
0
MALES
FEMALES
B.
Total Albumin 24h (mg)
40
30
20
10
0
MALES
FEMALES
C.
Males
Females
Ang II/DOCA
SHAM
D.
Ang II/DOCA
SHAM
M
F
E.
Ang II/DOCA
SHAM
M
F

References

1. Yang HC, Zuo Y, Fogo AB: **Models of chronic kidney disease**. *Drug Discov Today Dis Models* 2010, **7**(1-2):13-19.

2. Skarnes WC, Rosen B, West AP, Koutsourakis M, Bushell W, Iyer V, Mujica AO, Thomas M, Harrow J, Cox T *et al*: **A conditional knockout resource for the genome-wide study of mouse gene function**. *Nature* 2011, **474**(7351):337-342.

3. Zheng F, Striker GE, Esposito C, Lupia E, Striker LJ: **Strain differences rather than hyperglycemia determine the severity of glomerulosclerosis in mice**. *Kidney Int* 1998, **54**(6):1999-2007.

4. Kato N, Watanabe Y, Ohno Y, Inoue T, Kanno Y, Suzuki H, Okada H: **Mapping quantitative trait loci for proteinuria-induced renal collagen deposition**. *Kidney Int* 2008, **73**(9):1017-1023.

5. El-Meanawy A, Schelling JR, Iyengar SK, Hayden P, Barathan S, Goddard K, Pozuelo F, Elashi E, Nair V, Kretzler M *et al*: **Identification of nephropathy candidate genes by comparing sclerosis-prone and sclerosis-resistant mouse strain kidney transcriptomes**. *BMC Nephrol* 2012, **13**:61.

6. Kirchhoff F, Krebs C, Abdulhag UN, Meyer-Schwesinger C, Maas R, Helmchen U, Hilgers KF, Wolf G, Stahl RA, Wenzel U: **Rapid development of severe end-organ damage in C57BL/6 mice by combining DOCA salt and angiotensin II**. *Kidney Int* 2008, **73**(5):643-650.

7. Longo DL, Kasper, D. L., Jameson, J. L., Fauci, A. S., Hauser, S. L. & Loscalzo, J. : **Clinical and Laboratory Manifestations of Chronic Kidney Disease and Uremia**. In: *Harrison's PRINCIPLES OF INTERNAL MEDICINE.* Eighteenth edn: McGraw-Hill; 2012: 1410-1410.

8. Remuzzi G, Bertani T: **Pathophysiology of progressive nephropathies**. *The New England journal of medicine* 1998, **339**(20):1448-1456.

9. Atlas SA: **The renin-angiotensin aldosterone system: pathophysiological role and pharmacologic inhibition**. *Journal of managed care pharmacy : JMCP* 2007, **13**(8 Suppl B):9-20.

10. Gradman AH, Basile JN, Carter BL, Bakris GL, Materson BJ, Black HR, Izzo JL, Jr., Oparil S, Weber MA: **Combination therapy in hypertension**. *Journal of the American Society of Hypertension : JASH* 2010, **4**(2):90-98.

11. Gavrieli Y, Sherman Y, Ben-Sasson SA: **Identification of programmed cell death in situ via specific labeling of nuclear DNA fragmentation**. *The Journal of cell biology* 1992, **119**(3):493-501.

12. Raij L, Azar S, Keane W: **Mesangial immune injury, hypertension, and progressive glomerular damage in Dahl rats**. *Kidney Int* 1984, **26**(2):137-143.

13. Austyn JM, Gordon S: **F4/80, a monoclonal antibody directed specifically against the mouse macrophage**. *European journal of immunology* 1981, **11**(10):805-815.

14. Levey AS, Eckardt KU, Tsukamoto Y, Levin A, Coresh J, Rossert J, De Zeeuw D, Hostetter TH, Lameire N, Eknoyan G: **Definition and classification of chronic kidney disease: a position statement from Kidney Disease: Improving Global Outcomes (KDIGO)**. *Kidney international* 2005, **67**(6):2089-2100.

15. Kerr M, Bray B, Medcalf J, O'Donoghue DJ, Matthews B: **Estimating the financial cost of chronic kidney disease to the NHS in England**. *Nephrology, dialysis, transplantation : official publication of the European Dialysis and Transplant Association - European Renal Association* 2012, **27 Suppl 3**:iii73-80.

16. Jha V, Garcia-Garcia G, Iseki K, Li Z, Naicker S, Plattner B, Saran R, Wang AY, Yang CW: **Chronic kidney disease: global dimension and perspectives**. *Lancet* 2013, **382**(9888):260-272.

17. Remuzzi G, Perico N, Macia M, Ruggenenti P: **The role of renin-angiotensin-aldosterone system in the progression of chronic kidney disease**. *Kidney international Supplement* 2005(99):S57-65.

18. Turner JM, Bauer C, Abramowitz MK, Melamed ML, Hostetter TH: **Treatment of chronic kidney disease**. *Kidney international* 2012, **81**(4):351-362.

19. Hodgkins KS, Schnaper HW: **Tubulointerstitial injury and the progression of chronic kidney disease**. *Pediatric nephrology* 2012, **27**(6):901-909.

20. Levey AS, Coresh J: **Chronic kidney disease**. *Lancet* 2012, **379**(9811):165-180.

21. Kumar D, Robertson S, Burns KD: **Evidence of apoptosis in human diabetic kidney**. *Molecular and cellular biochemistry* 2004, **259**(1-2):67-70.

22. Liu G, Sun Y, Li Z, Song T, Wang H, Zhang Y, Ge Z: **Apoptosis induced by endoplasmic reticulum stress involved in diabetic kidney disease**. *Biochem Biophys Res Commun* 2008, **370**(4):651-656.

23. Woo D: **Apoptosis and loss of renal tissue in polycystic kidney diseases**. *The New England journal of medicine* 1995, **333**(1):18-25.

24. Sanz AB, Santamaria B, Ruiz-Ortega M, Egido J, Ortiz A: **Mechanisms of renal apoptosis in health and disease**. *Journal of the American Society of Nephrology : JASN* 2008, **19**(9):1634-1642.

25. Nath KA: **The tubulointerstitium in progressive renal disease**. *Kidney international* 1998, **54**(3):992-994.

26. Sean Eardley K, Cockwell P: **Macrophages and progressive tubulointerstitial disease**. *Kidney Int* 2005, **68**(2):437-455.

27. Wang Y, Harris DC: **Macrophages in renal disease**. *Journal of the American Society of Nephrology : JASN* 2011, **22**(1):21-27.

28. Rodriguez-Iturbe B, Pons H, Herrera-Acosta J, Johnson RJ: **Role of immunocompetent cells in nonimmune renal diseases**. *Kidney international* 2001, **59**(5):1626-1640.

29. Liu Y: **Renal fibrosis: new insights into the pathogenesis and therapeutics**. *Kidney international* 2006, **69**(2):213-217.

30. Strutz FM: **EMT and proteinuria as progression factors**. *Kidney international* 2009, **75**(5):475-481.

31. Duffield JS: **Macrophages and immunologic inflammation of the kidney**. *Seminars in nephrology* 2010, **30**(3):234-254.

32. Fogo AB: **Mechanisms of progression of chronic kidney disease**. *Pediatr Nephrol* 2007, **22**(12):2011-2022.

33. Aspromonte N, Cruz DN, Ronco C, Valle R: **Role of bioimpedance vectorial analysis in cardio-renal syndromes**. *Seminars in nephrology* 2012, **32**(1):93-99.

34. Lee WL, Cheng MH, Tarng DC, Yang WC, Lee FK, Wang PH: **The benefits of estrogen or selective estrogen receptor modulator on kidney and its related disease-chronic kidney disease-mineral and bone disorder: osteoporosis**. *Journal of the Chinese Medical Association : JCMA* 2013, **76**(7):365-371.

35. Dubey RK, Oparil S, Imthurn B, Jackson EK: **Sex hormones and hypertension**. *Cardiovascular research* 2002, **53**(3):688-708.

36. Silbiger SR, Neugarten J: **The impact of gender on the progression of chronic renal disease**. *American journal of kidney diseases : the official journal of the National Kidney Foundation* 1995, **25**(4):515-533.

37. Baylis C: **Age-dependent glomerular damage in the rat. Dissociation between glomerular injury and both glomerular hypertension and hypertrophy. Male gender as a primary risk factor**. *The Journal of clinical investigation* 1994, **94**(5):1823-1829.

38. Mulroney SE, Woda C, Johnson M, Pesce C: **Gender differences in renal growth and function after uninephrectomy in adult rats**. *Kidney international* 1999, **56**(3):944-953.

39. Hodeify R, Megyesi J, Tarcsafalvi A, Mustafa HI, Hti Lar Seng NS, Price PM: **Gender Differences control the susceptibility to ER stress-induced acute kidney injury**. *American journal of physiology Renal physiology* 2013.

40. Muller V, Szabo A, Viklicky O, Gaul I, Portl S, Philipp T, Heemann UW: **Sex hormones and gender-related differences: their influence on chronic renal allograft rejection**. *Kidney international* 1999, **55**(5):2011-2020.

41. Metcalfe W: **How does early chronic kidney disease progress? A background paper prepared for the UK Consensus Conference on early chronic kidney disease**. *Nephrol Dial Transplant* 2007, **22 Suppl 9**:ix26-30.

Chapter 3

Endoplasmic reticulum stress inhibition attenuates hypertensive chronic kidney disease through reduction in proteinuria

Summary and Significance:

This article comprises of a time point analysis to investigate the progression of CKD in the Ang II/DOCA salt model characterized in Chapter 2. The induction of ER stress was observed within 7 days on the model coinciding with increased proteinuria and hypertension. ER stress inhibition with 4-PBA resulted in diminished hypertension, albuminuria, fibrosis and inflammation. Our mRNA and protein analysis of kidney tissue revealed that Ang II/DOCA salt mice treated with 4-PBA experienced an increase in cubilin, an endocytic receptor responsible for tubular protein reabsorption. This suggests that the protein folding function of 4-PBA as a chaperon was allowing more cubilin to be available for albumin reabsorption thereby decreasing albuminuria. However, 4-PBA also decreased glomeruloscleorsis, therefore, 4-PBA could be attenuating CKD by reducing proteinuria through its action on both the glomerular and tubular compartment of the kidney. CHOP, a pro-apoptotic transcription factor induced by ER stress was upregulated early in the kidneys of mice treated with Ang II-DOCA salt and was inhibited by 4-PBA which was associated with CKD attenuation. When we applied the Ang II/DOCA salt model to CHOP deficient mice, we observed a decrease in albuminuria, glomerulosclerosis, protein cast formation, fibrosis and inflammation. However, CHOP deficient mice developed hypertension comparable to WT mice

due to Ang II/DOCA salt. Upon closer examination, CHOP deficient mice had higher levels of nephrin than WT mice upon Ang II/DOCA salt treatment. This finding suggested that CHOP deficiency could be diminishing proteinuria by preserving glomerular integrity. This study implicates ER stress inhibition as a therapeutic strategy and CHOP as a molecular drug target to treat CKD.

Title: Endoplasmic reticulum stress inhibition attenuates hypertensive chronic kidney disease through reduction in proteinuria

Author names and affiliations:

Zahraa Mohammed-Ali[1], Chao Lu[1], Mandeep K. Marway[1], Rachel E. Carlisle[1], Kjetil Ask[2], Dusan Lukic[3], Joan C. Krepinsky[1], Jeffrey G. Dickhout[1*].

[1]Department of Medicine, Division of Nephrology, McMaster University and St. Joseph's Healthcare Hamilton, Hamilton, Ontario, Canada.

[2]Department of Medicine, Division of Respirology, McMaster University and St. Joseph's Healthcare Hamilton, Hamilton, Ontario, Canada.

[3]Department of Pathology and Molecular Medicine, McMaster University and St. Joseph's Healthcare Hamilton, Ontario, Canada

Running title: ER stress inhibition attenuates CKD

SOURCES OF FUNDING:

This work was supported by research grants to Jeffrey G. Dickhout from the Canadian Institutes of Health Research (OSO-115895 and MOP-133484). Financial support from St. Joseph's Healthcare Hamilton, including salary support to Jeffrey G. Dickhout, is also acknowledged. Support from the Division of Nephrology in the Department of Medicine at McMaster University is acknowledged. Dr. Dickhout also holds a Kidney foundation of Canada, Krescent New Investigator award.

***Address Correspondence to:**
Jeffrey G. Dickhout, PhD
Department of Medicine, Division of Nephrology
McMaster University and St. Joseph's Healthcare Hamilton
50 Charlton Avenue East
Hamilton, ON, Canada, L8N 4A6
Tel: 905-522-1155 ext. 35334
Fax: 905-540-6589
Email: jdickhou@stjosham.on.ca

Abstract

Endoplasmic reticulum (ER) stress is implicated in chronic kidney disease (CKD) development in patients and in animal models. Here we show that ER stress inhibition through 4-phenylbutyric acid (4-PBA) administration decreases blood pressure, albuminuria, and tubular casts in an angiotensin II/deoxycorticosterone acetate/salt murine model of CKD. Lower albuminuria in 4-PBA-treated mice was associated with higher levels of cubilin protein in renal tissue membrane fractions. 4-PBA decreased renal interstitial fibrosis, renal $CD3^+$ T-cell and macrophage infiltration, mRNA expression of TGFβ1, Wnt signaling molecules, and ER stress-induced pro-inflammatory genes. CHOP deficient mice that underwent this model of CKD developed hypertension comparable to wild type mice, but had less albuminuria and tubular casts. CHOP deficiency resulted in higher nephrin levels and decreased glomerulosclerosis compared to wild type mice; this effect was accompanied by lower macrophage infiltration and fibrosis. Our findings portray ER stress inhibition as a means to alleviate hypertensive CKD by preserving glomerular barrier integrity and tubular function. These results demonstrate ER stress modulation as a novel target for preserving renal function in hypertensive CKD.

Introduction

Chronic kidney disease (CKD) can result from a variety of disorders that affect the structure and function of the kidney, and it is a rising global health concern due to its increasing prevalence (8-16%) worldwide[1]. There is presently no cure for CKD and the treatments available are primarily aimed at halting disease progression. Further, CKD can result in end stage renal disease (ESRD) and is associated with complications, such as cardiovascular disease, cognitive decline, anaemia, and mineral and bone disorders[1]. Individuals that progress to ESRD require renal replacement therapy that involves dialysis and/or renal transplants that are extremely costly, $35 billion per year in the United States of America. As well, access to renal replacement therapy is limited in developing and third world countries, causing 1 million people to die annually from ESRD[2].

The endoplasmic reticulum (ER) is responsible for the synthesis of transmembrane, secretory, and ER lumenal proteins[3]. During diseased states there may be a disruption of ER proteostasis, whereby there is an imbalance between protein folding capacity and protein folding demand[4]. The accumulation of misfolded proteins in the ER is known as ER stress and leads to the activation of the unfolded protein response (UPR). The UPR triggers the dissociation of GRP78 from three known transmembrane sensors in the ER: activating transcription factor 6 (ATF6), inositol-requiring enzyme I (IRE1), and PKR (double-stranded RNA-dependent protein kinase)-like ER protein kinase (PERK). The activation of these signal transduction pathways can result in cell death,

inflammation, and fibrosis in the context of CKD[5,6]. ER stress has been shown to play a role in the pathogenesis of various renal diseases in humans[3]. The upregulation of key UPR markers has been observed in patients with primary glomerular disease[7-9] and diabetic nephropathy[10], and has been strongly associated with proteinuria[11].

Our central hypothesis in this study is that inhibition of ER stress impedes CKD progression. In our experiments, we utilized two methods to inhibit ER stress, pharmacologically by dietary administration of 4-phenylbutyric acid (PBA) and genetically through the disruption of CHOP, a pro-apoptotic transcription factor that is induced by ER stress.

Results:

4-PBA inhibits hypertensive proteinuria in a model of CKD

This CKD model produced a significant increase in systolic (Figure 1A) and diastolic blood pressure (Figure 1B) at day 7 post-angiotensin (Ang) II/deoxycorticosterone acetate (DOCA) salt treatment, continuing until sacrifice at day 21. Hypertension was completely inhibited by 4-PBA treatment, as measured on day 21. An increase in albuminuria was observed at all time points in response to Ang II/DOCA salt treatment. 4-PBA treatment significantly reduced 24 h urinary albumin excretion at day 21 (Figure 1C). To investigate why 4-PBA treatment reduced albuminuria, we examined megalin and cubilin, two multi-ligand endocytic receptors, responsible for tubular protein reabsorption[12]. Proteinuric kidney

disease places an increased demand for synthesis of these receptors in the ER[13]. Since 4-PBA alleviates ER stress by aiding in protein folding, we hypothesized that mice treated with 4-PBA could produce higher amounts of megalin and cubilin in response to the Ang II/DOCA salt-induced CKD. Therefore, we measured megalin and cubilin expression at the RNA and protein level. Nanostring nCounter assay analysis showed an increase in megalin (Figure 1D) and cubilin (Figure 1E) mRNA in response to Ang II/DOCA salt treatment. 4-PBA treatment resulted in an even higher level of megalin and cubilin mRNA, suggesting that the action of 4-PBA increased endocytic receptor transcription. Western blotting showed an increase in cubilin protein expression (Figure 1F, 1G) in response to Ang II/DOCA salt treatment, with higher levels in 4-PBA-treated mice; however, no change was found in megalin protein levels (Figure 1H, 1I). To decipher whether this increase in cubilin protein reached the plasma membrane to become a functional endocytic receptor, we extracted plasma membrane fractions from our experimental groups and measured membrane cubilin expression. Figure 1J and 1K showed significantly increased cubilin in plasma membrane lysates from 4-PBA-treated animals compared to untreated animals in response to Ang II/DOCA salt. In attempting to measure megalin in these same membrane fractions, we were not able to obtain a reliable band in the 600 kDa range, the known molecular weight for the protein. The effect of albuminuria on renal pathology was examined through periodic acid-Schiff (PAS) staining by scoring glomerular damage and quantifying intratubular protein casts. In AngII/DOCA salt mice, 4-PBA treatment significantly

decreased glomerulosclerosis (Figure 1L, 1M) and significantly reduced intratubuluar protein cast formation in both the cortex and the medulla (Figure 1N, 1O).

4-PBA inhibits the UPR in a model of CKD

The NanoString nCounter determined the fold change of UPR gene expression over 21 days of Ang II/DOCA/salt-induced CKD (Figure 2A). Fold changes for the 4-PBA-treated Ang II/DOCA salt mice were compared to sham controls that were also sacrificed at day 21. Collagen-folding chaperones, such as *Hsp47* and *Fkbp65*[14,15], were induced in the Ang II/DOCA salt-treated mice at day 7 and remained elevated until the endpoint of the study. *Hmox-1*, a gene known to be upregulated during ER stress[16], and an important marker of human CKD progression[17] was shown to be significantly induced by the AngII/DOCA salt model at an early stage. Our CKD mouse model also showed an increase in apoptosis and authophagy genes that are induced by IRE1α phosphorylation and mediated by *Ask1* during ER stress. These genes include *Bcl2, Bad, Bax, Bak1, Bbc3, Trp53,* and *Beclin-1*[18,19]. As well, apoptotic genes that have been shown to be directly induced by ER stress, *Chop* and *phlda1,* are increased in our CKD model[20]. 4-PBA treatment inhibited the activation of UPR genes in response to Ang II/DOCA salt at the 21-day time point. *Pcsk9* was the only gene that was significantly induced by 4-PBA and was significantly higher in the 4-PBA-treated group compared to Ang II/DOCA salt mice without 4-PBA treatment. To examine the UPR activation in our

CKD model, kidneys were stained for CHOP (Figure 2B) and phosphorylated IRE1α (Figure 2C). Quantification of the staining showed an increase in CHOP (Figure 2D) and phosphorylated IRE1α (Figure 2E) at all time points; both CHOP and phosphorylated IRE1α were inhibited by 4-PBA treatment (Figures 2D, 2E).

4-PBA attenuated renal interstitial fibrosis in Ang II/DOCA salt-induced CKD

A Nanostring nCounter assay was performed to evaluate the fold changes in the expression of fibrosis genes illustrated in a heat map (Figure 3A). Genes encoding extracellular matrix (ECM) proteins collagen (*Col1a1, Col3a1*) and fibronectin (*Fn1*), myofibroblast marker α-smooth muscle actin (*Acta2*), as well as regulators of the ECM deposition process such as E-cadherin, *Mmp2, Mmp3, Mmp14, Timp1,* are shown to be upregulated early in CKD development at day 7 and continue to exhibit high levels of expression through all time points. The ECM deposition process is initiated by TGF-β and Wnt signaling pathways in various animal models of kidney disease, as well as in human CKD[21,22]. Our Ang II/DOCA salt model resulted in an early upregulation of TGF-β signaling and non-canonical Wnt signaling (*Wnt5a-Ror2*) as early as day 7 in the model and these pathways were significantly lowered with 4-PBA treatment. Although 4-PBA-treated mice still experienced a significant increase in pro-fibrotic genes *Col1a1, Mmp3, Fn1, Loxl2, Lgals3, Gremlin,* and *Timp-1*, there was an overall decrease in ECM components and fibrotic mediators. Kidneys were stained with α-smooth muscle actin (Figure 3B) and picrosirius red (Figure 3C) to examine renal fibrosis. Analysis of α-smooth

muscle actin expression (Figure 3D) and collagen deposition (Figure 3E) demonstrated that ECM deposition was increased at day 7 and continued rising until sacrifice at day 21. Although some α-smooth muscle actin and collagen deposition was observed in 4-PBA-treated Ang II/DOCA salt mice, it was significantly lower than Ang II/DOCA salt mice (Figures 3D, 3E).

4-PBA treatment attenuated inflammation in Ang II/DOCA salt-mediated CKD

Fold changes in the expression of inflammatory genes are demonstrated in a heat map (Figure 4A). Only a few genes appeared to be regulated at day 7 in the inflammatory gene codeset, whereas almost all inflammatory genes were upregulated by day 21. This temporality in response allowed us to isolate potential initiators of CKD development. These include pattern recognition receptors (PRRs) such as *Tlr2, Tlr4,* and *Nod-1* that have been shown to be associated with various models of kidney injury[23,24]. Transcription factors *NF-κB, AP-1*, and *Stat3,* which have been reported to be induced by ER stress[25,26] were also significantly increased at day 7 in our model. The NanoString data showed an increase in chemokines *IP-10* and *Ccl20*, which are known to attract various immune cells to the site of tissue injury. Therefore, staining for F4/80 and CD3, well-established cell-surface markers of macrophages (Figure 4B) and T-cells (Figure 4C), respectively, were used to assess inflammation in kidney micrographs. This CKD model resulted in significantly increased macrophage infiltration at day 14, 18 and 21 (Figure 4D) and T-cell infiltration at all time points (Figure 4E). The quantification

of F4/80 staining shows that 4-PBA treatment completely inhibited macrophage infiltration in response to Ang II/DOCA salt treatment (Figure 4D). However, 4-PBA-treated mice still experienced a certain level of T-cell infiltration in response to Ang II/DOCA/salt, although it was significantly lower than mice without 4-PBA treatment (Figure 4E).

CHOP deficiency inhibits proteinuria but not hypertension in a CKD model

Since CHOP is a key transcription factor in the UPR and was upregulated at the earliest time point, day 7, in our model, we examined the effect of genetic disruption of CHOP on CKD severity. In response to the Ang II/DOCA/salt model, $CHOP^{-/-}$ mice experienced an increase in both systolic (Figure 5A) and diastolic blood pressure (Figure 5B), which was comparable to wild type (WT) mice. However, Ang II/DOCA salt-treated $CHOP^{-/-}$ mice showed a significantly lower level of albuminuria compared with WT mice (Figure 5C). Therefore, we explored possible mechanisms for the decreased albumin levels found in $CHOP^{-/-}$ mice. Reports have established that eIF2α phosphorylation during ER stress results in general translation attenuation and CHOP induction. CHOP leads to the activation of GADD34, which is able to recover protein translation by dephosphorylating eIF2α[27]. During translation attenuation proteins with short open reading frames such as ATF4 are preferentially translated[28]. Nephrin, an integral component of the podocyte slit diaphragm, is another protein that is preferentially translated during eIF2α phosphorylation[28]. Our experiments show an increase in nephrin in

response to our CKD model and a significantly higher amount of nephrin in CHOP$^{-/-}$ mice treated with Ang II/DOCA salt than in WT mice at both the mRNA (Figure 5D) and the protein level (Figure 5E, 5F). As well, our data shows a significantly lower level of GADD34 in CHOP$^{-/-}$ mice (Figure 5G, 5H), confirming our suggested mechanism. Since nephrin is important in maintaining the renal filtration barrier, we then investigated the effect of CHOP deficiency on the maintenance of glomerular structure and renal pathology. Glomerular scoring showed a significantly lower degree of glomerular damage in CHOP$^{-/-}$ mice that underwent the Ang II/DOCA salt model compared to WT mice (Figure 5I, 5J). PAS staining demonstrated a significantly lower level of protein cast formation in the cortex and medulla of CHOP$^{-/-}$ mice compared to WT mice (Figure 5K, 5L, 5M) in response to Ang II/DOCA salt.

CHOP deficiency inhibits the UPR, inflammation, and fibrosis in CKD

CHOP deficiency reduced the number of genes regulated in response to Ang II/DOCA salt. Lower levels of UPR (Figure 6A), fibrotic (Figure 6B), and inflammatory (Figure 6C) genes were induced by the Ang II/DOCA salt model in the CHOP$^{-/-}$ mice compared to WT mice. Of note, *Pcsk9* is higher in the kidney in CHOP$^{-/-}$ mice treated with AngII/DOCA salt. Some UPR and apoptosis/autophagy genes were regulated in the opposite direction in CHOP$^{-/-}$ mice treated with Ang II/DOCA salt compared to WT, such as *PPARγ, Bad, Bif-1, Calreticulin,* and *Fkbp13*. Similarly, transcription factor *AP-1* and transmembrane protein *gp130* also

experienced downregulation in CHOP$^{-/-}$ mice treated with Ang II/DOCA salt, as opposed to upregulation in WT mice. Although certain ECM deposition components such as *Col1A1, Col3A1, Fn1*, showed a significant increase in CHOP$^{-/-}$ mice treated with Ang II/DOCA salt, the level of increase was attenuated. α-smooth muscle actin staining of renal tissue was significantly lower in the cortex and medulla of CHOP$^{-/-}$ mice treated with Ang II/DOCA salt than in WT mice (Figure 7A, 7B). Similarly, area density of F4/80 staining showed significantly lower macrophage infiltration in CHOP$^{-/-}$ mice treated with Ang II/DOCA salt compared with WT mice (Figure 8A, 8B&C).

The UPR is activated in human hypertensive nephrosclerosis

In order to translate our work into human CKD, we studied the renal pathology in patients with hypertensive nephrosclerosis in comparison to renal pathology in our mouse model. The similarities in pathology are demonstrated in terms of glomerular damage between our mouse model and CKD patients. Further, protein cast formation was present in both the cortex and the medulla of CKD patients, similar to the Ang II/DOCA salt mouse model (Figure 9A). Masson's trichrome staining showed glomerular and renal interstitial fibrosis in both human CKD and the Ang II/DOCA salt model (Figure 9B). Likewise, an increase in key UPR genes, specifically phosphorylated IRE1α (Figure 9C) and CHOP (Figure 9D), was found in the medullae of biopsies of human hypertensive CKD.

Discussion

In this study, we investigated the temporal relationships between the inflammatory, fibrotic, and UPR pathways in CKD. Our results implicate the UPR as an initiator of CKD, since key ER stress genes, *Grp78, Chop, Atf6* and *phlda1* were upregulated early in the disease process. ER stress-induced apoptotic and autophagy genes, *Ask1, Bad, Bax, Bcl2, Bbc3* and *Beclin-1*[18,19], were also upregulated early in our model. This model shows increased albuminuria and protein cast formation early in CKD development. These results indicate albuminuria and renal pathology occurs at the same time as UPR activation and are in accordance with previous reports[11,29].

4-PBA is a small molecular chaperone that alleviates ER stress by aiding in the protein folding in the ER[30,31]. We found 4-PBA significantly reduced albuminuria and CKD progression in our model while inhibiting the upregulation of key UPR genes. This result is in agreement with previous studies, where 4-PBA administration has been reported to decrease urinary protein excretion and glomerular damage in streptozotocin-induced diabetic nephropathy[30,32]. As well, 4-PBA has been shown to decrease outer medullary stripe damage in tunicamycin-induced acute kidney injury (AKI)[33]. Our experiments are the first to draw a link between the effect of 4-PBA treatment and albumin reabsorption mediated by megalin and cubilin in renal proximal tubules. In addition to abnormalities in the glomerular filtration barrier, defective tubular reabsorption may also contribute to albuminuria[34]. In our study, 4-PBA treatment resulted in lower albuminuria, as well

as a significant increase in megalin and cubilin mRNA. Protein analysis showed an increase in cubilin in both whole kidney tissue lysates, as well as plasma membrane extracts in 4-PBA-treated mice. In line with our findings, a recent study[35] showed a six-fold increase in urinary albumin excretion in cubilin-deficient mice. Similarly, patients with defective cubilin, resulting in Imerslund-Gräsbeck disease, also have higher urinary excretion of albumin, along with other ligands of cubilin[36,37]. It appears that 4-PBA increased the folding and delivery of cubilin to the apical membrane of the proximal tubule allowing for a greater reabsorption of albumin, thereby reducing 24 h albumin excretion. However, further experiments are necessary to conclude that 4-PBA increased cubilin directly through its chaperone activity, since 4-PBA treatment augmented both mRNA and protein cubilin levels. Therefore, the significantly lower albuminuria in 4-PBA-treated mice could be attributed to the increased cubilin levels in these mice.

Albuminuria is an important risk factor for CKD progression[38,39]. Albumin excretion associated with renal injury has been shown to cause TGF-β activation[40-42]. Our study shows increased TGF-β1 signalling, which stimulates resident fibroblasts, myofibroblasts, and tubular epithelial cells to produce ECM components, collagens type I and III, FN1, and α-smooth muscle actin, resulting in fibrosis[21]. 4-PBA treatment inhibited α-smooth muscle actin and collagen protein deposition in response to Ang II/DOCA/salt. Our experiments, along with others on the unilateral ureteral obstruction (UUO) model, have shown 4-PBA treatment to impart protection against apoptosis and renal interstitial fibrosis[43,44], suggesting a

causative role for ER stress in renal fibrosis. Further, in a study by El Karoui *et al.*[45] 4-PBA treatment resulted in decreased tubular lesions, interstitial fibrosis and tubular apoptosis in $WT1^{+/mut}$ mice which develop glomerular disease due to a mutation in WT1, an important regulator of podocyte function. In this study, 4-PBA was also administered in a model of doxorubicin-induced nephropathy where it caused a reduction in protein cast formation, apoptosis and ER stress in the kidney[45]. The effect of 4-PBA was partly linked to its inhibition of Lipocalin 2, a gene requiring calcium release-induced ER stress for its induction. Lipocalin 2 induction was shown to generate tubular apoptosis and renal lesions. Interestingly, the authors demonstrated that albumin is able to activate calcium-dependent ER stress. They speculate that this may occur through albumin binding to megalin in a calcium-dependent manner thereby triggering intracellular ER calcium release and ER stress [45]. Our study adds to this data by showing further association between ER stress inhibition and decreased albuminuria through the increase in membrane cubilin available for albumin reabsorption.

The IRE1α and PERK pathways of the UPR result in inflammation through the activation of *NF-κB* and *AP-1*, transcription factors responsible for the upregulation of cytokines, chemokines, complement, and acute phase proteins[6,25]. In our study, both *NF-κB* and *AP-1* were significantly upregulated in our CKD model. Immune cell recruitment was increased with Ang II/DOCA/salt CKD, with an increased infiltration of $CD3^+$ and $F4/80^+$ cells in the kidneys of mice with CKD. Macrophage and T-cell infiltration has been shown in human and animal models

of kidney disease and is associated with disease progression and proteinuria[46]. Studies on the streptozotocin model of diabetic nephropathy have shown that in addition to lowering urinary protein excretion, 4-PBA attenuates inflammatory mediators NF-kB and MCP-1[30,47]. MCP-1 is responsible for the recruitment of macrophages, and its urinary levels in humans have shown strong association with proteinuria[48]. In fact, MCP-1 deficiency has been shown to prevent renal fibrosis, proteinuria, and macrophage infiltration in various animal models of disease[48]. 4-PBA significantly reduced inflammatory cell infiltration and inflammatory gene expression including NF-kB and MCP-1 in our study. In addition to reducing albuminuria and renal injury, 4-PBA is able to prevent disease progression through its inhibitory effect on pro-inflammatory and pro-fibrotic mediators.

Since CHOP was upregulated early in our CKD model, we examined the efficacy of CHOP knockout to inhibit CKD progression. $CHOP^{-/-}$ mice have previously been studied in the context of renal fibrosis, where they have been shown to protect against apoptosis, fibrosis, and inflammation in UUO and AKI[33,44,49,50]. Our experiments have shown that in response to Ang II/DOCA/salt, $CHOP^{-/-}$ mice exhibit significantly lower albuminuria, glomerular injury, and protein cast formation compared to WT mice. Interestingly, unlike the 4-PBA treatment group, they experienced an increase in blood pressure similar to WT mice.

Nephrin is a key component of the slit diaphragm in glomerular podocytes, which helps maintain the glomerular filtration barrier[51]. Cybulsky *et al.*[28] provided evidence that, analogous to ATF4, nephrin could be preferentially translated in

stressed cells during eIF2α phosphorylation, owing to its short upstream open reading frames. General translation attenuation due to eIF2α phosphorylation is relieved by GADD34, a phosphatase induced by CHOP. Prolonged translation attenuation and subsequently lower levels of GADD34, achieved through CHOP deficiency, would allow increased preferential translation of nephrin during ER stress. Our experiments have shown a significant increase in nephrin mRNA with Ang II/DOCA salt treatment and even higher expression in CHOP$^{-/-}$ mice. At the protein level, however, WT Ang II/DOCA salt mice have similar levels of nephrin as WT sham animals, whereas CHOP$^{-/-}$ mice expressed significantly higher levels of nephrin. Taken together, our findings indicate a link between diminished CHOP expression and improved glomerular permselectivity.

Our experiments show lower ER stress and apoptotic gene expression with CHOP deficiency. UPR genes *Atf6, Atf4, Calnexin* and *Calreticulin,* as well as apoptotic and autophagy genes upregulated by the UPR, *Bax, Bad* and *Beclin-1,* show reduced expression in CHOP$^{-/-}$ mice. The inhibition of UPR genes by CHOP deficiency has been demonstrated previously[49]. CHOP has also been shown to downregulate pro-survival gene *Bcl2*, thereby resulting in the activation of apoptosis via Bax/Bak proteins and Beclin-1[18,52]. In addition, CHOP$^{-/-}$ mice had an overall trend of attenuated expression of fibrotic and inflammatory genes, as compared to their WT counterparts. Upregulation of key inflammatory transcription factors *NF-κB* and *AP-1* was diminished in CHOP$^{-/-}$ mice. In fact, *AP-1* is downregulated with CHOP deficiency; this could be due to the reported ability of

CHOP to enhance the transcriptional activation of *AP-1*[53]. The weakened inflammatory gene expression in CHOP$^{-/-}$ mice on Ang II/DOCA salt was also reflected by lower macrophage infiltration. A recent study by Zhang *et al.*[49] has shown CHOP deficiency reduces fibrosis, macrophage infiltration, and TLR4-NFκB signaling in a unilateral ureteral obstruction model of kidney disease. This group attributed the reduction in fibrosis to the decreased TLR4-NFκB signalling, which results in significantly lower levels of TGF-β activity[49]. Our experiments also show a decrease in renal fibrosis in line with previous reports on CHOP knockouts; CHOP deficiency attenuated *Tlr4, NF-κB,* and *TGF-β* activity in response to Ang II/DOCA salt.

The finding that CHOP and phosphorylated IRE1α are upregulated in patients with hypertensive nephrosclerosis aids in translating our work to human CKD. Both methods of ER stress inhibition, 4-PBA treatment and CHOP knockdown, were shown to decrease renal fibrosis, inflammation, and albuminuria, important predictors of disease progression in humans. Taken together, these studies provide strong support for a potential therapeutic benefit of 4-PBA in patients with hypertensive kidney disease.

Methods and Materials

Mouse model of CKD

A combination of uninephrectomy, Ang II/DOCA infusion, as well as salt in the drinking water was used to induce CKD, as previously documented[8,54]. Briefly, 10-

week-old male mice were subjected to a uninephrectomy under isofluorane anesthesia. Upon recovery, Ang II (1.5 ng/min/g body weight) was administered via osmotic pump along with a 50 mg 21-day release DOCA pellet. Mice were then provided with 1% salt in drinking water and sacrificed at 7, 14, 18 and 21 days. For each time point, a sham operation was performed on a group of mice for both the uninephrectomy and osmotic pump and pellet implantation; these mice were used as controls. 4-PBA (Scandinavian Formulas) was administered in the drinking water upon pump and pellet implantation at 1 g/kg/day to determine if this treatment would affect the endpoint of CKD development for the 21-day group. Dose was adjusted through measurement of water intake in metabolic cages. Mice placed on 4-PBA were also provided with 1% salt in the drinking water while factoring in the contribution of 4-PBA to the sodium content. Age-matched $CHOP^{-/-}$ mice were obtained from a breeding colony held at McMaster University Central Animal Facility along with their wild type littermate controls. The founders of the colony were purchased from Jackson Laboratories (Stock number: 05530). All animal work was done in accordance with and approved by the McMaster University Animal Research Ethics Board.

Human Kidney Biopsies

Kidney biopsies were obtained from the Department of Pathology at St. Joseph's Healthcare Hamilton, Canada. Human CKD kidney biopsies were obtained from patients diagnosed with purely hypertensive nephrosclerosis. Uninvolved, normal

renal tissue was obtained from kidneys resected from renal cell carcinoma patients. Work on these tissues was approved by the Hamilton Integrated Research Ethics Board.

Blood pressure measurements and urinalysis

Blood pressure measurements were obtained through the tail cuff method using a CODA blood pressure analyzer (Kent Scientific), as done previously[54]. Metabolic cages were used to collect 24 h urine before the surgical procedure and after 3 weeks on treatment with AngII/DOCA/salt. Albuminuria, an important risk factor for CKD progression[55,56], was assessed using an ELISA (Bethyl Laboratories) to measure mouse urine albumin concentration in 24 h urine.

Western blotting

Total cell lysates were obtained using 4X SDS lysis buffer with protease inhibitor cocktail (Roche) and phosphatase inhibitor cocktail (Roche) added. Plasma membrane lysates were obtained using the Mem-PER plus kit (ThermoFisher Scientific). Protein levels were determined using BioRad DC Protein Assay (BioRad) for control of protein loading. Tissue lysates were subjected to electrophoretic separation in an SDS-PAGE reducing gel (BioRad). Primary antibodies were detected using appropriate horseradish peroxidase-conjugated secondary antibodies and ECL Western Blotting Detection Reagents (GE Healthcare), as described previously[33]. Nephrin antibody (AF3159, R& D Systems)

was diluted 1:10,000, GADD34 antibody (sc-8327, Santa Cruz) was diluted 1:200, cubilin antibody (sc-20609, Santa Cruz) was diluted 1:200, megalin antibody (sc-25470, Santa Cruz) was diluted 1:100, vinculin antibody (Sigma) was diluted 1:500 and β-actin antibody (Sigma) was diluted 1:5000. Results were densitometrically quantified using ImageLab software (BioRad) and expressed as a ratio of loading controls.

Immunohistochemistry

At sacrifice, renal tissue was fixed in 4% paraformaldehyde and subsequently sectioned using a microtome. To evaluate renal pathology, PAS staining was performed to assess protein cast formation, and picrosirius red (PSR) and α-smooth muscle actin staining was used to assess fibrosis. For PSR staining, kidney tissue sections were processed with saturated picric acid solution and then stained with Sirius red F3B (Colour Index 35782). For T-cell staining, rabbit anti-human CD3 antibody (Dakocytomation) was used at a concentration of 0.6 g/L and a dilution of 1:100 in normal goat serum (Vector). For macrophage staining, rat antibody to F4/80 (ab6640, Abcam) was used at a dilution of 1:30 in normal rabbit serum. For CHOP staining, rabbit anti-GADD153 (sc-575, Santa Cruz) was used at 1:40 dilution. To detect IRE1α phosphorylation, anti-IRE1 (phospho S724) antibody (ab48187, Abcam) was used at a dilution of 1:100. Horseradish peroxidase streptavidin (Vector SA-5004) was used in combination with Nova Red (Vector) and hematoxylin (Sigma) to visualize the stained cells.

Assessment of renal pathology

Immunohistochemistry sections were imaged using an Olympus BX41 microscope. Images of PSR-stained kidneys were taken using the U-POT polarizer and U-ANT analyzer (Olympus) for transmitted light. The diaphragm and polarizer allowed the detection of birefringence of collagen fibres. All other stained kidneys were imaged without the polarizer and analyzer. Five random images of each of the cortex and the medulla per mouse were taken to analyze the pathological features in renal tissue. The Metamorph program was used to assess the area density for PSR, α-smooth muscle actin, CHOP, phosphorylated IRE1α, and F4/80 staining. This method involves setting a colour threshold in the Metamorph program to express the area density of the stain as a percentage of the image total area. The quantification of PAS staining was performed in the same program by manually selecting the casts and then calculating the percentage area of casts per image and then per mouse cortex or medulla. As well, glomerular scoring was assessed based on the scale and method used in previous studies[57,58]. CD3-stained sections were processed using the cell count tool in Image J software.

RNA Isolation and NanoString Analysis

Total RNA was isolated from flash frozen mouse kidney tissue using the RNeasy Mini Kit (Qiagen). RNA integrity was assessed using the Agilent 2100 bioanalyzer and Agilent RNA 6000 Nano reagents (Agilent Technologies). Only RNA with

RIN>5 was used in our NanoString analyses. The code set for NanoString analysis was established based on literature searches of pathways that are important in determining therapeutic targets for the treatment of CKD. NanoString data was normalized against 7 housekeeping genes, IPO8, GUSB, TBP, YWHAZ, ACTB, GAPDH and RPLP2. P-values were corrected for multiple comparisons using the Benjamin-Hochberg procedure in R programming language and heat maps were produced using Java Treeview software. Fold changes were log-transformed and hierarchical gene clustering was performed on heat maps using Euclidean distance and complete linkage. On the heat maps, each column represents a time point or the effect of 4-PBA or CHOP deficiency on the 21 day Ang II/DOCA salt model. Each box represents the fold change for a particular gene in Ang II/DOCA salt-treated mice compared to their respective sham controls at the designated time point, treatment, or genotype manipulation. Fold changes were $\log_2$-transformed. Down-regulation is denoted by blue and up-regulation is denoted by red.

Statistical Analysis

Data are shown as the mean±standard error of the mean. Student's T-test was used to analyze difference between groups. Differences among multiple groups were analyzed with analysis of variance followed by post-hoc Bonferroni tests in Graphpad Prism 5.0. A P-value of ≤ 0.05 was considered significant.

Figure Legends

FIGURE 1: ***Effect of 4-PBA treatment on the development of hypertensive proteinuria.*** Mice treated with Ang II/DOCA salt showed a significant increase in (A) systolic and (B) diastolic blood pressures at the day 7 (7D), 14 (14D), 18 (18D) and 21 (21D) time points (n=5 per group) compared to their corresponding SHAM controls (n=3-5 per group). Ang II/DOCA salt animals treated with 4-PBA (n=5) did not show any change in (A) systolic and (B) diastolic blood pressure. (C) Total 24 h urinary albumin excretion was significantly increased by Ang II/DOCA salt at all time points, 7D (n=5), 14D (n=5), 18D (n=4) and 21D (n=6) compared to SHAM controls (n=5-6), and was significantly reduced by 4-PBA treatment (n=6). Normalized total counts for endocytic receptor mRNA (D) cubilin and (E) megalin show a significant increase with Ang II/DOCA salt (n=3) treatment, and a further significant increase with 4-PBA treatment (n=4) compared to SHAM controls (n=3). (F, G) Protein levels of cubilin in whole kidney tissue lysates were significantly increased with Ang II/DOCA salt treatment (n=3) and showed significantly higher levels with 4-PBA treatment (n=3). (H, I) There was no change in kidney megalin protein levels with Ang II/DOCA salt treatment or 4-PBA treatment (n=3 per group). (J, K) Membrane extracts from kidney tissue lysates showed significantly increased levels of membrane-embedded cubilin in the Ang II/DOCA salt group treated with 4-PBA (n=3 per group). (L, M) 4-PBA significantly decreased glomerulosclerosis in Ang II/DOCA salt mice (n=3 per group). (N, O) An increase in protein cast formation (arrows) was observed in Ang II/DOCA salt mice at all time points (n=4-5 per group)

compared to their respective SHAMs (n=5-6), and is decreased with 4-PBA treatment (n=6). 21D SHAM (n=5) is used as a representative image for all shams. * denotes significantly different than the corresponding SHAM; # indicates significantly different in the D21 Ang II/DOCA salt + 4-PBA compared to day 21 Ang II/DOCA salt. Scale bars=100 μm in (L) and 200 μm in (N).

FIGURE 2: ***Effect of 4-PBA treatment on the UPR activation.*** (A) Hierarchical clustering of ER stress and apoptotic genes is demonstrated using a heat map. Fold changes represent the changes in gene expression with Ang II/DOCA salt treatment at days 7 (7D; n=4), 14 (14D; n=5), 18 (18D; n=3), 21 (21D; n=5) and 21D+4-PBA (n=5) compared to their respective sham-operated controls. (B, D) CHOP and (C, E) phosphorylated IRE1α staining (60X) in the kidney was increased by Ang II/DOCA salt (n=5 for 7D, 14D and 21D, n=4 for 18D), as indicated by arrows, and inhibited by 4-PBA treatment (n=5). The 21D SHAM group (n=5 for cortex, n=3 for medulla) is representative of all shams. * indicates that the Ang II/DOCA salt group is significantly different than corresponding SHAM at that time point; # indicates that the 21D+4-PBA is significantly different than the 21D Ang II/DOCA salt group. Scale bars=100 μm in (B) and (C).

FIGURE 3: ***Effect of 4-PBA treatment on renal fibrosis.*** (A) Hierarchical clustering of fibrotic genes is demonstrated in a heat map. Fold changes represent the changes in gene expression with Ang II/DOCA salt treatment at days 7 (7D; n=4), 14 (14D; n=5), 18 (18D; n=3), 21 (21D; n=5) and 21D+4-PBA (n=5)

compared to their respective sham-operated controls. (B, D) α-smooth muscle actin staining (arrows) (20X) is increased at all timepoints (n=4 per group). (C, E) Collagen deposition (arrows), demonstrated using picrosirius red staining (20X), was significantly elevated at all timepoints (n=5 for 7D, 14D and 18D and n=4 for 21D). 4-PBA treatment (n=3) significantly decreased both collagen and α-smooth muscle actin deposition in response to Ang II/DOCA salt. Only the representative sham, 21D SHAM group (n=4 for cortex, n=3 for medulla), is shown. * indicates that the Ang II/DOCA salt treatment is significantly different than corresponding sham at that time point; # indicates that the 21D+4-PBA group is significantly different than the 21D Ang II/DOCA salt group. Scale bars=200 μm in (B) and (C).

FIGURE 4: ***Effect of 4-PBA treatment on renal inflammation.*** (A) A heat map demonstrates hierarchical clustering of inflammatory genes. Fold changes represent the changes in gene expression with Ang II/DOCA salt treatment at days 7 (7D; n=4), 14 (14D; n=5), 18 (18D; n=3), 21 (21D; n=5) and 21D+4-PBA (n=5), compared to their respective sham-operated controls. (B, D) F4/80 staining (40X; arrows) shows an increase in $F4/80^{+}$ macrophage infiltration at 14D (n=4), 18D (n=5) and 21D (n=5), but not at 7D (n=6). (C, E) CD3 staining (60X; arrows) demonstrates significant T-cell infiltration at all time points (n=4 per group). 4-PBA treatment (n=3) significantly decreased macrophage and T-cell infiltration in response to Ang II/DOCA salt. Only the representative 21D SHAM is included in the figure (n=5 for F4/80 staining, n=4 for CD3 staining). * indicates that the Ang

II/DOCA salt is significantly different than corresponding sham at that time point (n=4-5 per group); # indicates that the 21D+4-PBA is significantly different than the 21D Ang II/DOCA salt group. Scale bars= 100 μm in (B) and (C).

FIGURE 5: ***Effect of CHOP knockout on the development of hypertensive proteinuria.*** Both wild type (WT) (n=6) and $CHOP^{-/-}$ (n=5) mice treated with the CKD model experienced an increase in (A) systolic and (B) diastolic blood pressures, compared to their respective SHAM controls (n=6 for WT SHAM and n=5 for $CHOP^{-/-}$ SHAM). (C) Although $CHOP^{-/-}$ mice (n=5) showed an increase in albuminuria with CKD development compared to $CHOP^{-/-}$ SHAM mice (n=6), they had significantly lower albuminuria compared to WT mice (n=7). (D) Nephrin mRNA levels increase with Ang II/DOCA salt treatment compared to sham controls (n=3 per group) and are significantly higher in $CHOP^{-/-}$ animals treated with Ang II/DOCA salt (n=5) compared to WT Ang II/DOCA salt animals (n=5). (E, F) Protein levels of nephrin were significantly increased in whole kidney tissue lysates (n=3 per group) in $CHOP^{-/-}$ mice. (G, H) Significantly lower levels of GADD34 were observed in $CHOP^{-/-}$ mice. (I, J) $CHOP^{-/-}$ mice (n=5) showed significantly lower glomerular sclerosis (arrows) compared to WT mice (n=5) in response to Ang II/DOCA salt. (K, L, M) Protein cast formation (arrows; 20X) demonstrates less damage in $CHOP^{-/-}$ mice (n=5) in response to Ang II/DOCA salt compared to treated WT mice (n=5). There was no difference in glomerular score or protein cast formation between $CHOP^{-/-}$ sham (n=6) and WT sham (n=6). * indicates significantly different than the

respective sham-operated controls; # indicates significant difference between the CHOP$^{-/-}$ Ang II/DOCA salt mice compared to WT Ang II/DOCA salt mice. Scale bars= 50 μm in (I) and 200 μm (K).

FIGURE 6: ***Effect of CHOP deficiency on UPR, fibrosis, and inflammatory gene expression.*** Heat maps demonstrate hierarchical clustering of (A) UPR, (B) fibrotic, and (C) inflammatory genes. "WT" column represents fold changes in gene expression with Ang II/DOCA salt treatment in wild type (WT; n=6) compared to WT SHAM (n=3). "CHOP$^{-/-}$" column represents fold changes in treated CHOP$^{-/-}$ mice (n=5) compared to CHOP$^{-/-}$ sham mice (n=3). Genes included in these heat maps are those that were significantly regulated in WT Ang II/DOCA salt-treated mice compared to WT sham at day 21. CHOP deficiency attenuated the upregulation of important pathways underlying CKD. * indicates that Ang II/DOCA salt CHOP$^{-/-}$ is significantly different than corresponding sham in CHOP$^{-/-}$ mice; # indicates that the gene is regulated in the opposite direction in CHOP$^{-/-}$ Ang II/DOCA salt mice compared to WT Ang II/DOCA salt mice.

FIGURE 7: ***Effect of CHOP deficiency on the development of fibrosis.*** (A, B and C) α-smooth muscle actin staining (arrows; 20X) is reduced with CHOP deficiency. Extracellular matrix deposition was significantly increased by Ang II/DOCA salt in wild type (WT) mice (n=5), but not in CHOP$^{-/-}$ mice (n=5). * indicates that the Ang II/DOCA salt is significantly different than corresponding sham; #

indicates that the CHOP$^{-/-}$ mice are significantly different than WT mice. Scale bars= 200 μm in (A).

FIGURE 8: ***Effect of CHOP deficiency on the development of inflammation.*** (A, B and C) F4/80 staining (arrows; 40X) demonstrates that macrophage infiltration was significantly increased by Ang II/DOCA salt in wild type (WT; n=4) but not in CHOP$^{-/-}$ mice (n=5), compared to their corresponding sham controls (n=4). * indicates that the Ang II/DOCA salt mice are significantly different than corresponding sham; # indicates that the CHOP$^{-/-}$ mice are significantly different than WT mice. Scale bars= 100 μm in (A).

FIGURE 9: ***Similarities in pathology between human and murine chronic kidney disease.*** This Ang II/DOCA salt mouse model of chronic kidney disease (CKD) produces (A) protein cast formation, demonstrated by periodic acid-Schiff staining, and (B) fibrosis, demonstrated by Masson's trichrome staining, at a comparable level to the kidney damage found in hypertensive nephrosclerotic human patients. Human CKD patients (n=2) show an increase in medullary (C) phosphorylated IRE1α and (D) CHOP staining (arrows) compared to non-CKD patients. Scale bars= 100 μm in (A-D).

FIGURE 1:

A.

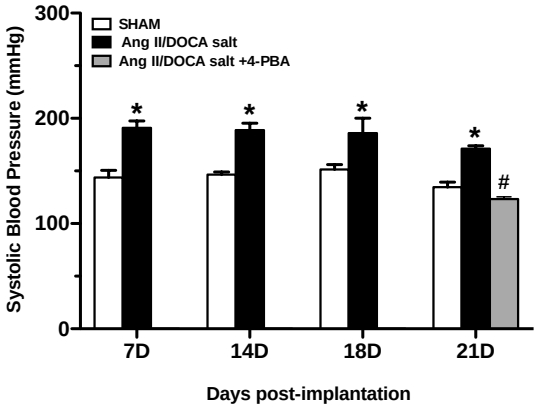
SHAM
Ang II/DOCA salt
Ang II/DOCA salt +4-PBA
Systolic Blood Pressure (mmHg)
300
200
100
0
*
*
*
*
#
7D
14D
18D
21D
Days post-implantation

B.

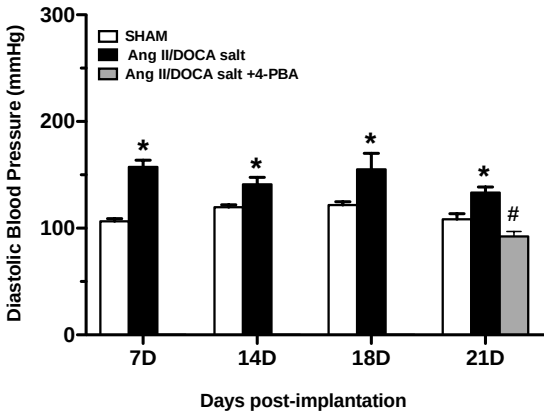
SHAM
Ang II/DOCA salt
Ang II/DOCA salt +4-PBA
Diastolic Blood Pressure (mmHg)
300
200
100
0
*
*
*
*
#
7D
14D
18D
21D
Days post-implantation

C.

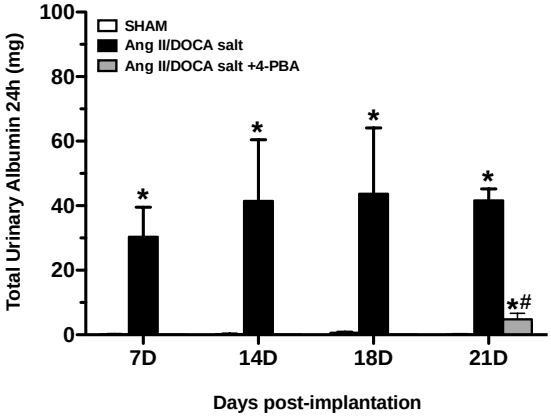
SHAM
Ang II/DOCA salt
Ang II/DOCA salt +4-PBA
Total Urinary Albumin 24h (mg)
100
80
60
40
20
0
*
*
*
*
*#
7D
14D
18D
21D
Days post-implantation

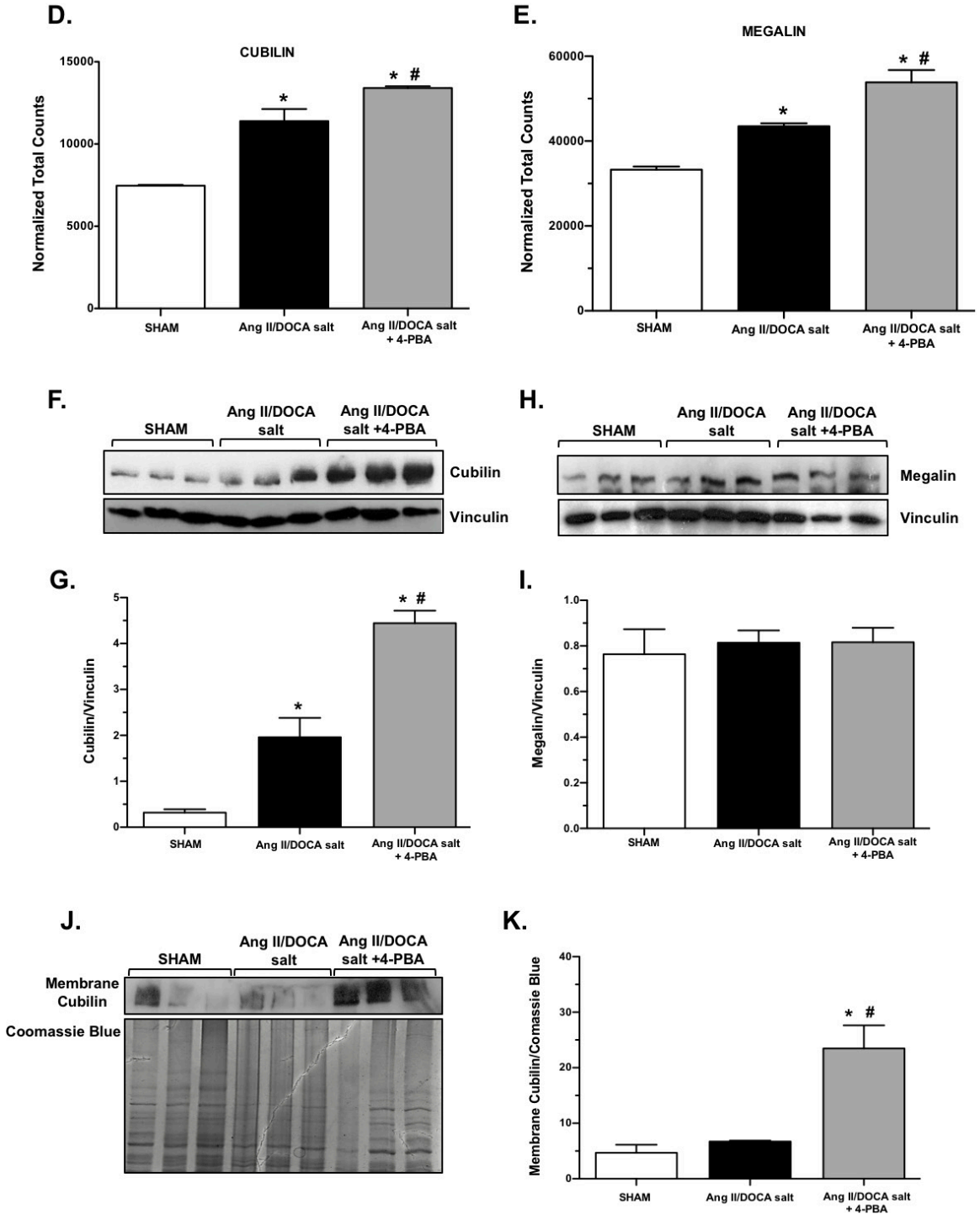
D.
CUBILIN
Normalized Total Counts
15000
10000
5000
0
*
* #
SHAM
Ang II/DOCA salt
Ang II/DOCA salt + 4-PBA
E.
MEGALIN
Normalized Total Counts
60000
40000
20000
0
*
* #
SHAM
Ang II/DOCA salt
Ang II/DOCA salt + 4-PBA
F.
SHAM
Ang II/DOCA salt
Ang II/DOCA salt +4-PBA
Cubilin
Vinculin
H.
SHAM
Ang II/DOCA salt
Ang II/DOCA salt +4-PBA
Megalin
Vinculin
G.
Cubilin/Vinculin
5
4
3
2
1
0
*
* #
SHAM
Ang II/DOCA salt
Ang II/DOCA salt + 4-PBA
I.
Megalin/Vinculin
1.0
0.8
0.6
0.4
0.2
0.0
SHAM
Ang II/DOCA salt
Ang II/DOCA salt + 4-PBA
J.
SHAM
Ang II/DOCA salt
Ang II/DOCA salt +4-PBA
Membrane Cubilin
Coomassie Blue
K.
Membrane Cubilin/Comassie Blue
40
30
20
10
0
* #
SHAM
Ang II/DOCA salt
Ang II/DOCA salt + 4-PBA

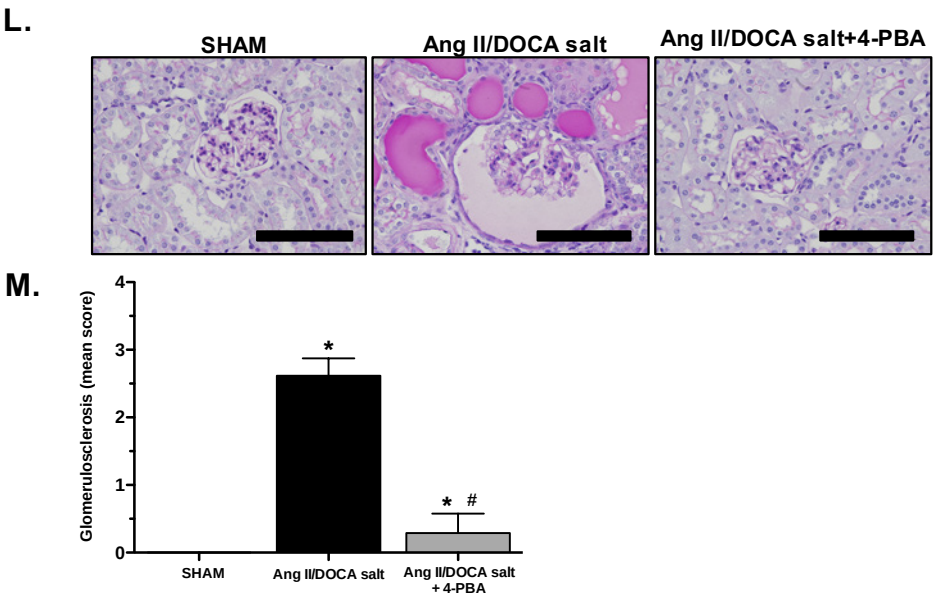
L.
SHAM
Ang II/DOCA salt
Ang II/DOCA salt+4-PBA
M.
Glomerulosclerosis (mean score)
SHAM
Ang II/DOCA salt
Ang II/DOCA salt + 4-PBA
N.
SHAM
7D
21D
21D+4-PBA
PAS staining
Cortex
Medulla
O.
Area density of protein casts (%)
Cortex
Medulla
SHAM
7D
14D
18D
21D
21D+4-PBA

FIGURE 2:

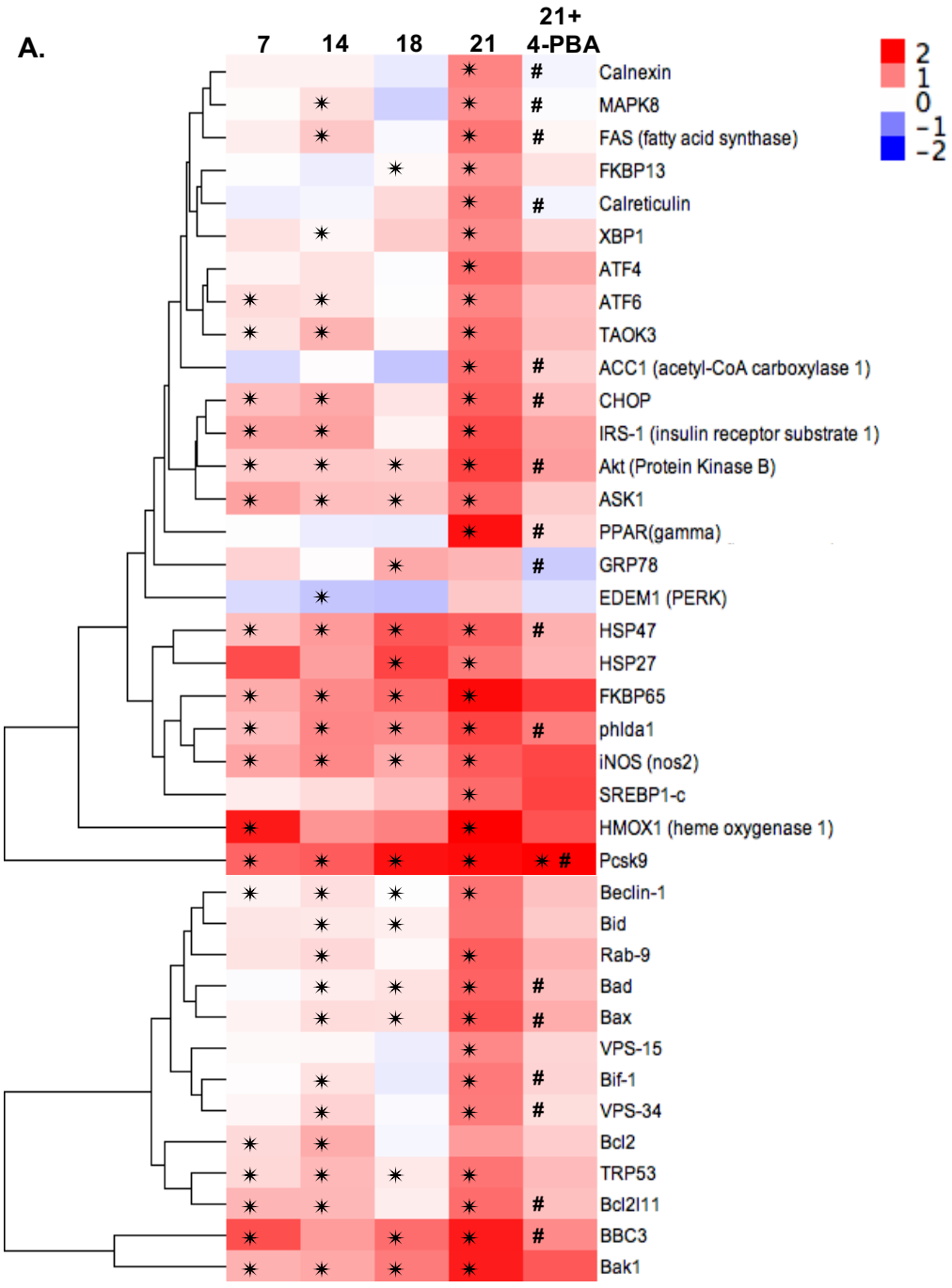
A.
7
14
18
21
21+ 4-PBA
2
1
0
-1
-2
Calnexin
MAPK8
FAS (fatty acid synthase)
FKBP13
Calreticulin
XBP1
ATF4
ATF6
TAOK3
ACC1 (acetyl-CoA carboxylase 1)
CHOP
IRS-1 (insulin receptor substrate 1)
Akt (Protein Kinase B)
ASK1
PPAR(gamma)
GRP78
EDEM1 (PERK)
HSP47
HSP27
FKBP65
phlda1
iNOS (nos2)
SREBP1-c
HMOX1 (heme oxygenase 1)
Pcsk9
Beclin-1
Bid
Rab-9
Bad
Bax
VPS-15
Bif-1
VPS-34
Bcl2
TRP53
Bcl2l11
BBC3
Bak1

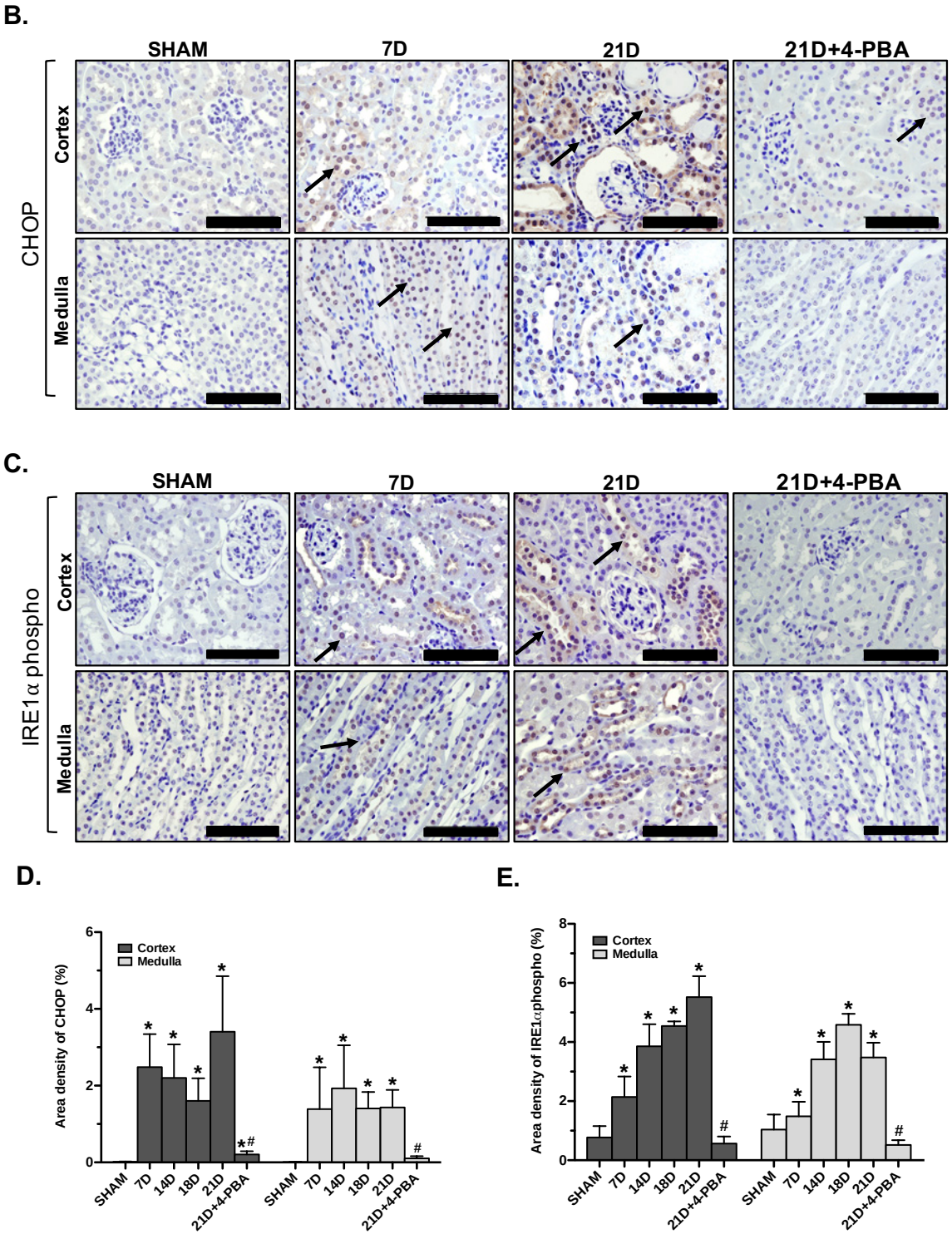
B.
SHAM
7D
21D
21D+4-PBA
CHOP
Cortex
Medulla
C.
SHAM
7D
21D
21D+4-PBA
IRE1α phospho
Cortex
Medulla
D.
Area density of CHOP (%)
Cortex
Medulla
SHAM
7D
14D
18D
21D
21D+4-PBA
E.
Area density of IRE1αphospho (%)
Cortex
Medulla
SHAM
7D
14D
18D
21D
21D+4-PBA

FIGURE 3:

A.

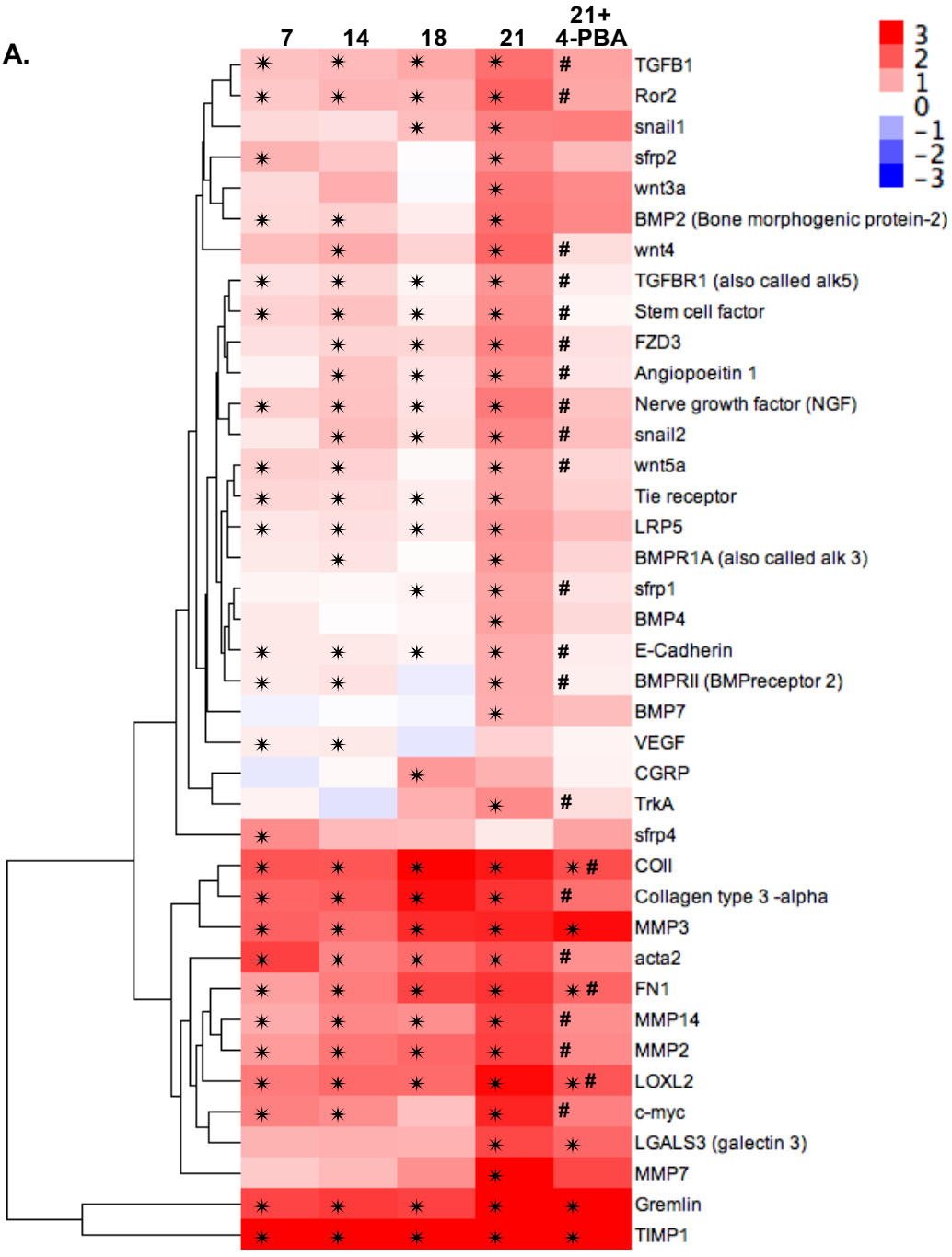
7
14
18
21
21+ 4-PBA
3
2
1
0
-1
-2
-3
TGFB1
Ror2
snail1
sfrp2
wnt3a
BMP2 (Bone morphogenic protein-2)
wnt4
TGFBR1 (also called alk5)
Stem cell factor
FZD3
Angiopoeitin 1
Nerve growth factor (NGF)
snail2
wnt5a
Tie receptor
LRP5
BMPR1A (also called alk 3)
sfrp1
BMP4
E-Cadherin
BMPRII (BMPreceptor 2)
BMP7
VEGF
CGRP
TrkA
sfrp4
COII
Collagen type 3 -alpha
MMP3
acta2
FN1
MMP14
MMP2
LOXL2
c-myc
LGALS3 (galectin 3)
MMP7
Gremlin
TIMP1

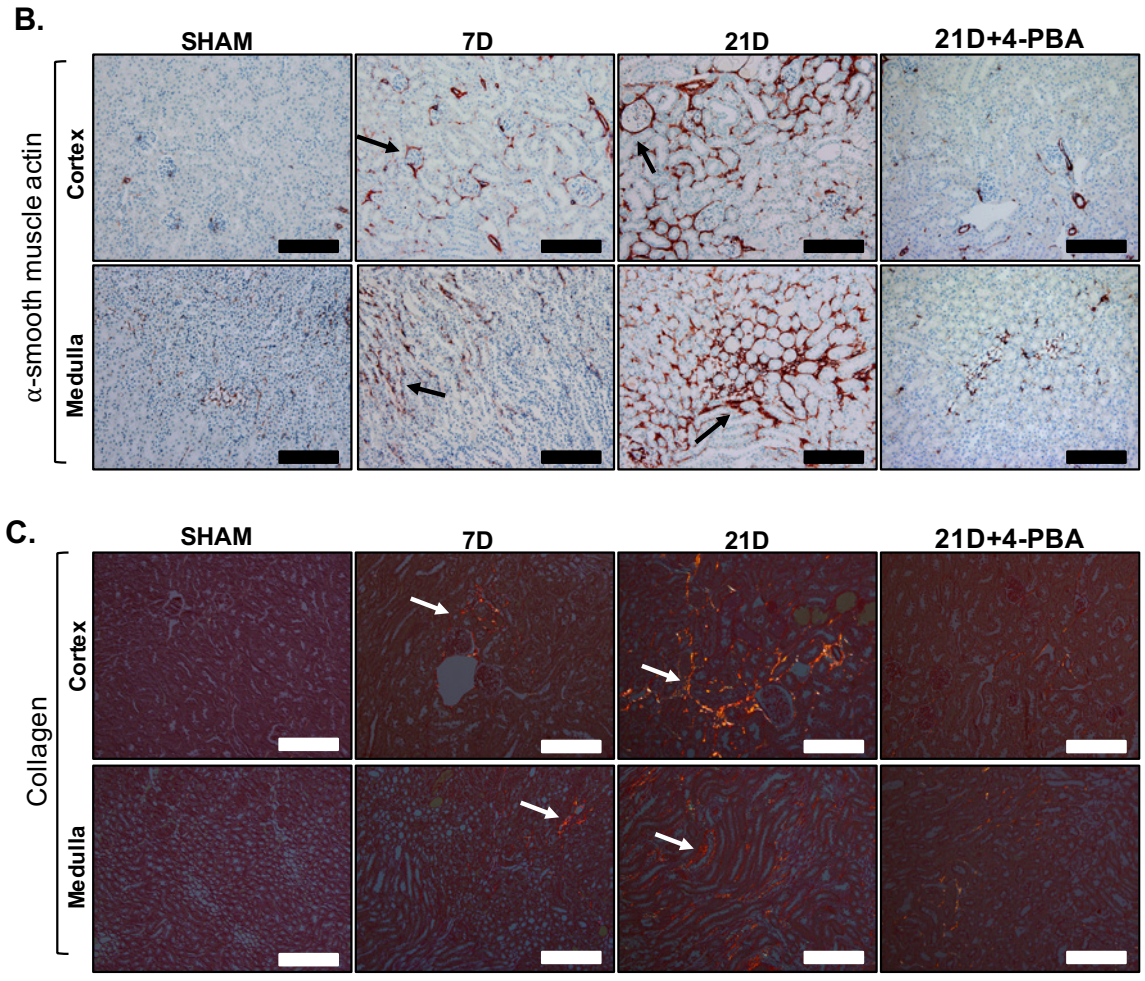
B.
SHAM
7D
21D
21D+4-PBA
α-smooth muscle actin
Cortex
Medulla
C.
SHAM
7D
21D
21D+4-PBA
Collagen
Cortex
Medulla
D.
Area density of α-smooth muscle actin (%)
Cortex
Medulla
SHAM
7D
14D
18D
21D
21D+4-PBA
E.
Area density of Collagen (%)
Cortex
Medulla
SHAM
7D
14D
18D
21D
21D+4-PBA

FIGURE 4:

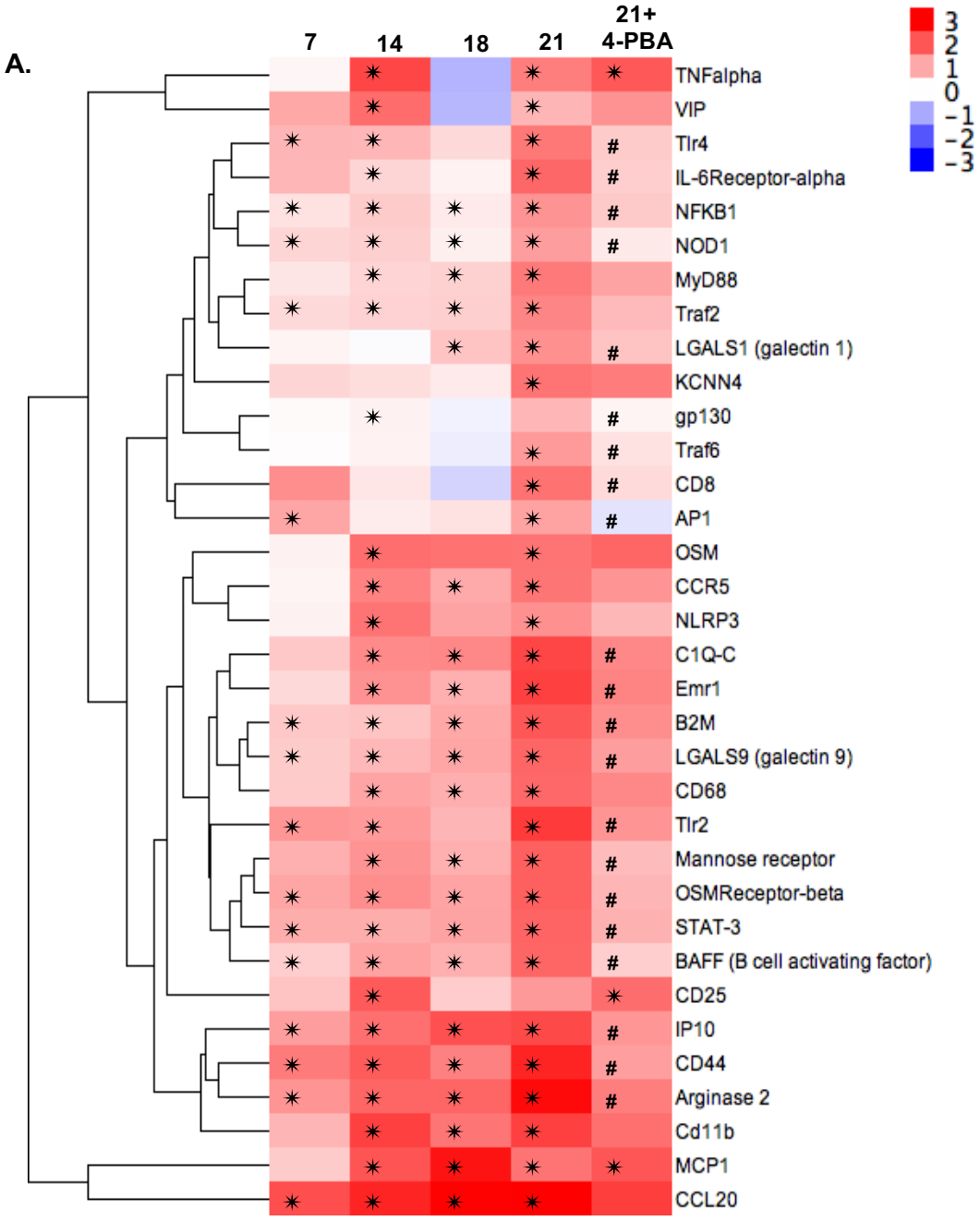
A.
7
14
18
21
21+ 4-PBA
3
2
1
0
-1
-2
-3
TNFalpha
VIP
Tlr4
IL-6Receptor-alpha
NFKB1
NOD1
MyD88
Traf2
LGALS1 (galectin 1)
KCNN4
gp130
Traf6
CD8
AP1
OSM
CCR5
NLRP3
C1Q-C
Emr1
B2M
LGALS9 (galectin 9)
CD68
Tlr2
Mannose receptor
OSMReceptor-beta
STAT-3
BAFF (B cell activating factor)
CD25
IP10
CD44
Arginase 2
Cd11b
MCP1
CCL20

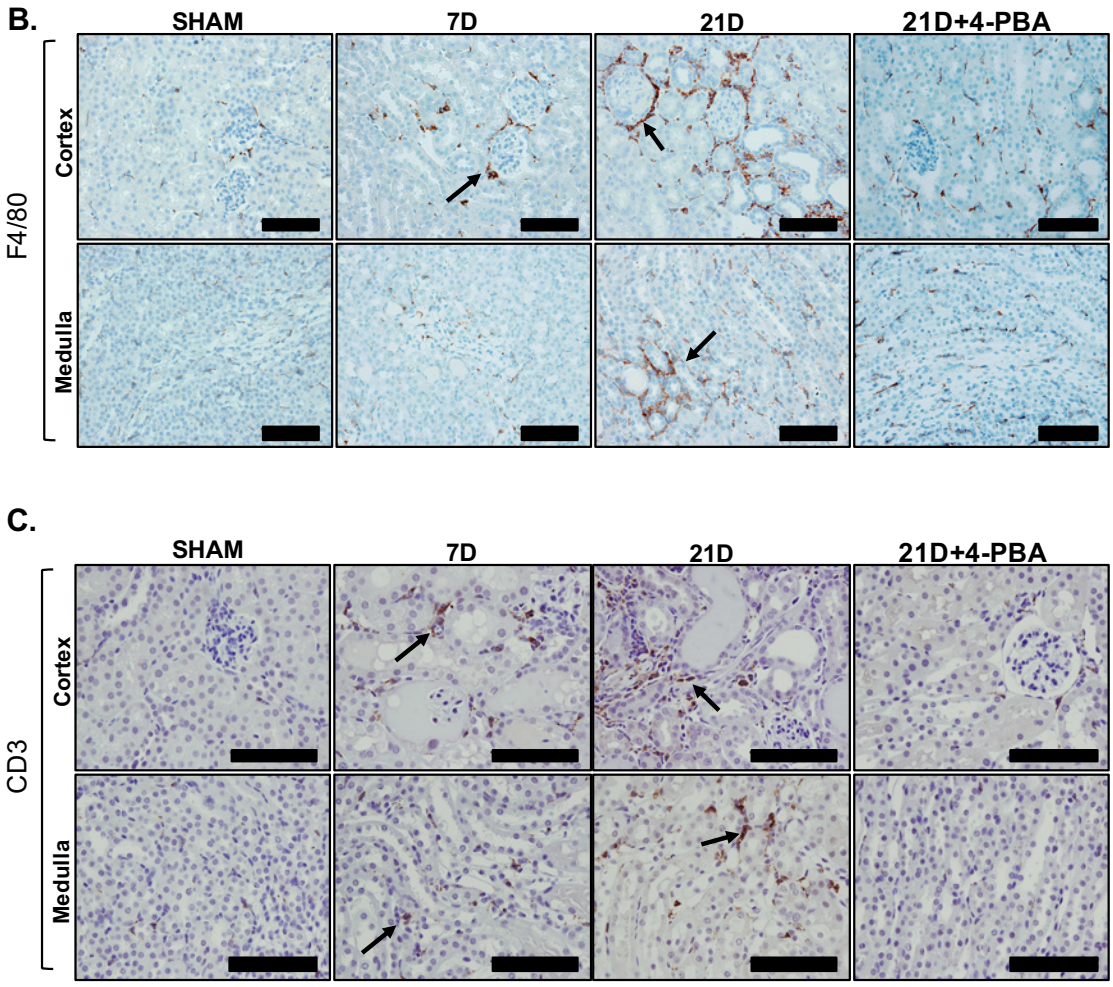
B.
SHAM
7D
21D
21D+4-PBA
F4/80
Cortex
Medulla
C.
SHAM
7D
21D
21D+4-PBA
CD3
Cortex
Medulla
D.
Area density of F4/80+ cells (%)
Cortex
Medulla
SHAM
7D
14D
18D
21D
21D+4-PBA
E.
CD3 + cells/mm2
Cortex
Medulla
SHAM
7D
14D
18D
21D
21D+4-PBA

FIGURE 5:

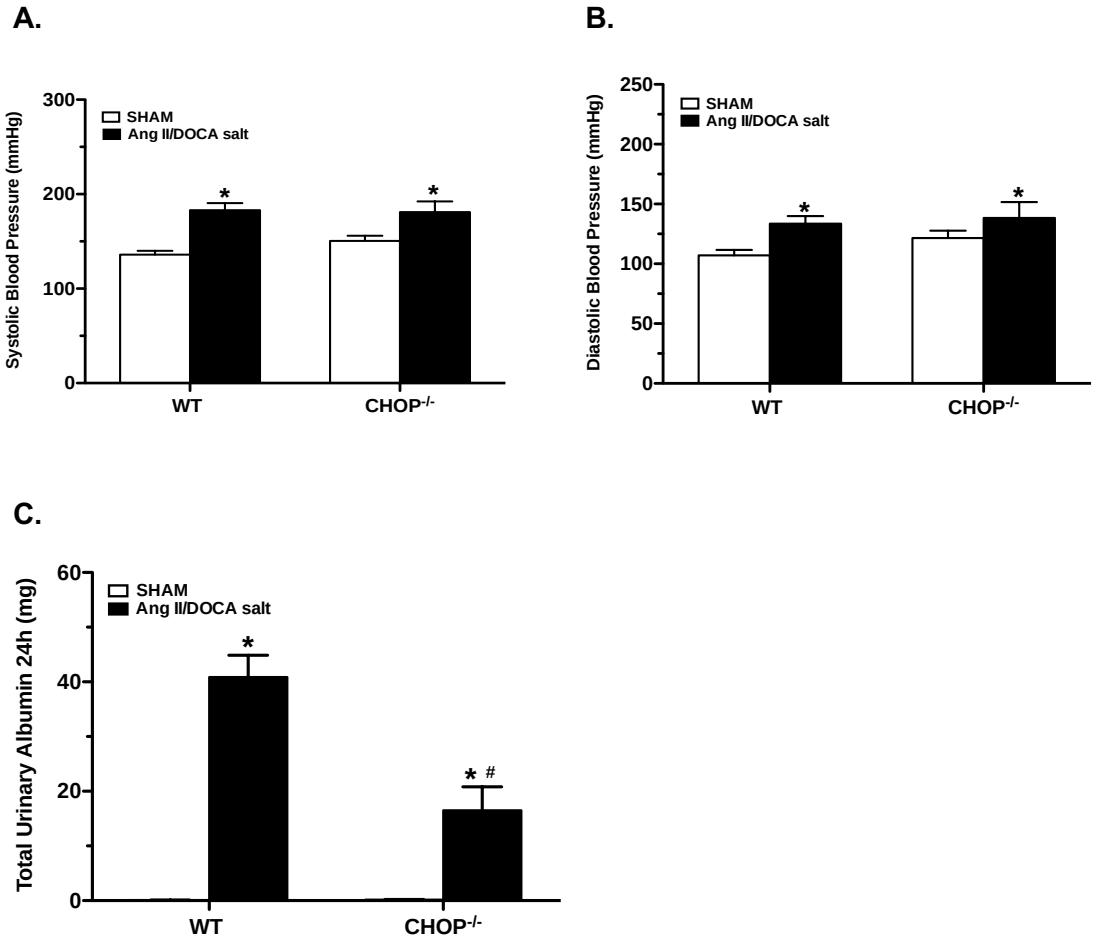
A.
Systolic Blood Pressure (mmHg)
300
200
100
0
SHAM
Ang II/DOCA salt
*
*
WT
CHOP-/-
B.
Diastolic Blood Pressure (mmHg)
250
200
150
100
50
0
SHAM
Ang II/DOCA salt
*
*
WT
CHOP-/-
C.
Total Urinary Albumin 24h (mg)
60
40
20
0
SHAM
Ang II/DOCA salt
*
* #
WT
CHOP-/-

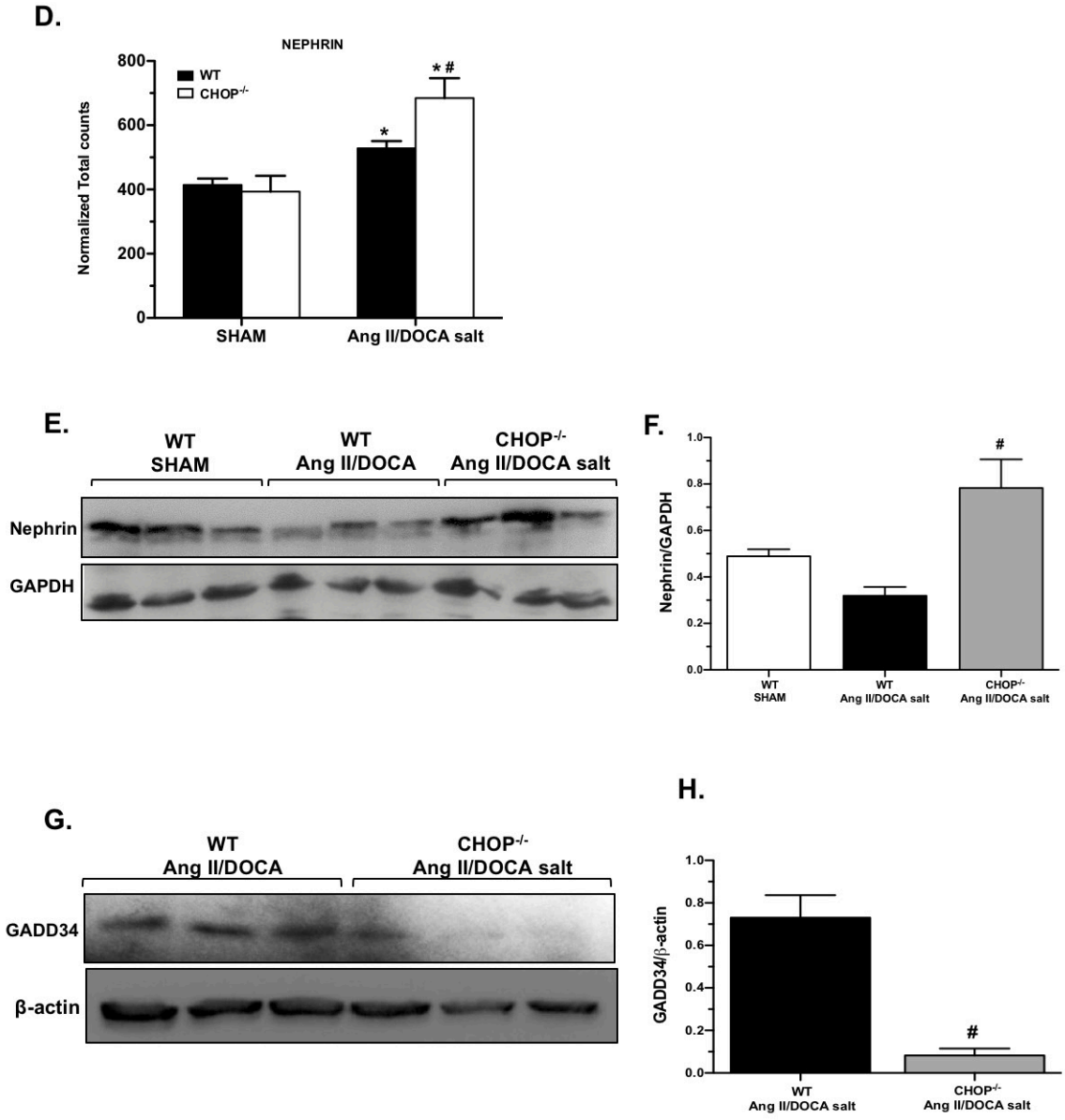
D.
NEPHRIN
WT
CHOP-/-
Normalized Total counts
800
600
400
200
0
*
* #
SHAM
Ang II/DOCA salt
E.
WT
SHAM
WT
Ang II/DOCA
CHOP-/-
Ang II/DOCA salt
Nephrin
GAPDH
F.
Nephrin/GAPDH
1.0
0.8
0.6
0.4
0.2
0.0
#
WT
SHAM
WT
Ang II/DOCA salt
CHOP-/-
Ang II/DOCA salt
G.
WT
Ang II/DOCA
CHOP-/-
Ang II/DOCA salt
GADD34
β-actin
H.
GADD34/β-actin
1.0
0.8
0.6
0.4
0.2
0.0
#
WT
Ang II/DOCA salt
CHOP-/-
Ang II/DOCA salt

I.

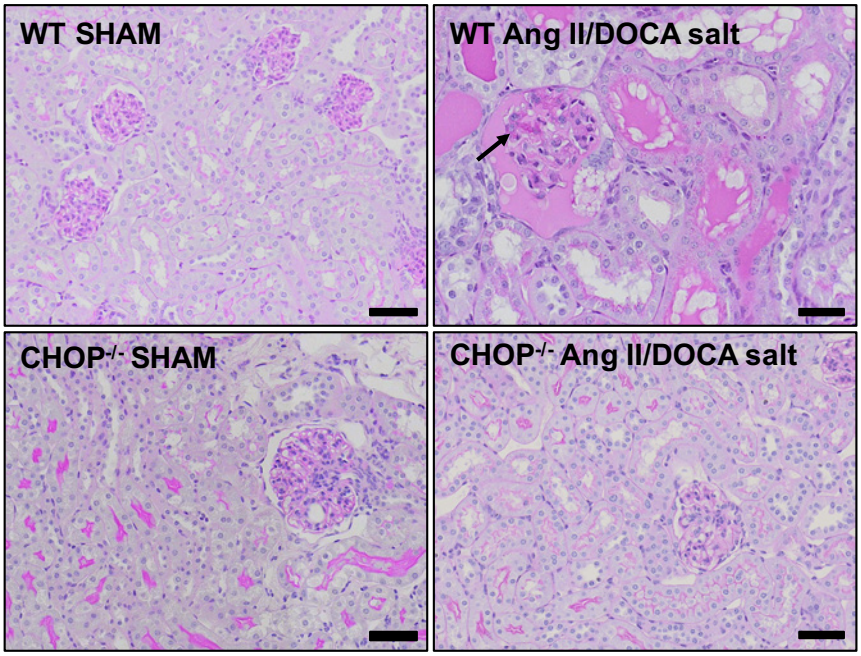
WT SHAM
WT Ang II/DOCA salt
CHOP-/- SHAM
CHOP-/- Ang II/DOCA salt

J.

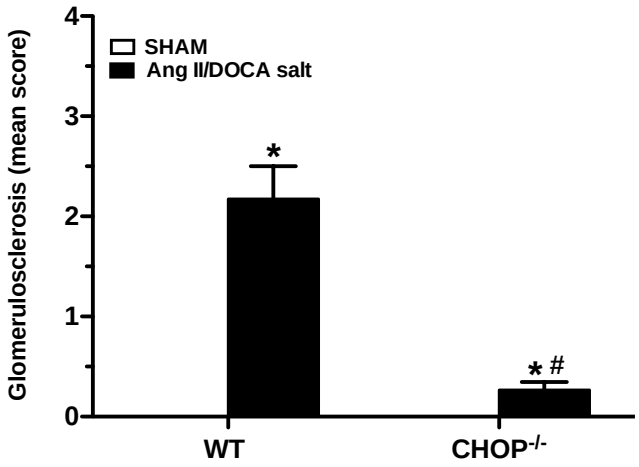
Glomerulosclerosis (mean score)
SHAM
Ang II/DOCA salt
0
1
2
3
4
*
* #
WT
CHOP-/-

K.

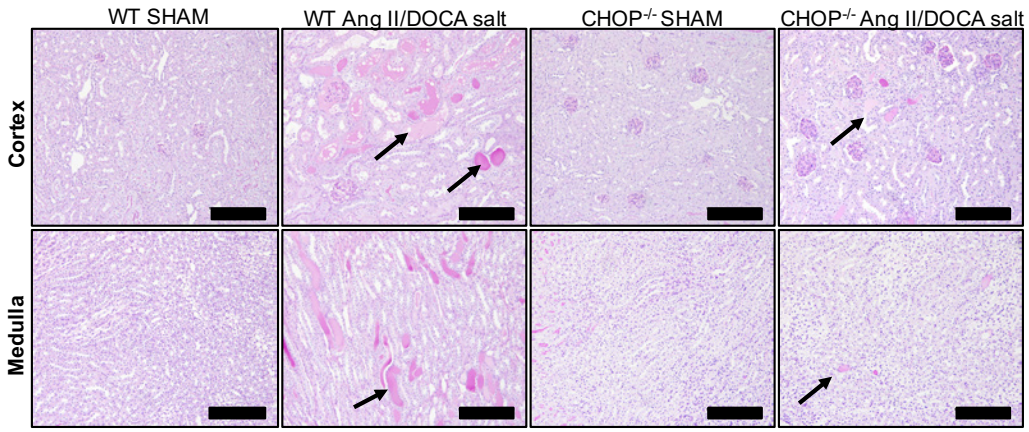
WT SHAM
WT Ang II/DOCA salt
CHOP-/- SHAM
CHOP-/- Ang II/DOCA salt
Cortex
Medulla

L.

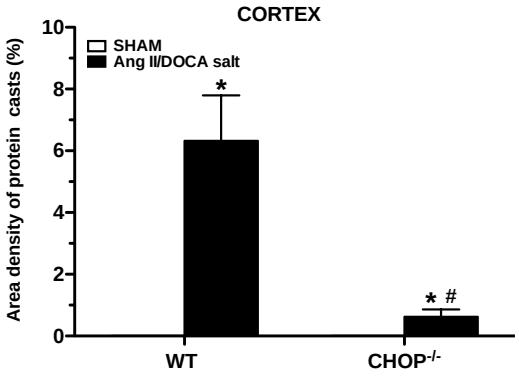
CORTEX
SHAM
Ang II/DOCA salt
Area density of protein casts (%)
10
8
6
4
2
0
*
* #
WT
CHOP-/-

M.

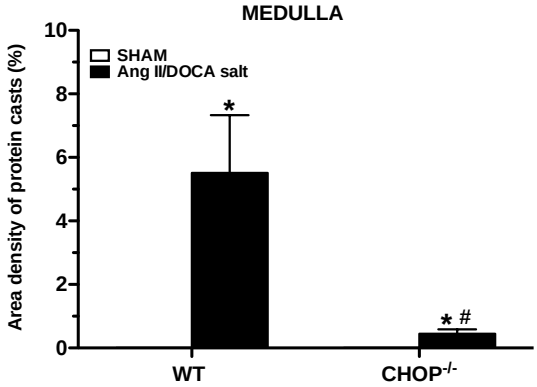
MEDULLA
SHAM
Ang II/DOCA salt
Area density of protein casts (%)
10
8
6
4
2
0
*
* #
WT
CHOP-/-

FIGURE 6:

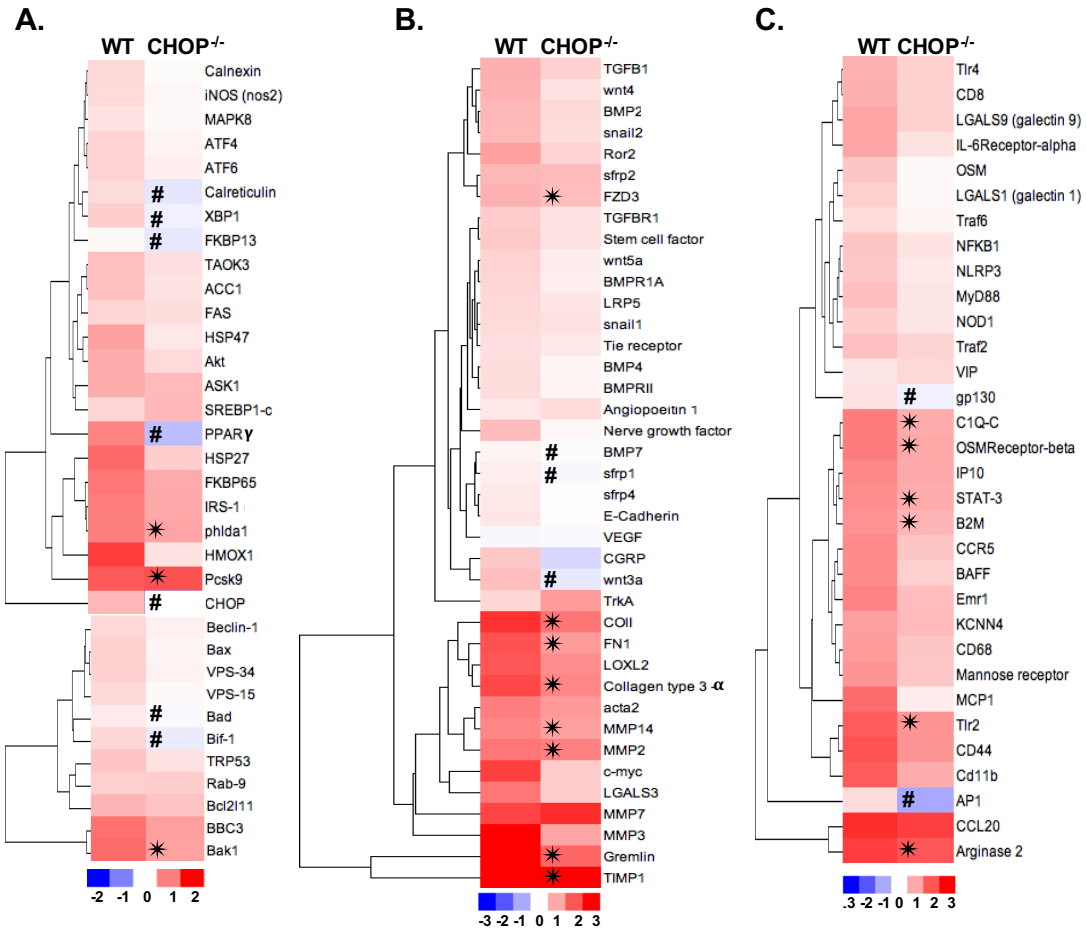
A.
WT CHOP-/-
Calnexin
iNOS (nos2)
MAPK8
ATF4
ATF6
Calreticulin
XBP1
FKBP13
TAOK3
ACC1
FAS
HSP47
Akt
ASK1
SREBP1-c
PPARγ
HSP27
FKBP65
IRS-1
phlda1
HMOX1
Pcsk9
CHOP
Beclin-1
Bax
VPS-34
VPS-15
Bad
Bif-1
TRP53
Rab-9
Bcl2l11
BBC3
Bak1
-2 -1 0 1 2
B.
WT CHOP-/-
TGFB1
wnt4
BMP2
snail2
Ror2
sfrp2
FZD3
TGFBR1
Stem cell factor
wnt5a
BMPR1A
LRP5
snail1
Tie receptor
BMP4
BMPRII
Angiopoietin 1
Nerve growth factor
BMP7
sfrp1
sfrp4
E-Cadherin
VEGF
CGRP
wnt3a
TrkA
COII
FN1
LOXL2
Collagen type 3 -α
acta2
MMP14
MMP2
c-myc
LGALS3
MMP7
MMP3
Gremlin
TIMP1
-3 -2 -1 0 1 2 3
C.
WT CHOP-/-
Tlr4
CD8
LGALS9 (galectin 9)
IL-6Receptor-alpha
OSM
LGALS1 (galectin 1)
Traf6
NFKB1
NLRP3
MyD88
NOD1
Traf2
VIP
gp130
C1Q-C
OSMReceptor-beta
IP10
STAT-3
B2M
CCR5
BAFF
Emr1
KCNN4
CD68
Mannose receptor
MCP1
Tlr2
CD44
Cd11b
AP1
CCL20
Arginase 2
-3 -2 -1 0 1 2 3

FIGURE 7:

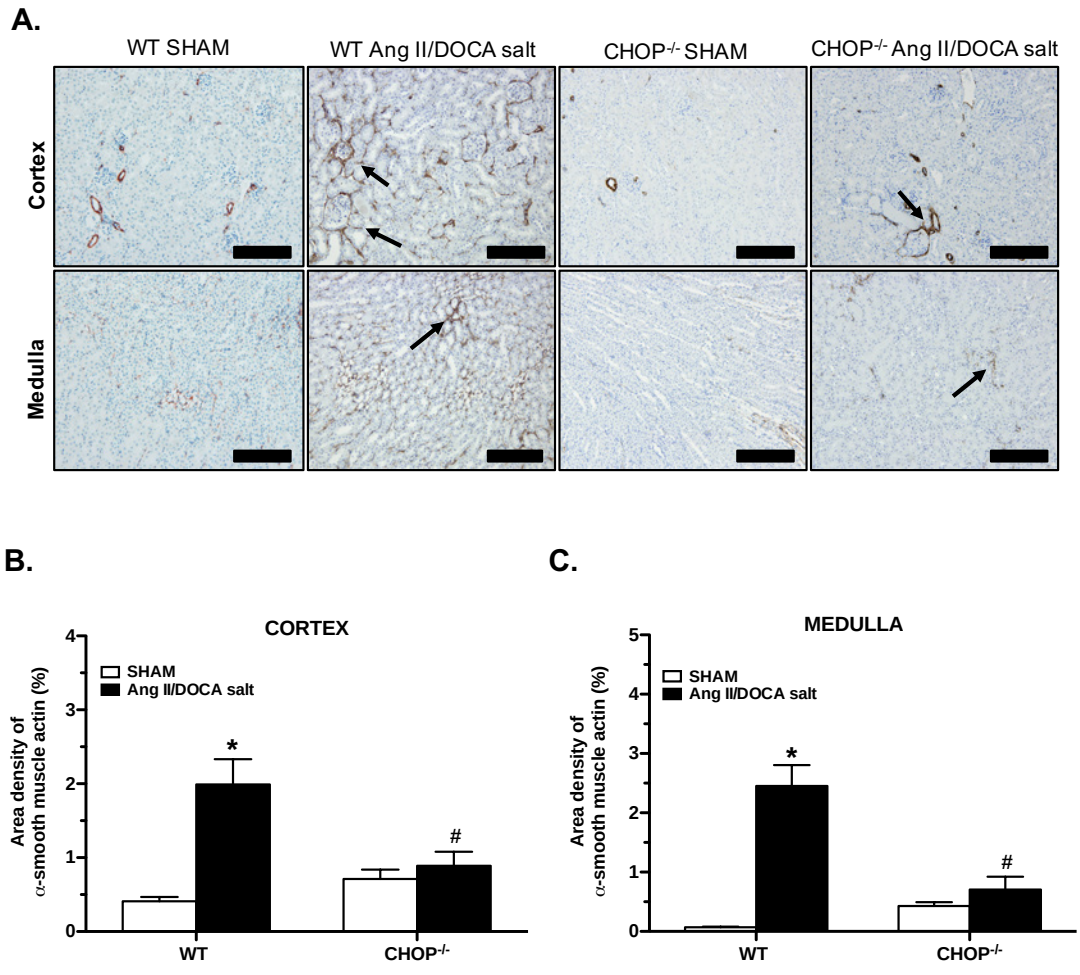
A.
WT SHAM
WT Ang II/DOCA salt
CHOP-/- SHAM
CHOP-/- Ang II/DOCA salt
Cortex
Medulla
B.
CORTEX
SHAM
Ang II/DOCA salt
Area density of α-smooth muscle actin (%)
WT
CHOP-/-
C.
MEDULLA
SHAM
Ang II/DOCA salt
Area density of α-smooth muscle actin (%)
WT
CHOP-/-

FIGURE 8:

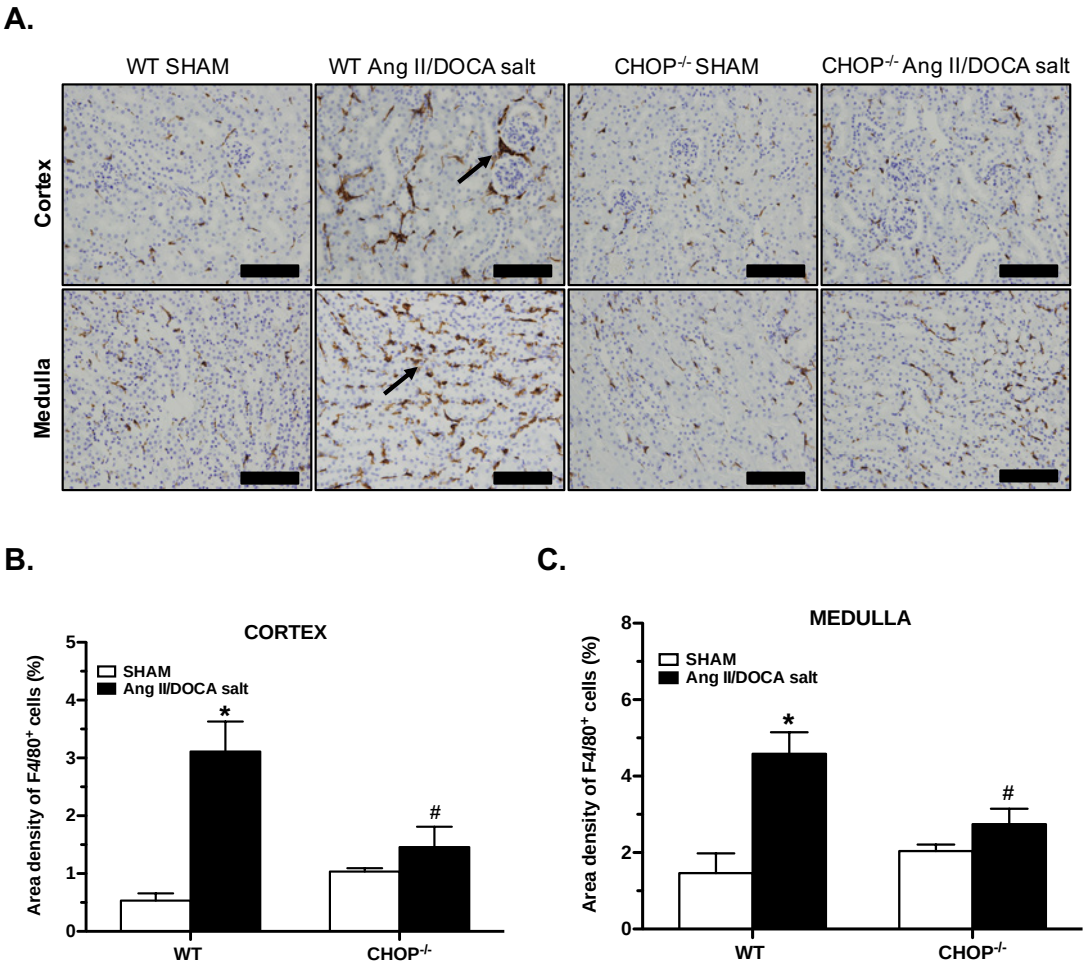
A.
WT SHAM
WT Ang II/DOCA salt
CHOP-/- SHAM
CHOP-/- Ang II/DOCA salt
Cortex
Medulla
B.
CORTEX
SHAM
Ang II/DOCA salt
Area density of F4/80+ cells (%)
WT
CHOP-/-
C.
MEDULLA
SHAM
Ang II/DOCA salt
Area density of F4/80+ cells (%)
WT
CHOP-/-

FIGURE 9:

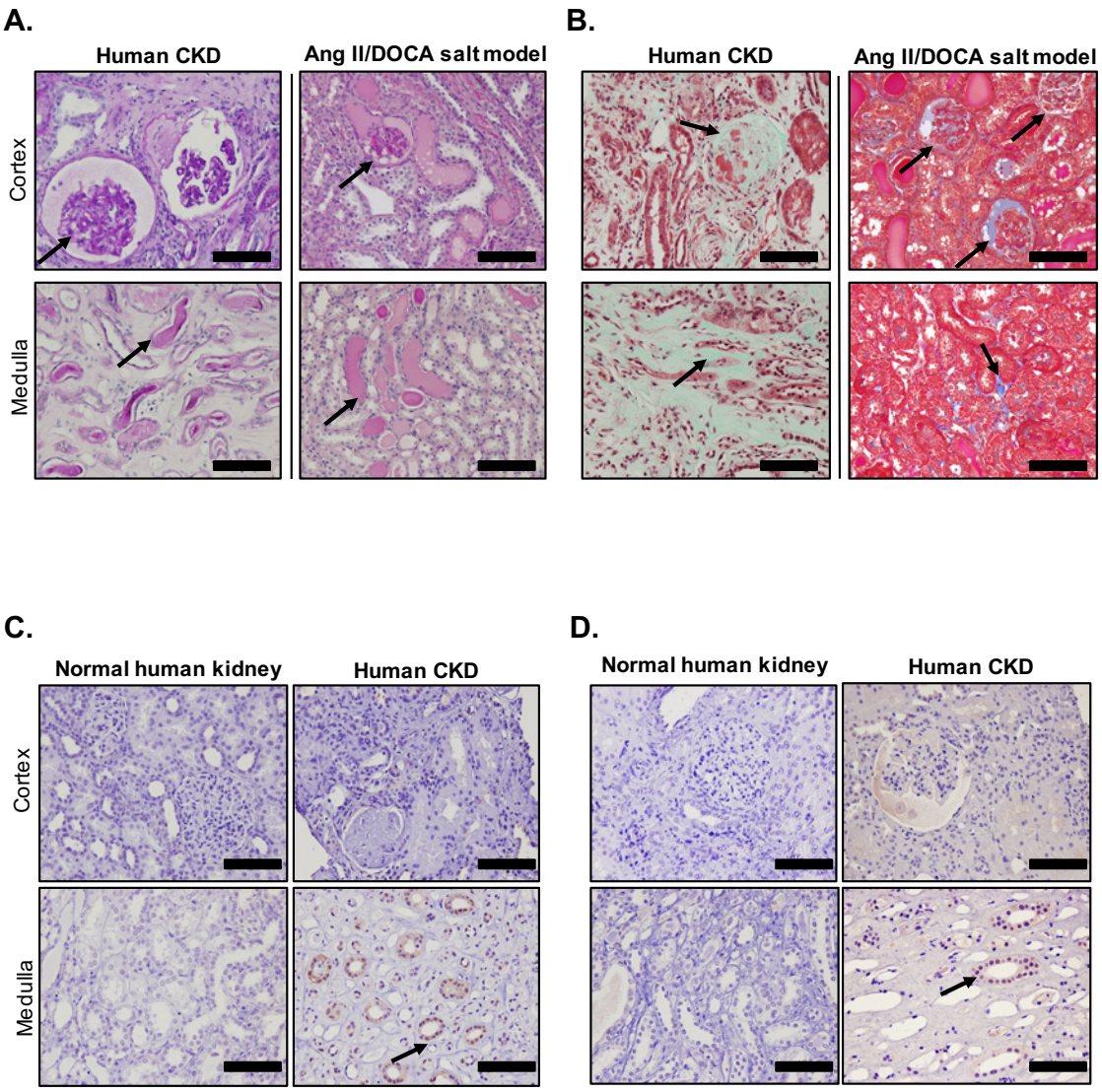
A.
Human CKD
Ang II/DOCA salt model
Cortex
Medulla
B.
Human CKD
Ang II/DOCA salt model
C.
Normal human kidney
Human CKD
Cortex
Medulla
D.
Normal human kidney
Human CKD

References:

1 Jha, V. *et al.* Chronic kidney disease: global dimension and perspectives. *Lancet* **382**, 260-272, (2013).

2 Ojo, A. Addressing the global burden of chronic kidney disease through clinical and translational research. *Trans Am Clin Climatol Assoc* **125**, 229-243, (2014).

3 Dickhout, J. G. & Krepinsky, J. C. Endoplasmic reticulum stress and renal disease. *Antioxid Redox Signal* **11**, 2341-2352, (2009).

4 Inagi, R., Ishimoto, Y. & Nangaku, M. Proteostasis in endoplasmic reticulum--new mechanisms in kidney disease. *Nat Rev Nephrol* **10**, 369-378, (2014).

5 Dickhout, J. G., Carlisle, R. E. & Austin, R. C. Interrelationship between cardiac hypertrophy, heart failure, and chronic kidney disease: endoplasmic reticulum stress as a mediator of pathogenesis. *Circ Res* **108**, 629-642, (2011).

6 Mohammed-Ali, Z., Cruz, G. L. & Dickhout, J. G. Crosstalk between the unfolded protein response and NF-kappaB-mediated inflammation in the progression of chronic kidney disease. *J Immunol Res* **2015**, 428508, (2015).

7 Bek, M. F. *et al.* Expression and function of C/EBP homology protein (GADD153) in podocytes. *Am J Pathol* **168**, 20-32, (2006).

8 Kirchhoff, F. *et al.* Rapid development of severe end-organ damage in C57BL/6 mice by combining DOCA salt and angiotensin II. *Kidney Int* **73**, 643-650, (2008).

9 Markan, S. *et al.* Up regulation of the GRP-78 and GADD-153 and down regulation of Bcl-2 proteins in primary glomerular diseases: a possible involvement of the ER stress pathway in glomerulonephritis. *Mol Cell Biochem* **324**, 131-138, (2009).

10 Lindenmeyer, M. T. *et al.* Proteinuria and hyperglycemia induce endoplasmic reticulum stress. *J Am Soc Nephrol* **19**, 2225-2236, (2008).

11 Cybulsky, A. V. Endoplasmic reticulum stress in proteinuric kidney disease. *Kidney Int* **77**, 187-193, (2010).

12 Christensen, E. I. & Birn, H. Megalin and cubilin: multifunctional endocytic receptors. *Nat Rev Mol Cell Biol* **3**, 256-266, (2002).

13 Verroust, P. J., Birn, H., Nielsen, R., Kozyraki, R. & Christensen, E. I. The tandem endocytic receptors megalin and cubilin are important proteins in renal pathology. *Kidney Int* **62**, 745-756, (2002).

14 Ishida, Y. & Nagata, K. Hsp47 as a collagen-specific molecular chaperone. *Methods Enzymol* **499**, 167-182, (2011).

15 Ishikawa, Y., Vranka, J., Wirz, J., Nagata, K. & Bachinger, H. P. The rough endoplasmic reticulum-resident FK506-binding protein FKBP65 is a

molecular chaperone that interacts with collagens. *J Biol Chem* **283**, 31584-31590, (2008).
16 Louise L Dunn, R. G. M., Jun Ni, Hafizah A Hamin, Christopher R Parish, Roland Stocker. New Insights into intracellular locations and functions of Heme Oxygenas-1. *Antioxidants & Redox signaling* **20,** 1723-1742 (2014).
17 Perco, P. *et al.* Protein biomarkers associated with acute renal failure and chronic kidney disease. *Eur J Clin Invest* **36**, 753-763, (2006).
18 Szegezdi, E., Logue, S. E., Gorman, A. M. & Samali, A. Mediators of endoplasmic reticulum stress-induced apoptosis. *EMBO Rep* **7**, 880-885, (2006).
19 Sano, R. & Reed, J. C. ER stress-induced cell death mechanisms. *Biochim Biophys Acta* **1833**, 3460-3470, (2013).
20 Liu, Z., Lv, Y., Zhao, N., Guan, G. & Wang, J. Protein kinase R-like ER kinase and its role in endoplasmic reticulum stress-decided cell fate. *Cell Death Dis* **6**, e1822, (2015).
21 Lopez-Hernandez, F. J. & Lopez-Novoa, J. M. Role of TGF-beta in chronic kidney disease: an integration of tubular, glomerular and vascular effects. *Cell Tissue Res* **347**, 141-154, (2012).
22 Kawakami, T., Ren, S. & Duffield, J. S. Wnt signalling in kidney diseases: dual roles in renal injury and repair. *J Pathol* **229**, 221-231, (2013).
23 Gluba, A. *et al.* The role of Toll-like receptors in renal diseases. *Nat Rev Nephrol* **6**, 224-235, (2010).
24 Anders, H. J. & Muruve, D. A. The inflammasomes in kidney disease. *J Am Soc Nephrol* **22**, 1007-1018, (2011).
25 Zhang, K. & Kaufman, R. J. From endoplasmic-reticulum stress to the inflammatory response. *Nature* **454**, 455-462, (2008).
26 Meares, G. P. *et al.* PERK-dependent activation of JAK1 and STAT3 contributes to endoplasmic reticulum stress-induced inflammation. *Mol Cell Biol* **34**, 3911-3925, (2014).
27 Marciniak, S. J. *et al.* CHOP induces death by promoting protein synthesis and oxidation in the stressed endoplasmic reticulum. *Genes Dev* **18**, 3066-3077, (2004).
28 Cybulsky, A. V., Takano, T., Papillon, J. & Bijian, K. Role of the endoplasmic reticulum unfolded protein response in glomerular epithelial cell injury. *J Biol Chem* **280**, 24396-24403, (2005).
29 Inagi, R. Endoplasmic reticulum stress as a progression factor for kidney injury. *Curr Opin Pharmacol* **10**, 156-165, (2010).
30 Luo, Z. F. *et al.* Effects of 4-phenylbutyric acid on the process and development of diabetic nephropathy induced in rats by streptozotocin: regulation of endoplasmic reticulum stress-oxidative activation. *Toxicol Appl Pharmacol* **246**, 49-57, (2010).
31 Kolb, P. S. *et al.* The therapeutic effects of 4-phenylbutyric acid in maintaining proteostasis. *Int J Biochem Cell Biol* **61**, 45-52, (2015).

32 Ayala, P. *et al.* Attenuation of endoplasmic reticulum stress using the chemical chaperone 4-phenylbutyric acid prevents cardiac fibrosis induced by isoproterenol. *Exp Mol Pathol* **92**, 97-104, (2012).

33 Carlisle, R. E. *et al.* 4-Phenylbutyrate inhibits tunicamycin-induced acute kidney injury via CHOP/GADD153 repression. *PLoS One* **9**, e84663, (2014).

34 Nielsen, R. & Christensen, E. I. Proteinuria and events beyond the slit. *Pediatr Nephrol* **25**, 813-822, (2010).

35 Amsellem, S. *et al.* Cubilin is essential for albumin reabsorption in the renal proximal tubule. *J Am Soc Nephrol* **21**, 1859-1867, (2010).

36 Storm, T. *et al.* A patient with cubilin deficiency. *N Engl J Med* **364**, 89-91, (2011).

37 Wahlstedt-Froberg, V., Pettersson, T., Aminoff, M., Dugue, B. & Grasbeck, R. Proteinuria in cubilin-deficient patients with selective vitamin B12 malabsorption. *Pediatr Nephrol* **18**, 417-421, (2003).

38 Gansevoort, R. T., Nauta, F. L. & Bakker, S. J. Albuminuria: all you need to predict outcomes in chronic kidney disease? *Curr Opin Nephrol Hypertens* **19**, 513-518, (2010).

39 Methven, S. *et al.* Comparison of urinary albumin and urinary total protein as predictors of patient outcomes in CKD. *Am J Kidney Dis* **57**, 21-28, (2011).

40 Wolf, G., Schroeder, R., Ziyadeh, F. N. & Stahl, R. A. Albumin up-regulates the type II transforming growth factor-beta receptor in cultured proximal tubular cells. *Kidney Int* **66**, 1849-1858, (2004).

41 Fogo, A. B. Mechanisms of progression of chronic kidney disease. *Pediatr Nephrol* **22**, 2011-2022, (2007).

42 Metcalfe, W. How does early chronic kidney disease progress? A background paper prepared for the UK Consensus Conference on early chronic kidney disease. *Nephrol Dial Transplant* **22 Suppl 9**, ix26-30, (2007).

43 Liu, S. H. *et al.* Chemical chaperon 4-phenylbutyrate protects against the endoplasmic reticulum stress-mediated renal fibrosis in vivo and in vitro. *Oncotarget*, **7**, 22116-22127, (2016).

44 Chiang, C. K. *et al.* Endoplasmic reticulum stress implicated in the development of renal fibrosis. *Mol Med* **17**, 1295-1305, (2011).

45 El Karoui, K. *et al.* Endoplasmic reticulum stress drives proteinuria-induced kidney lesions via Lipocalin 2. *Nat Commun* **7**, 10330, (2016).

46 Imig, J. D. & Ryan, M. J. Immune and inflammatory role in renal disease. *Compr Physiol* **3**, 957-976, (2013).

47 Qi, W. *et al.* Attenuation of diabetic nephropathy in diabetes rats induced by streptozotocin by regulating the endoplasmic reticulum stress inflammatory response. *Metabolism* **60**, 594-603, (2011).

48 Sean Eardley, K. & Cockwell, P. Macrophages and progressive tubulointerstitial disease. *Kidney Int* **68**, 437-455, (2005).

49 Zhang, M. *et al.* Chop deficiency prevents UUO-induced renal fibrosis by attenuating fibrotic signals originated from Hmgb1/TLR4/NFkappaB/IL-1beta signaling. *Cell Death Dis* **6**, e1847, (2015).

50 Chen, B. L. *et al.* CCAAT-Enhancer-Binding Protein Homologous Protein Deficiency Attenuates Oxidative Stress and Renal Ischemia-Reperfusion Injury. *Antioxid Redox Signal* **23**, 1233-1245, (2015).

51 Welsh, G. I. & Saleem, M. A. Nephrin-signature molecule of the glomerular podocyte? *J Pathol* **220**, 328-337, (2010).

52 Liu, K. *et al.* CHOP mediates ASPP2-induced autophagic apoptosis in hepatoma cells by releasing Beclin-1 from Bcl-2 and inducing nuclear translocation of Bcl-2. *Cell Death Dis* **5**, e1323, (2014).

53 Ubeda, M., Vallejo, M. & Habener, J. F. CHOP enhancement of gene transcription by interactions with Jun/Fos AP-1 complex proteins. *Mol Cell Biol* **19**, 7589-7599 (1999).

54 Z Mohammed-Ali, G. L. C., C Lu, R E Carlisle, K E Werner, K Ask, J G Dickhout. Development of a model of Chronic Kidney Disease in the C57BL/6 mouse with Properties of progressive human CKD. *BioMed Research International* **2015,** 172302 (2015).

55 Peterson, J. C. *et al.* Blood pressure control, proteinuria, and the progression of renal disease. The Modification of Diet in Renal Disease Study. *Ann Intern Med* **123**, 754-762 (1995).

56 Ruggenenti, P., Perna, A., Mosconi, L., Pisoni, R. & Remuzzi, G. Urinary protein excretion rate is the best independent predictor of ESRF in non-diabetic proteinuric chronic nephropathies. "Gruppo Italiano di Studi Epidemiologici in Nefrologia" (GISEN). *Kidney Int* **53**, 1209-1216, (1998).

57 Raij, L., Azar, S. & Keane, W. Mesangial immune injury, hypertension, and progressive glomerular damage in Dahl rats. *Kidney Int* **26**, 137-143 (1984).

58 Cowley, A. W., Jr. *et al.* Brown Norway chromosome 13 confers protection from high salt to consomic Dahl S rat. *Hypertension* **37**, 456-461 (2001).

Contributions

Conceived and designed the experiments: Z.M., J.G.D. Performed the experiments: Z.M., C.L., M.K.M., J.G.D. Analyzed the data: Z.M., M.K.M., J.G.D Contributed reagents/materials/analysis tools: K.A., D.L., J.C.K. J.G.D Wrote the paper: Z.M., R.E.C., J.C.K., J.G.D.

Competing interests

The authors declare no competing financial interests.

Chapter 4

GRP78 heterozygosity imparts protection against Angiotensin II/DOCA salt-induced CKD in the C57BL/6 mouse.

Summary and significance:

This article is focused on examining the effects of GRP78 heterozygosity on CKD development in the Ang II/DOCA salt model. GRP78 is the key regulator of the UPR and interacts with the three known UPR sensors PERK, IRE1α and ATF6. GRP78 heterozygous mice were used in this study since total knockdown of GRP78 has been shown to be embryonically lethal. GRP78 heterozygosity was demonstrated to impart protection against proteinuria, albuminuria and protein cast formation due to Ang II/DOCA salt treatment. GRP78 heterozygous mice also exhibited significantly lower fibrosis and macrophage infiltration compared to WT mice in the Ang II/DOCA salt model. This study is descriptive, however, mRNA analysis using Nanostring showed an increase in Arginase 1, CD23 and Foxp3 in GRP78 heterozygous mice undergoing Ang II/DOCA salt treatment compared to WT mice. This finding points to a potential role for immune cells in the development of pathology through their interaction with ER stress pathways, however, further studies are required to fully elucidate the identity of the immune cells involved and their role.

Title: GRP78 heterozygosity imparts protection against Angiotensin II/DOCA salt-induced CKD in the C57BL/6 mouse.

Author names and affiliations:

Zahraa Mohammed-Ali[1], Chao Lu[1], Mandeep K. Marway[1], Edward G Lynn[1], Kjetil Ask[2], Richard C. Austin[1], Jeffrey G. Dickhout[1].

[1]Department of Medicine, Division of Nephrology, McMaster University and St. Joseph's Healthcare Hamilton, Hamilton, Ontario, Canada.

[2]Department of Medicine, Division of Respirology, McMaster University and St. Joseph's Healthcare Hamilton, Hamilton, Ontario, Canada.

Running title: GRP78 heterozygosity diminishes CKD

SOURCES OF FUNDING:

This work was supported by research grants to Jeffrey G. Dickhout from the Canadian Institutes of Health Research (OSO-115895 and MOP-133484). This work was also supported, in part, by research grants to Richard C. Austin from the Heart and Stroke Foundation of Canada (G-15-0009389) and the Canadian Institutes of Health Research (MOP-286787). Financial support from St. Joseph's Healthcare Hamilton, including salary support to Jeffrey G. Dickhout, is acknowledged. Support from the Division of Nephrology in the Department of Medicine at McMaster University and St. Joseph's Healthcare Hamilton is acknowledged. Dr. Dickhout also holds a Kidney Foundation of Canada, Krescent New Investigator award. Richard C. Austin is a Career Investigator of the Heart and Stroke Foundation of Ontario and holds the Amgen Canada Research Chair in the Division of Nephrology at St. Joseph's Healthcare and McMaster University.

Address Correspondence to:
Jeffrey G. Dickhout, PhD
Department of Medicine, Division of Nephrology
McMaster University and St. Joseph's Healthcare Hamilton
50 Charlton Avenue East
Hamilton, ON, Canada, L8N 4A6
Tel: 905-522-1155 ext. 35334
Fax: 905-540-6589
Email: jdickhou@stjosham.on.ca

Abstract

The unfolded protein response (UPR) is upregulated in experimental and human renal diseases and its inhibition has been demonstrated to impede renal injury. In this study we investigated the effect of modulating the ER resident chaperone, GRP78, the main regulator of the UPR on chronic kidney disease (CKD) development. GRP78 heterozygous mice on a C57BL/6 background were used in a mouse model of CKD involving uninephrectomy, Angiotensin II/DOCA administration and high salt in the drinking water. $GRP78^{+/-}$ mice developed hypertension when subjected to this model, however, compared to wildtype mice they had significantly lower urinary protein excretion. Histology and immunohistochemistry analysis showed a decrease in protein cast formation, $F4/80^{+}$ macrophage infiltration and α-smooth muscle actin and collagen deposition in the kidneys $GRP78^{+/-}$ mice, compared to wildtype controls. RNA analysis of whole kidney tissue showed comparable upregulation of key fibrotic and inflammatory mediators in both WT and $GRP78^{+/-}$ mice. These mediators include TGF-β1, gremlin, extracellular matrix components, collagen Type1A and 3A, fibronectin1 and α-smooth muscle actin, metalloproteinases, MMP2, MMP14 and MMP7, NF-κB, IP-10 and C1Q complement. The only genes found to be regulated differently in $GRP78^{+/-}$ mice were Foxp3, a marker of regulatory T cells, Arginase 1, a marker for M2 macrophages and CD23, an IgE receptor expressed on B cells, T cells, follicular dendritic cells, eosinophils and activated macrophages. Therefore, our findings provide evidence that GRP78

heterozygosity protects against CKD development through modulation of the immune response.

Introduction

Endoplasmic reticulum (ER) stress results from an imbalance between protein-folding capacity and protein-folding demand in the ER and has been implicated in the development of kidney disease in experimental models and in the human population (8, 14). The aggregation of unfolded proteins in the ER activates the unfolded protein response (UPR) to alleviate protein overload. Three main ER signaling pathways mediate the UPR, PKR-like endoplasmic reticulum kinase (PERK), inositol requiring-1 (IRE-1) α and activating transcription factor (ATF) 6 (10).

The 78-kDa glucose-regulated protein (GRP78), also known as BiP (immunoglobulin heavy chain binding protein) or *hspa5*, is a an ER resident protein-folding chaperone and the master regulator of the UPR (32). During ER stress, GRP78 dissociates from the three UPR mediators and assists in the folding of newly synthesized polypeptides. This dissociation also activates the production of more protein-folding chaperones through the ATF6 and IRE1α pathways in an effort to ameliorate ER stress (32). Under conditions of severe ER stress, IRE1α activation and the induction of CHOP, a pro-apoptotic transcription factor, through the PERK arm of the UPR both stimulate apoptosis (28, 29). IRE1α and PERK activation also result in NF-κB activation causing ER stress-induced inflammation (21).

ER stress underlies a myriad of diseases including chronic kidney disease (CKD) (8, 14), obesity (5), Type II diabetes (4), rheumatoid arthritis (22) and

chronic obstructive pulmonary disease (24). Therefore, various attempts have been made to investigate the precise role of the UPR in these diseases by modulating GRP78 levels. The homozygous deletion of GRPP78 is embryonically lethal, however, GRP78 heterozygous mice are viable and fertile (19) and have been used in a number of studies to explore the effect of modifying the UPR by a partial reduction of GRP78 (3, 35-37). For example, $GRP78^{+/-}$ mice were shown to be protected against high fat diet-induced obesity due to the activation of the adaptive UPR characterized by higher levels of ER stress-induced chaperones GRP94, protein disulfide isomerase (PDI), calnexin and calreticulin, compared to WT mice (35). Similarly, our recent findings show that inhibition of bleomycin-induced pulmonary fibrosis in $GRP78^{+/-}$ mice was attributed to the upregulation of CHOP in airway macrophages, thereby contributing to macrophage apoptosis (3). Thus, GRP78 heterozygosity has a significant effect on UPR activation and can be used to study the effect of UPR modulation on a variety of diseases where ER stress is implicated in the development and progression of pathology.

In our previous study, we have shown an upregulation of GRP78 mRNA in response to Angiotensin II/DOCA salt-induced CKD. The administration of 4-phenylbutyrate, a low molecular weight chaperone used to inhibit ER stress, in this model resulted in significantly lower GRP78 mRNA levels and attenuated CKD. Therefore, the regulation of the UPR by GRP78 may influence key processes involved in CKD development. In this study, we sought to elucidate the effects of GRP78 heterozygosity on CKD development.

Methods and Materials

Chronic kidney disease (CKD) mouse model

CKD was induced in C57BL/6 mice by combining uninephrectomy with Angiotensin II (Ang II)/ deoxycorticosterone acetate (DOCA) infusion and high salt in the drinking water, as reported by us previously (17, 38). Ten-week-old male mice were subjected to a uninephrectomy under isofluorane anesthesia. Upon recovery, 1.5 ng Ang II (Sigma) per minute per gram body weight was administered via osmotic pump along, while DOCA was provided with a 50 mg 21-day release pellet (Innovative Research of America, M-121). Mice were then provided with 1% salt in drinking water. Age-matched GRP78$^{+/-}$ mice were obtained from a breeding colony held at the McMaster University Animal Facility along with their Wildtype (WT) littermate controls. All animal work was performed in accordance with and approved by the McMaster University Animal Research Ethics Board.

Blood pressure measurements and urine analysis

Blood pressure measurements were obtained through the tail cuff method using a CODA (Kent Scientific, Torrington, CT) blood pressure analyzer as examined previously (38). Metabolic cages were used to collect 24-hour urine before the surgical procedure and after 3 weeks following treatment with AngII/DOCA salt. Urine samples were sent to an in-house laboratory to assess total 24h urinary protein. ELISA was used to measure mouse urine albumin concentration

(BETHYL Laboratories, Montgomery, TX).

Western blotting

Total cell lysates were obtained using 4X SDS lysis buffer containing the protease inhibitor and phosphatase inhibitor cocktails (complete Mini; Roche; Laval, Canada). Protein levels were determined using BioRad DC Protein Assay (BioRad, Mississauga, Canada) for control of protein loading. Tissue lysates were subjected to electrophoretic separation in an SDS-PAGE reducing gel (BioRad). Primary antibodies were detected using appropriate horseradish peroxidase-conjugated secondary antibodies and ECL Western Blotting Detection Reagents (GE Healthcare, Mississauga, Canada), as described previously (7). GRP78 mouse Ab (BD Transduction Laboratories #610979) was diluted 1:1000 and β-actin antibody (Sigma) was diluted 1:5000. Results were densitometrically quantified using ImageLab software (BioRad) and expressed as a ratio of β-actin loading control.

Immunohistochemistry and assessment of renal pathology

Renal tissue was fixed in 4% paraformaldehyde upon sacrificing the animal. The tissue was then embedded in paraffin blocks and sectioned using a microtome. For T cell staining, a polyclonal rabbit, anti-human CD3 antibody (Dakocytomation) was used at a concentration of 0.6 g/L and a dilution of 1:100 in normal goat serum (Vector) at 1:20. The secondary antibody was an anti-rabbit

IgG (H+L) from Vector BA-1000 biotinylated (1:500) in TBS. For macrophage staining, a rat monoclonal antibody to F4/80 (abcam, ab6640) was used at a dilution of 1:30 in normal rabbit serum at 1:20 and in combination with secondary biotinylated anti-rat IgG (H+L) (Vector), mouse absorbed, affinity purified, made in rabbit at a dilution of 1:500 in TBS. Sections were stained with horseradish peroxidase Streptavidin (Vector SA-5004) in combination with Nova Red (Vector) and Hematoxylin (Sigma) to visualize the stained cells. To evaluate renal pathology, (Periodic Acid Schiff) PAS stain was performed to assess protein cast formation and Picro-Sirius Red (PSR) and α-smooth muscle actin staining was used to assess fibrosis. For PSR staining, kidney tissue sections were processed with saturated picric acid solution and then stained with Sirius red F3B (Colour Index 35782). Immunohistochemistry sections were imaged with a 20X objective lens. Five random images from the cortex and the medulla per mouse were taken to analyze the pathological features in renal tissue. PSR sections were analyzed using an Olympus BX41 microscope. Polarized light microscopic images of PSR staining were obtained using a U-POT polarizer and U-ANT analyzer (Olympus) in transmitted light. The diaphragm and polarizer allowed the detection of birefringence of collagen fibers. The Metamorph program was used to assess the area density for PSR, α-smooth muscle actin and F4/80 staining. This method involves setting a color threshold in the Metamorph program to express the area density of the stain as a percentage of the image total area. The quantification of PAS staining was performed in the same program by manually selecting the

casts and then calculating the percentage area of casts per image and then per mouse cortex or medulla. CD3 positive cells were quantified using the cell count tool in Image J software (NIH).

RNA isolation and Nanostring Analysis

Total RNA was isolated from flash frozen mouse kidney tissue using the RNeasy Mini Kit (Qiagen, Cat. No. 74104). RNA integrity was assessed using the Agilent 2100 bioanalyzer and Agilent RNA 6000 Nano reagents, Cat. No. 5067-1511 (Agilent Technologies, Mississauga, Canada). Only RNA with RIN>5 was used in our nanostring analyses. The code set for Nanostring analysis was established based on literature searches of pathways that are important in determining therapeutic targets for the treatment of CKD. Nanostring data was normalized against 4 housekeeping genes, IPO8, YWHAZ, GAPDH and RPLP2. P values were corrected for multiple comparisons using the Benjamin-Hochberg procedure in R programming language and heatmaps were produced using Java Treeview software. Fold changes were log-transformed and Hierarchical gene clustering was performed on heatmaps using Euclidean distance and complete linkage. On the heatmaps, each column represents the response to the AngII/DOCA salt model by WT or $GRP78^{+/-}$ mice. Each box represents the fold change for a particular gene in AngII/DOCA salt treated mice, compared to their respective sham controls. Fold changes were log_2-transformed. Down-regulation is denoted by blue and up-regulation is denoted by red.

Statistical Analysis

Data are shown as the mean± standard error of the mean. Student's T-test was used to analyze difference between groups. Differences among multiple groups were analyzed with analysis of variance followed by post-hoc Bonferroni tests in Graphpad Prism 5.0. A p-value of ≤ 0.05 was considered significant.

Results

GRP78 heterozygosity attenuates proteinuria and protein cast formation but does not affect hypertension development in CKD.

GR78$^{+/-}$ mice showed a reduction of ~50% in GRP78 protein expression compared to WT when treated with the Ang II/DOCA salt model (Figure 1A and 1B) This effect allowed us to study the impact of a 50% reduction in GRP78 in the context of CKD. The Ang II/DOCA salt model induced an increase in systolic and diastolic blood pressure in both WT and GRP78$^{+/-}$ mice (Figure 1C and 1D), compared to sham-operated controls. GRP78 heterozygosity had no effect on hypertension development due to Ang II/DOCA salt. Urine collected over a 24h time period showed an increase in total protein and albumin with CKD development in both WT and GRP78$^{+/-}$ mice (Figure 1E and 1F). However, GRP78 heterozygosity significantly attenuated proteinuria and albuminuria in response to Ang II/DOCA salt. Next, we wanted to observe whether the decrease in proteinuria also translated to decreased renal tubular damage. Therefore, PAS staining was performed and the percentage of protein cast area density was calculated. This showed an increase in protein casts formation in the cortex and medulla of Ang II/DOCA salt mice (Figure 2A-2D). Although both WT and GRP78$^{+/-}$ mice developed protein casts, GRP78$^{+/-}$ mice had a significantly lower area density of protein cast deposition.

GRP78 heterozygosity decreases fibrosis and macrophage infiltration in CKD.

The Ang II/DOCA salt model increases the deposition of both α-smooth muscle actin (Figure 3A-3D) and collagen (Figure 3E-3H) in the cortex and medulla of WT mice. Although GRP78$^{+/-}$ mice also experienced some level of increase in extracellular matrix (ECM) deposition due to Ang II/DOCA salt treatment, GRP78 heterozygosity significantly reduced fibrosis in CKD. Since macrophages have been shown to play an important role in fibrosis in various diseased states (6, 25), we next assessed the area density of macrophage infiltration using F4/80 staining. Although both WT and GRP78$^{+/-}$ mice have increased F4/80^{+} macrophage infiltration, GRP78 heterozygosity significantly reduced the area density of F4/80 positive staining in response to Ang II/DOCA salt treatment (Figure 4A and 4C). To evaluate whether GRP78 heterozygosity resulted in reduction in T cell infiltration in the CKD context, we performed CD3 staining. Our results show comparable increased levels of average CD3+ T cell numbers in the kidneys of WT and GRP78$^{+/-}$ mice with CKD development (Figure 4B and 4D).

The effect of GRP78 heterozygosity on mRNA expression of fibrosis, UPR and inflammatory genes

Nanostring gene expression analysis was performed to evaluate the pathways underlying the protection of GRP78$^{+/-}$ mice against proteinuria, protein cast formation, fibrosis and macrophage infiltration in CKD. Overall, GRP78

heterozygosity did not impact mRNA expression of genes important in fibrosis such as ECM components including collagen type1a1 and 3a1, fibronectin (FN1) and α-smooth muscle actin (acta 2) (Figure 5A). As well, there was comparable activation of key regulators of renal fibrosis TGFβ1, TGFβ1-induced collagen crosslinking enzyme, LOXL2, type I collagen folding chaperon, FKBP65, TGFβ1 inhibitor, gremlin and matrix metalloproteinases MMP2, MMP7 and MMP14. Our CKD model also caused the increase in ER stress genes, CHOP, phlda1 and pro-apoptotic genes downstream of the UPR, Bcl2l11, BBC3 and Bak1. These genes were regulated in both WT and GRP78$^{+/-}$ mice. Similarly, GRP78$^{+/-}$ mice showed an increase in inflammatory gene expression with CKD development comparable to WT mice (Figure 5B). NF-κB and AP-1, pro-inflammatory transcription factors known to be induced by ER stress were observed to increase with Ang II/DOCA salt treatment. Our CKD model also resulted in an increase in TLR2 and TLR4, pattern recognition receptors associated with innate immune responses, as well as various cytokines and chemokines, IP-10, IL-6, CCL20 and CXCR3. Upregulation of macrophage markers Arginase 2, CD68 and mannose receptor also indicated a role for macrophages in both WT and GRP78$^{+/-}$ groups in CKD renal pathology. Genes that showed a significantly higher expression in the GRP78$^{+/-}$ mice compared to their WT counterparts included SREBP1-c (1.68-fold higher), Arginase 1 (9.86-fold higher) and CD23 (4.19-fold higher). GRP78$^{+/-}$ mice with CKD induced by Ang II/DOCA salt also showed a 2.85-fold higher level of T regulatory cell marker Foxp3 mRNA

compared to WT mice, however, this difference was not statistically significant (p-value=0.17).

Discussion

Various reports have defined an association between ER stress and the development of progressive renal pathology in both animal and human CKD (8, 9, 14, 30). In addition to its role in protein folding and assembly, GRP78 interacts with the three known UPR sensors PERK, IRE1α and ATF6 to repress UPR activation (35). Therefore, GRP78 heterozygous mice on a C57BL/6 background have been utilized to study the role of ER stress in diverse disease contexts (3, 16, 19, 35-37). A study by Kimura *et al.* investigated the role of ER stress in chronic renal injury using C57BL/6 mice heterozygous for mutant-BiP (16). The mutant-BiP mouse is deficient in the carboxyl-terminal-Lys-Asp-Glu-Leu (KDEL) sequence that, under normal conditions, mediates the retrieval of BiP to the ER after it is secreted from post-ER compartments. This mutation results in an aberrant folding environment in the ER and can also affect quality control in post-ER compartments (20). Mutant BiP is functional only as long as it remains in the ER and this is dependent on ER retrieval of BiP via the KDEL receptor in the golgi. Mice homozygous for mutant-BiP suffered from ER stress and died several hours after birth due to impaired pulmonary surfactant biosynthesis and respiratory failure (20). The heterozygous mutant-BiP mice studied in the context of renal injury, however, showed significantly increased tubular-interstitial lesion

with aging compared to WT (16). The mutant-BiP mice also showed exacerbated tubular damage and apoptosis in response to a CKD model consisting of a uninephrectomy and protein overload. However, urinary protein excretion did not differ between mutant-BiP mice and WT in response to protein overload (16). Further, the authors reported that the pathological renal changes in response to protein overload were strain dependent and were absent in the C57BL/6 mice, which were used in their study (16). In our Ang II/DOCA salt model of CKD, C57BL/6 mice experienced robust CKD responses that included features of human CKD such as proteinuria, protein cast formation, inflammation and fibrosis. Our findings show that GRP78 heterozygosity imparted a protection against proteinuria, albuminuria and protein cast formation. GRP78 heterozygous mice have been shown to exhibit modulated UPR activation (3, 35), whereas mutations in BiP impair ER function (16, 20). Therefore, the effect that we observed in our Ang II/DOCA salt model is influenced by both our model of CKD and the use of GRP78 deficient mice rather than heterozygous mutant-BiP mice.

GRP78$^{+/-}$ mice on Ang II/DOCA salt also experienced significantly lower fibrosis and macrophage infiltration compared to WT. These results are in agreement with studies on mouse models of pulmonary fibrosis (3) and rheumatoid arthritis (37) where GRP78 heterozygosity has been associated with decreased fibrosis and inflammatory cell/macrophage infiltration. In a study by Ayaub et al. (3), the decreased fibrosis in GRP78$^{+/-}$ mice in a model of bleomycin-induced pulmonary fibrosis was shown to result from a higher level of

CHOP and apoptosis in pro-fibrotic M2 macrophages found in the alveoli of GRP78$^{+/-}$ compared to WT. In the context of CKD, macrophages are involved in a myriad of processes, renal inflammation, interstitial fibrosis and tissue remodeling and resolving renal injury, that influence CKD progression (6, 25, 33). In animal studies, depletion of macrophages using either liposomal clodronate or the CD11b-DTR mouse resulted in decreased fibrosis in unilateral ureteral obstruction as well as decreased proteinuria and improved renal function in models of nephrotoxic nephritis (26). Although our study shows a decrease in F4/80^{+} macrophages with GRP78 heterozygosity in CKD indicating decreased renal injury progression, we have yet to demonstrate that this occurs due to an increase in CHOP-induced apoptosis as suggested by Ayaub *et al.* (3) in a model of pulmonary fibrosis.

Another future direction involves the identification of macrophage subsets within GRP78 and WT mice in the Ang II/DOCA salt model. Numerous studies show that macrophage polarization plays an important role in the progression of several kidney diseases including obstructive nephropathy, ischemia-reperfusion injury, glomerulonephritis and diabetic nephropathy (31). Our nanostring analysis shows significantly higher levels of Arginase 1 in GRP78$^{+/-}$ mice subjected to Ang II/DOCA salt compared to WT. Arginase 1 is cytosolic enzyme that is constitutively expressed in the liver where it plays a role in nitrogen elimination by catalyzing arginine hydrolysis to urea and ornithine (23). This enzyme is also expressed in alternatively activated M2 macrophages, however, its expression is

dependent on exogenous stimuli including Th2 cytokines IL-4 and IL-13 (23, 25). Interestingly, CD23, which is significantly higher in GRP78$^{+/-}$ mice on Ang II/DOCA salt compared to WT, is a Fc receptor specific for IgE that is also reported to be a marker of activated M2 macrophages. CD23 is expressed on the surface of macrophages and has been shown to regulate their cytokine expression (27). However, CD23 is also expressed in T and B lymphocytes, follicular dendritic cells, intestinal epithelial cells and bone marrow stromal cells and imparts pleiotropic effects based on different stimuli (1).

Due to their small number within the lumen of proximal tubules, however, macrophages are not considered the main cell type responsible for the clearance of debris in the context of kidney disease. Nevertheless, F4/80^{+} macrophages have been shown to engulf debris coated with apoptosis inhibitor of macrophages (AIM), a protein that is present at high levels in the blood and that accumulates on intraluminal debris and enhances their clearance (2). Cell debris not only contributes to cellular casts but also blocks tubular cell resorption and promotes the precipitation of Tamm-Horsfall glycoprotein, the most abundant excreted protein, to form hyaline casts. Under these conditions, serum proteins such as albumin or immunoglobulin light chains are also prone to precipitate resulting in granular casts (18). Therefore, the phagocytic function of macrophages could play a role in regeneration following tissue injury. Whether macrophages are involved in protecting GRP78$^{+/-}$ mice against protein cast formation in the Ang II/DOCA salt model is a subject of future experiments.

The increase in protein levels of UPR markers such as CHOP, ATF4, GADD34 and ATF6 and ER stress-induced chaperones PDI, calnexin and calreticulin in GRP78$^{+/-}$ mice compared to WT has also been demonstrated in a model of diet-induced obesity (35). In this study, GRP78 heterozygosity was shown to promote the adaptive UPR, i.e. it was shown to attenuate the translational block caused by eIF2α phosphorylation downstream of PERK and increased ER chaperone levels to improve ER folding capacity. Since ER stress has been linked to obesity and glucose tolerance, the ability to activate the adaptive UPR explained how GRP78 heterozygosity attenuated high fat diet-induced obesity and protected against hyperinsulinemia, liver steatosis, white adipose tissue inflammation and hyperglycemia (6). Our gene analysis, however, did not show any difference in mRNA levels of CHOP or other apoptotic genes induced by ER stress such as Bak1, BBC3 or phlda1 between GRP78$^{+/-}$ and WT mice on the Ang II/DOCA salt model. In fact, only three genes were significantly higher in the GPR78$^{+/-}$ mice on the model compared to WT, SREBP-1c, Arginase 1 and CD23. SREBP-1c is a transcription factor involved in glucose utilization and fatty acid synthesis. Our results are in agreement with experiments where GRP78 overexpression resulted in the inhibition of SREBP-1c cleavage and the reduced expression of SREBP-1c target genes (15).

Foxp3 is a transcription factor gene that induces a regulatory T cell (Treg phenotype) and the depletion of Tregs has been shown to exacerbate renal

disease in various animal models (13). In a model of adriamycin-induced nephropathy, Foxp3-transduced T cells that showed a regulatory phenotype protected against renal injury and resulted in lower urinary protein excretion, less glomerulosclerosis, tubular damage and interstitial infiltrates (34). In db/db mice, adoptive transfer of CD4+Foxp3+ T regs significantly improved insulin sensitivity and diabetic nephropathy whereas Treg depletion enhanced insulin resistance, albuminuria and glomerular hyperfiltration (11). ER stress has been shown to drive a regulatory T cell phenotype in Foxp3+ human T reg clones by enhancing IL-10 transcription (12). The modulation of the UPR using GRP78 heterozygosity resulted in higher levels of Foxp3 mRNA in whole kidney tissue of $GRP78^{+/-}$ mice compared to WT. Therefore, GRP78 heterozygosity may impact Foxp3+ T reg populations in the kidney and this could influence renal injury progression, however additional experiments are required to explore this effect.

Collectively, our results show reduced renal injury in $GRP78^{+/-}$ mice on the Ang II/DOCA salt model. Our gene expression analysis points to potential immune pathways that could be underlying this effect. However, further analysis is required to determine the precise mechanisms involved in protection against CKD brought about by GRP78 heterozygosity.

Figure Legends

Figure 1. ***Effect of GRP78 heterozygosity on the development of hypertensive proteinuria.*** Wild type (WT) and GRP78$^{+/-}$ mice were uninephrectomized and then chronic 1% NaCl was added to the drinking water (Ang II/DOCA salt). WT and GRP78 sham-operated (SHAM) mice were utilized as controls. **(A, B)** Western blotting and quantification (n=3 per group) showed a ~50% reduction in GRP78 in GRP78 heterozygous mice in response to our Ang II/DOCA salt model. GRP78$^{+/-}$ mice (n=7) experienced a similar increase in systolic **(C)** and **(D)** diastolic blood pressure as WT mice (n=6) in response to Ang II/DOCA salt, compared to their respective SHAM controls (n=5-6). Measurements of **(E)** total 24h protein and **(F)** albumin demonstrate significantly higher urinary protein and albumin levels in WT and GRP78$^{+/-}$ mice on Ang II/DOCA salt (n=5-6 per group), compared to their respective shams (n=3-4 for total protein analysis and n=5-6 for total albumin analysis). GRP78$^{+/-}$ mice, however, showed lower urinary protein and albumin compared to WT. Error bars are shown as mean ± S.E.M. in **(B-F)**. *indicates that the measurement is significantly different in the Ang II/DOCA salt group compared to SHAM, while # indicates significantly lower in GRP78$^{+/-}$ mice compared to WT mice.

FIGURE 2: ***Effect of GRP78 heterozygosity on protein cast formation.*** The percentage of protein cast formation in the **(A, B)** cortex and the **(C, D)** medulla is increased with CKD development in both WT and GRP78$^{+/-}$ mice compared to

their respective sham-operated controls (n=5 per group). However, GRP78 heterozygosity significantly reduced protein cast formation in response to the CKD mouse model. Error bars are shown as mean ± S.E.M. in **(B)** and **(D)**. *indicates that the measurement is significantly different in CKD compared to sham-operated mice while # indicates significantly lower in GRP78$^{+/-}$ mice compared to WT mice.

FIGURE 3: ***Effect of GRP78 heterozygosity on fibrosis.*** Alpha-smooth muscle actin deposition is increased in the cortex **(A, B)** and medulla **(C, D)** of WT and GRP78$^{+/-}$ mice compared to sham-operated controls (n=5 per group for cortex analysis and n=3-4 for medulla analysis). Collagen deposition is also increased in the cortex **(E, F)** and medulla **(G, H)** of WT (n=5) and GRP78$^{+/-}$ (n=6) mice compared to sham-operated controls (n=4-5). GRP78 heterozygosity significantly decreased α-smooth muscle actin and collagen deposition, indicating lower fibrosis in a CKD mouse model. Error bars are shown as mean ± S.E.M. in **(B, D, F and H)**. *indicates that the measurement is significantly different in CKD compared to sham-operated mice while # indicates significantly lower in GRP78$^{+/-}$ mice compared to WT mice.

FIGURE 4: ***Effect of GRP78 heterozygosity on inflammatory cell infiltration.*** Renal F4/80+ macrophages **(A, C)** and CD3+ T cell infiltration **(B, D)** is increased in our CKD model in both WT and GRP78$^{+/-}$ mice (n=4 per group for CD3^{+}

staining and n=5-6 per group for F4/70 staining) compared to sham-operated controls (n=3-4). GRP78$^{+/-}$ mice had similar T cell numbers but significantly lower macrophage infiltration compared to WT mice with CKD development. Error bars are shown as mean ± S.E.M. in **(C)** and **(D)**. *indicates that the measurement is significantly different in CKD compared to sham-operated mice while # indicates significantly lower in GRP78$^{+/-}$ mice compared to WT mice.

FIGURE 5: ***Effect of GRP78 heterozygosity on mRNA expression of fibrosis, UPR and inflammatory genes.*** Heatmaps showing hierarchical clustering of **(A)** fibrosis and UPR and **(B)** inflammatory genes. Column **1** represents the fold changes in gene expression between WT Ang II/DOCA salt (n=5) and WT SHAM (n=5) whereas column **2** represents the fold changes in gene expression between GRP78$^{+/-}$ Ang II/DOCA salt mice (n=5) and GRP78$^{+/-}$ (n=4) sham-operated controls. *indicates that the Ang II/DOCA salt treated group is significantly different than corresponding SHAM whereas # indicates significantly higher in GRP78$^{+/-}$ Ang II/DOCA salt mice compared to WT Ang II/DOCA salt mice.

FIGURE 1

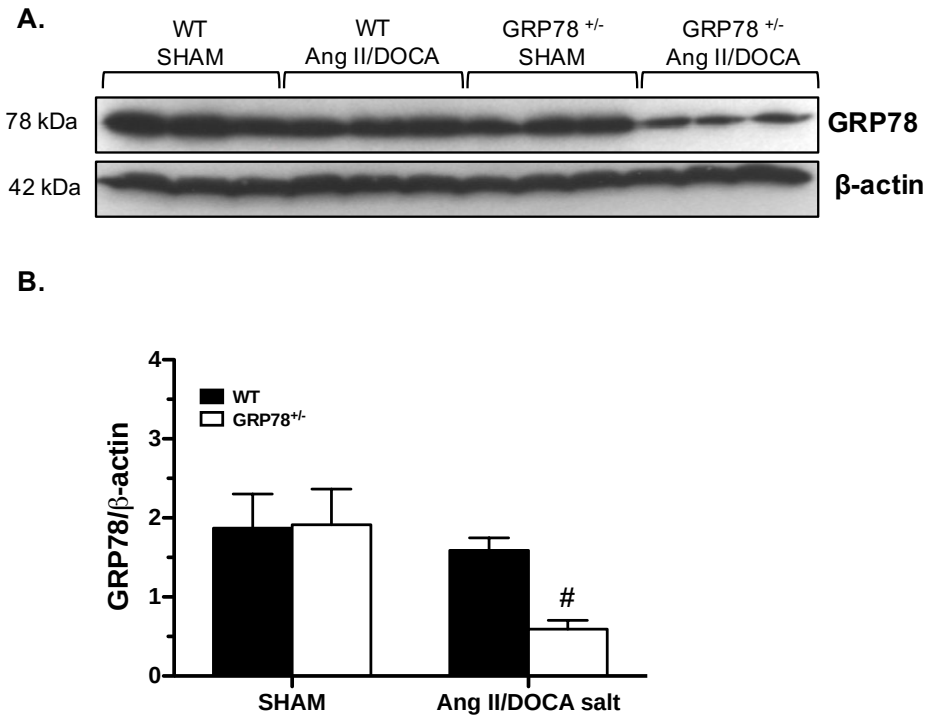
A.
WT
SHAM
WT
Ang II/DOCA
GRP78 +/-
SHAM
GRP78 +/-
Ang II/DOCA
78 kDa
GRP78
42 kDa
β-actin
B.
GRP78/β-actin
WT
GRP78+/-
4
3
2
1
0
#
SHAM
Ang II/DOCA salt

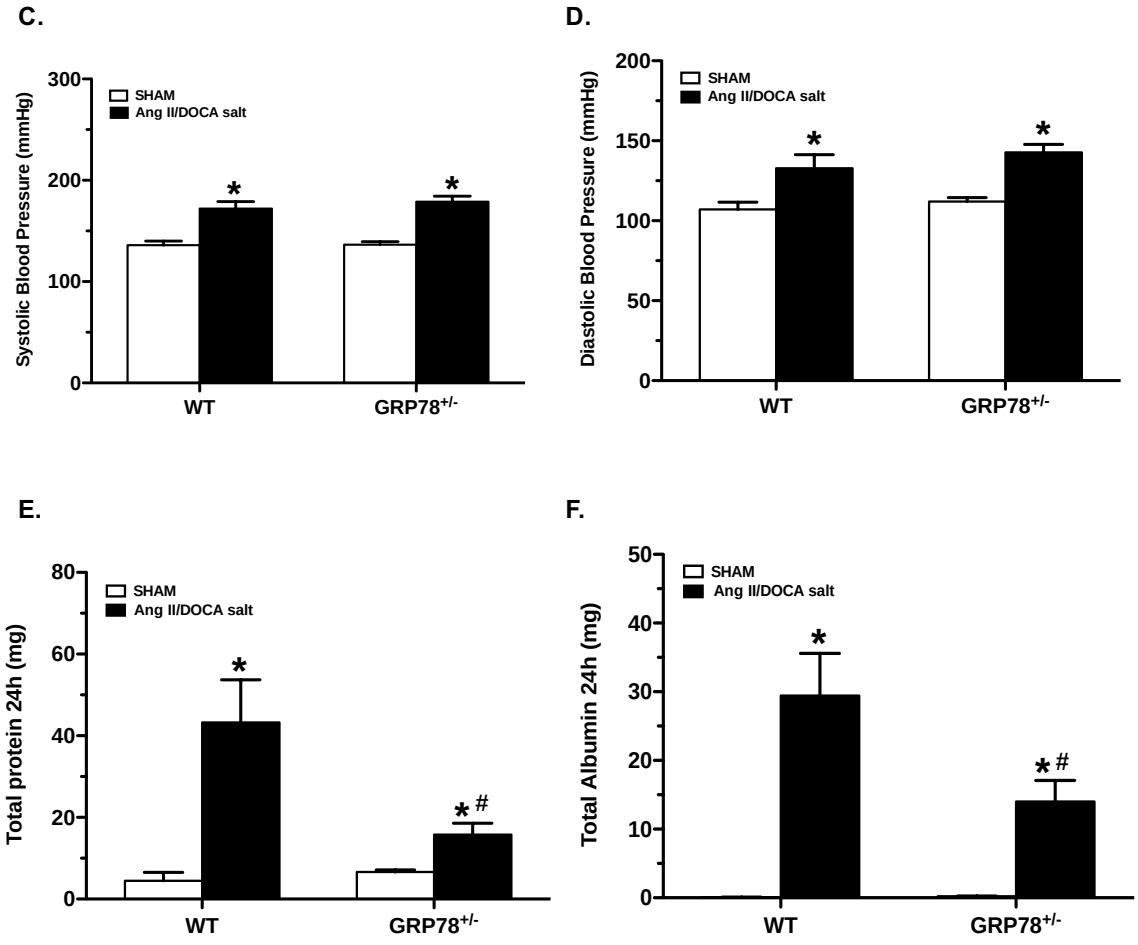
C.
Systolic Blood Pressure (mmHg)
300
200
100
0
SHAM
Ang II/DOCA salt
*
*
WT
GRP78+/-
D.
Diastolic Blood Pressure (mmHg)
200
150
100
50
0
SHAM
Ang II/DOCA salt
*
*
WT
GRP78+/-
E.
Total protein 24h (mg)
80
60
40
20
0
SHAM
Ang II/DOCA salt
*
*#
WT
GRP78+/-
F.
Total Albumin 24h (mg)
50
40
30
20
10
0
SHAM
Ang II/DOCA salt
*
*#
WT
GRP78+/-

FIGURE 2

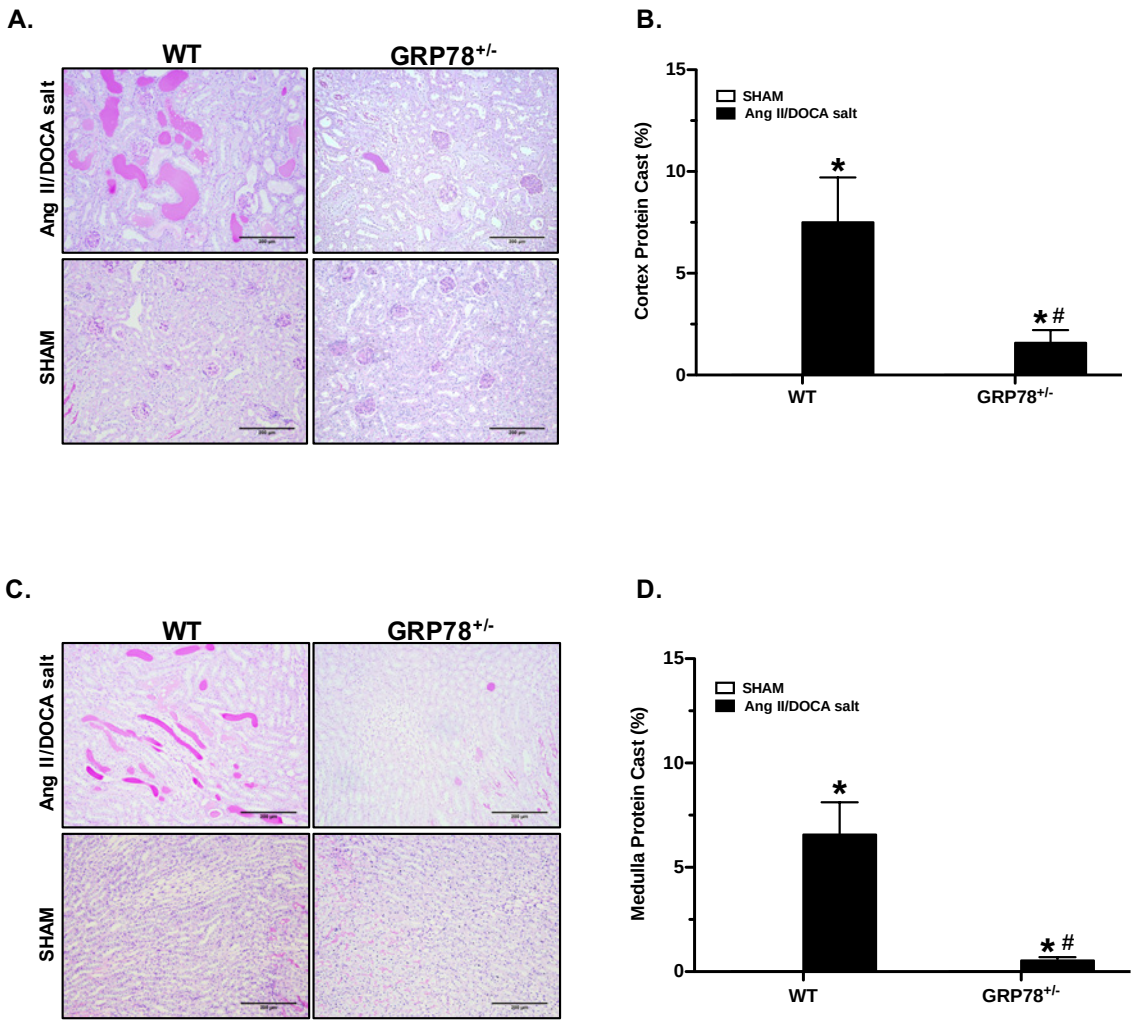
A.
WT
GRP78+/-
Ang II/DOCA salt
SHAM
B.
SHAM
Ang II/DOCA salt
Cortex Protein Cast (%)
15
10
5
0
*
*#
WT
GRP78+/-
C.
WT
GRP78+/-
Ang II/DOCA salt
SHAM
D.
SHAM
Ang II/DOCA salt
Medulla Protein Cast (%)
15
10
5
0
*
*#
WT
GRP78+/-

FIGURE 3

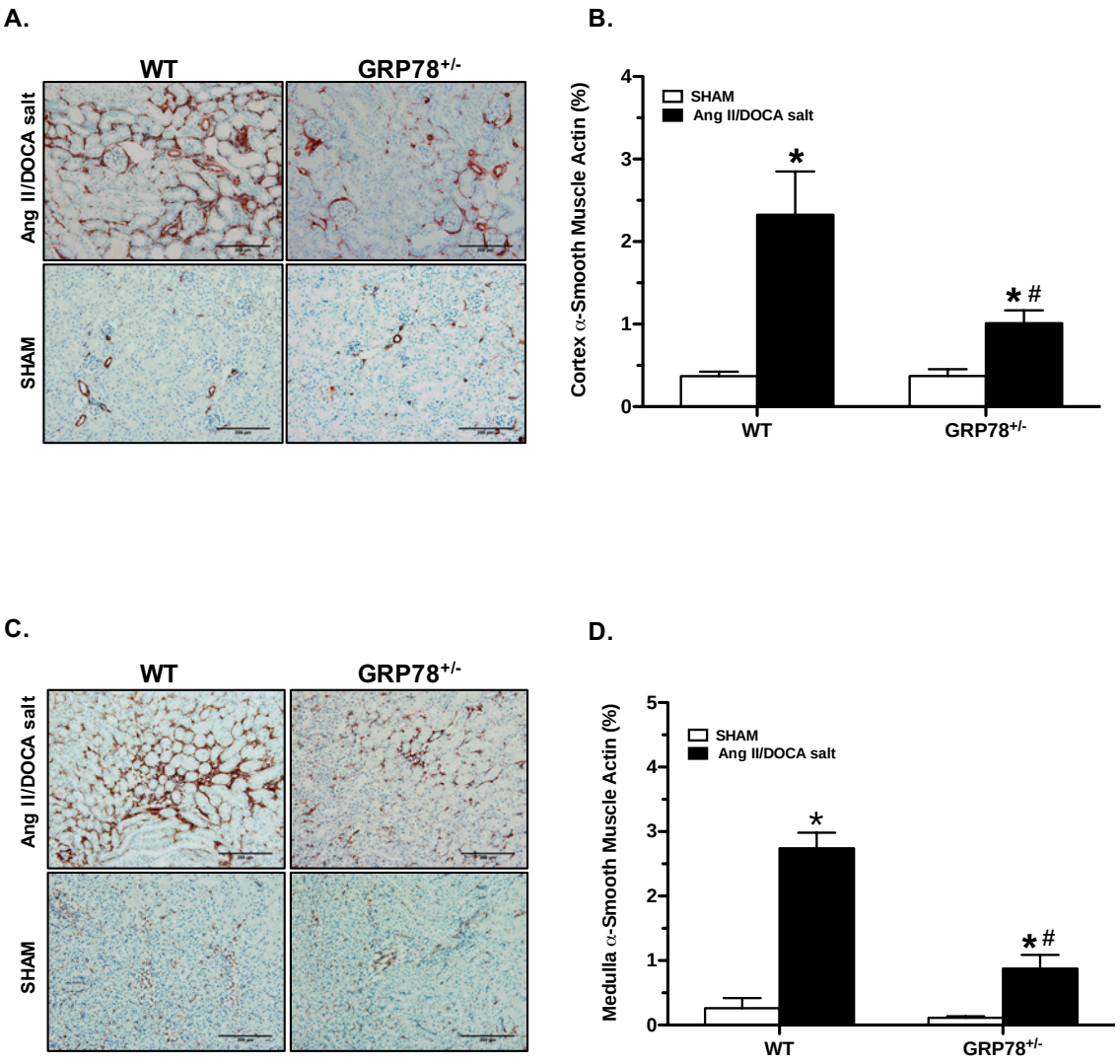
A.
WT
GRP78+/-
Ang II/DOCA salt
SHAM
B.
Cortex α-Smooth Muscle Actin (%)
SHAM
Ang II/DOCA salt
*
*#
WT
GRP78+/-
C.
WT
GRP78+/-
Ang II/DOCA salt
SHAM
D.
Medulla α-Smooth Muscle Actin (%)
SHAM
Ang II/DOCA salt
*
*#
WT
GRP78+/-

E.

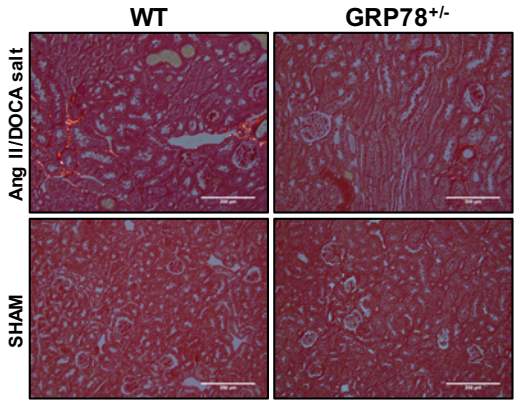
WT
GRP78+/-
Ang II/DOCA salt
SHAM

F.

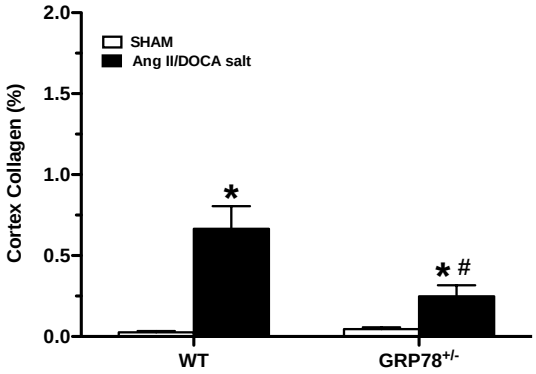
SHAM
Ang II/DOCA salt
Cortex Collagen (%)
2.0
1.5
1.0
0.5
0.0
*
* #
WT
GRP78+/-

G.

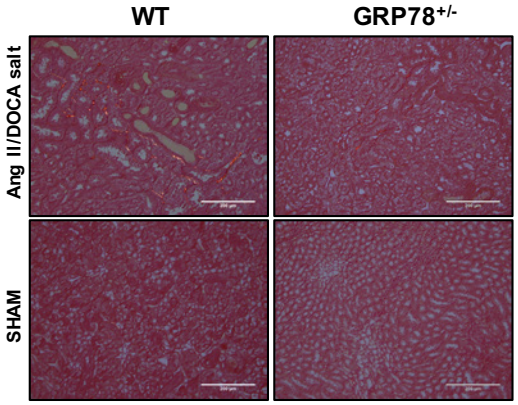
WT
GRP78+/-
Ang II/DOCA salt
SHAM

H.

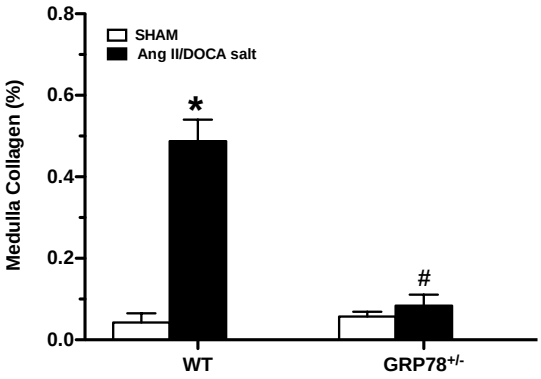
SHAM
Ang II/DOCA salt
Medulla Collagen (%)
0.8
0.6
0.4
0.2
0.0
*
#
WT
GRP78+/-

FIGURE 4

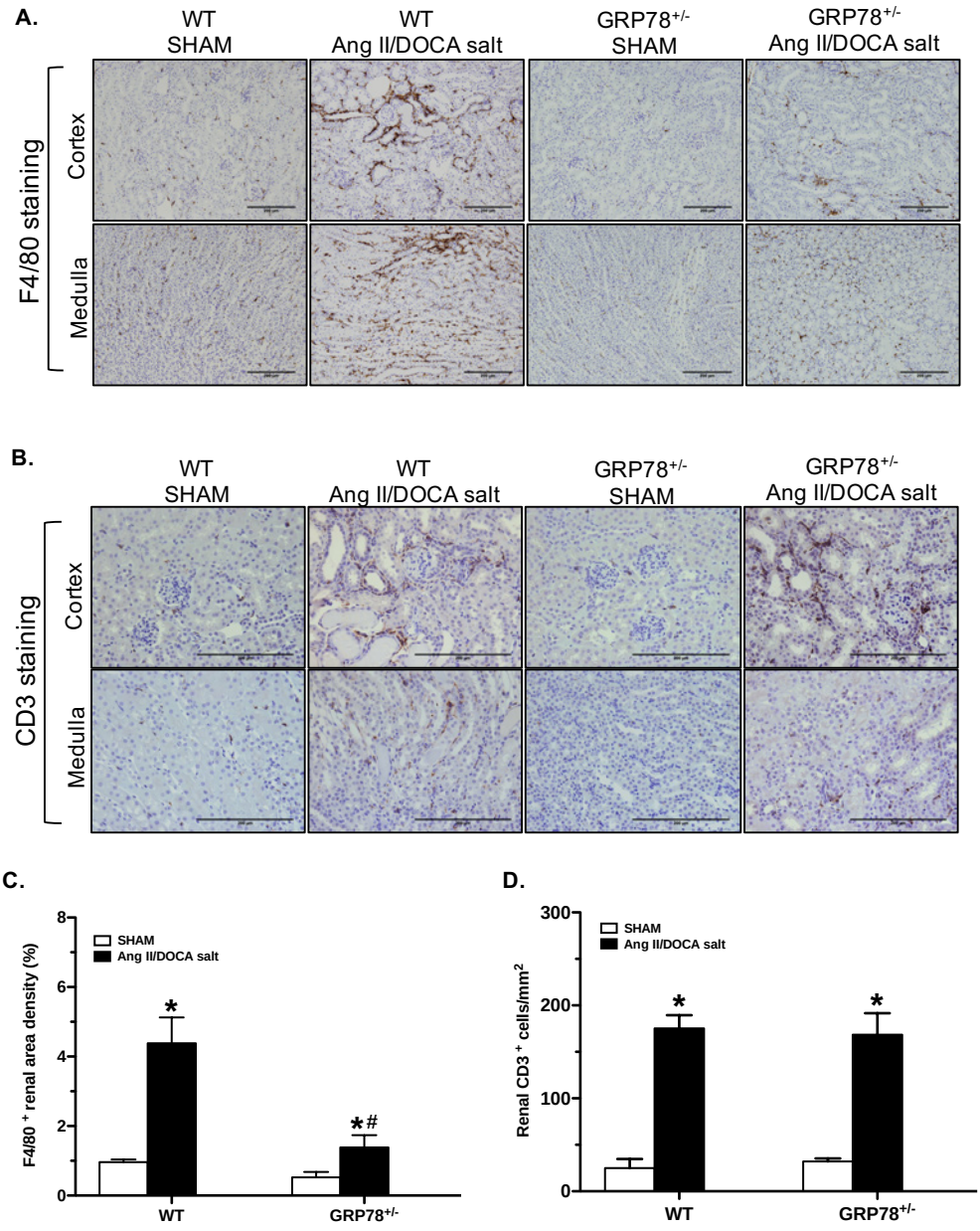
A.
WT SHAM
WT Ang II/DOCA salt
GRP78+/- SHAM
GRP78+/- Ang II/DOCA salt
F4/80 staining
Cortex
Medulla
B.
WT SHAM
WT Ang II/DOCA salt
GRP78+/- SHAM
GRP78+/- Ang II/DOCA salt
CD3 staining
Cortex
Medulla
C.
SHAM
Ang II/DOCA salt
F4/80+ renal area density (%)
0
2
4
6
8
*
*#
WT
GRP78+/-
D.
SHAM
Ang II/DOCA salt
Renal CD3+ cells/mm2
0
100
200
300
*
*
WT
GRP78+/-

FIGURE 5

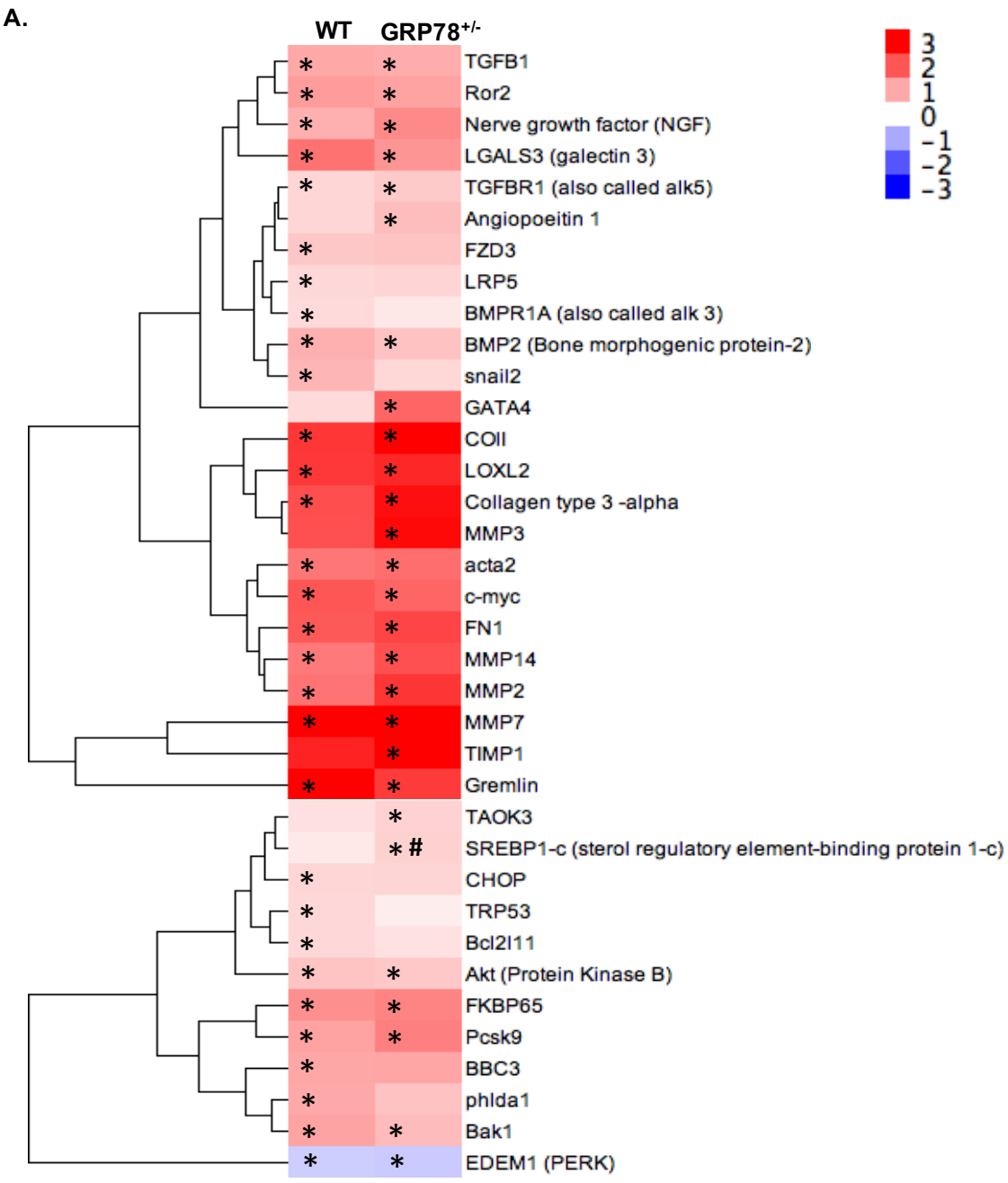
A.
WT
GRP78+/-
3
2
1
0
-1
-2
-3
TGFB1
Ror2
Nerve growth factor (NGF)
LGALS3 (galectin 3)
TGFBR1 (also called alk5)
Angiopoeitin 1
FZD3
LRP5
BMPR1A (also called alk 3)
BMP2 (Bone morphogenic protein-2)
snail2
GATA4
COII
LOXL2
Collagen type 3 -alpha
MMP3
acta2
c-myc
FN1
MMP14
MMP2
MMP7
TIMP1
Gremlin
TAOK3
SREBP1-c (sterol regulatory element-binding protein 1-c)
CHOP
TRP53
Bcl2l11
Akt (Protein Kinase B)
FKBP65
Pcsk9
BBC3
phlda1
Bak1
EDEM1 (PERK)

B.

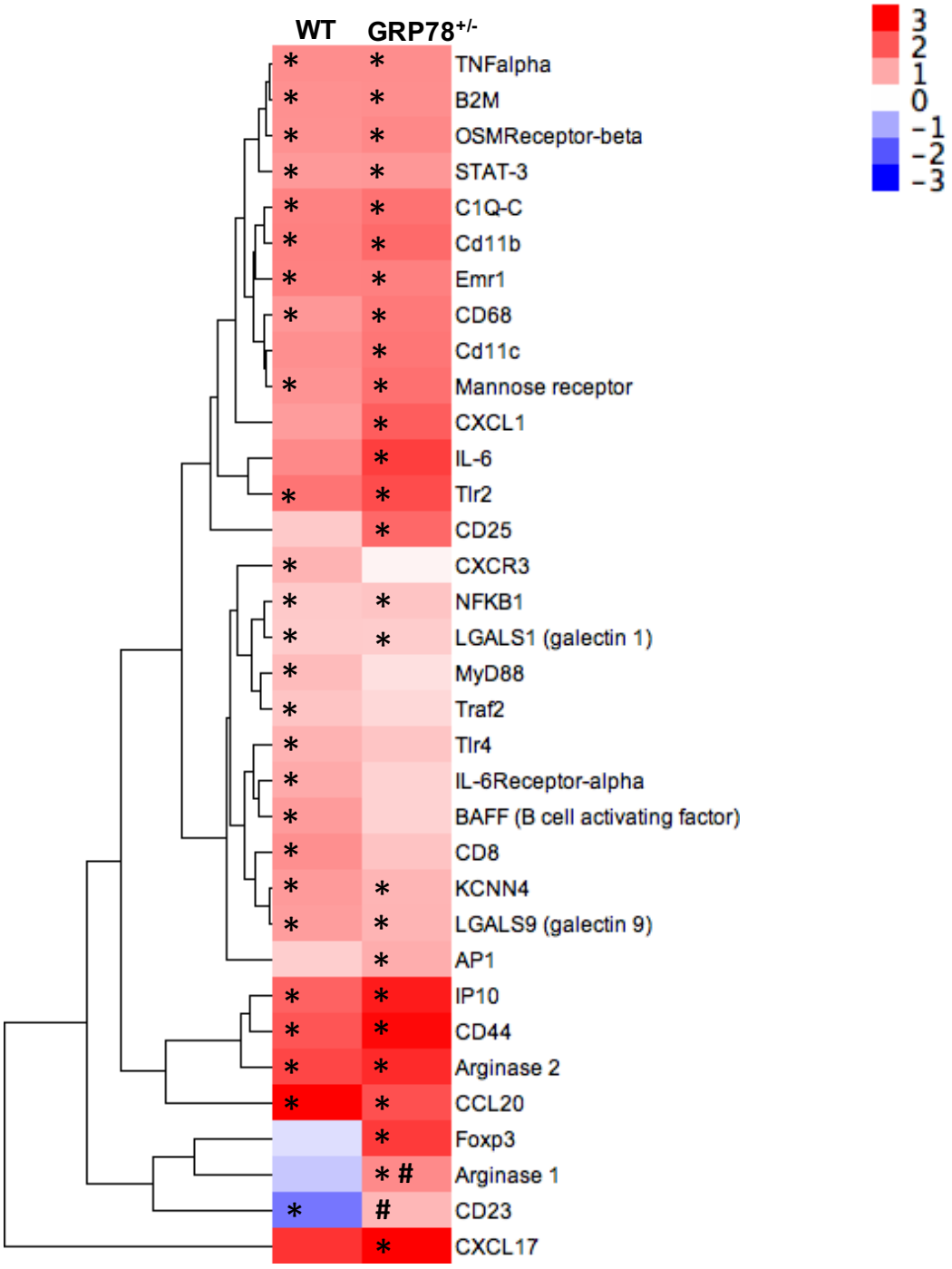
WT
GRP78+/-
TNFalpha
B2M
OSMReceptor-beta
STAT-3
C1Q-C
Cd11b
Emr1
CD68
Cd11c
Mannose receptor
CXCL1
IL-6
Tlr2
CD25
CXCR3
NFKB1
LGALS1 (galectin 1)
MyD88
Traf2
Tlr4
IL-6Receptor-alpha
BAFF (B cell activating factor)
CD8
KCNN4
LGALS9 (galectin 9)
AP1
IP10
CD44
Arginase 2
CCL20
Foxp3
Arginase 1
CD23
CXCL17
3
2
1
0
-1
-2
-3

References

1. **Acharya M, Borland G, Edkins AL, Maclellan LM, Matheson J, Ozanne BW, and Cushley W**. CD23/FcepsilonRII: molecular multi-tasking. *Clin Exp Immunol* 162: 12-23, 2010.

2. **Arai S, Kitada K, Yamazaki T, Takai R, Zhang X, Tsugawa Y, Sugisawa R, Matsumoto A, Mori M, Yoshihara Y, Doi K, Maehara N, Kusunoki S, Takahata A, Noiri E, Suzuki Y, Yahagi N, Nishiyama A, Gunaratnam L, Takano T, and Miyazaki T**. Apoptosis inhibitor of macrophage protein enhances intraluminal debris clearance and ameliorates acute kidney injury in mice. *Nat Med* 22: 183-193, 2016.

3. **Ayaub EA, Kolb PS, Mohammed-Ali Z, Tat V, Murphy J, Bellaye PS, Shimbori C, Boivin FJ, Lai R, Lynn EG, Lhotak S, Bridgewater D, Kolb MR, Inman MD, Dickhout JG, Austin RC, and Ask K**. GRP78 and CHOP modulate macrophage apoptosis and the development of bleomycin-induced pulmonary fibrosis. *J Pathol* 239: 411-425, 2016.

4. **Back SH, and Kaufman RJ**. Endoplasmic reticulum stress and type 2 diabetes. *Annu Rev Biochem* 81: 767-793, 2012.

5. **Boden G**. Endoplasmic reticulum stress: another link between obesity and insulin resistance/inflammation? *Diabetes* 58: 518-519, 2009.

6. **Braga TT, Agudelo JS, and Camara NO**. Macrophages During the Fibrotic Process: M2 as Friend and Foe. *Front Immunol* 6: 602, 2015.

7. **Carlisle RE, Brimble E, Werner KE, Cruz GL, Ask K, Ingram AJ, and Dickhout JG**. 4-Phenylbutyrate inhibits tunicamycin-induced acute kidney injury via CHOP/GADD153 repression. *PLoS One* 9: e84663, 2014.

8. **Cybulsky AV**. Endoplasmic reticulum stress in proteinuric kidney disease. *Kidney Int* 77: 187-193, 2010.

9. **Dickhout JG, Carlisle RE, and Austin RC**. Interrelationship between cardiac hypertrophy, heart failure, and chronic kidney disease: endoplasmic reticulum stress as a mediator of pathogenesis. *Circ Res* 108: 629-642, 2011.

10. **Dickhout JG, and Krepinsky JC**. Endoplasmic reticulum stress and renal disease. *Antioxid Redox Signal* 11: 2341-2352, 2009.

11. **Eller K, Kirsch A, Wolf AM, Sopper S, Tagwerker A, Stanzl U, Wolf D, Patsch W, Rosenkranz AR, and Eller P**. Potential role of regulatory T cells in

reversing obesity-linked insulin resistance and diabetic nephropathy. *Diabetes* 60: 2954-2962, 2011.

12. **Franco A, Almanza G, Burns JC, Wheeler M, and Zanetti M**. Endoplasmic reticulum stress drives a regulatory phenotype in human T-cell clones. *Cell Immunol* 266: 1-6, 2010.

13. **Hu M, Wang YM, Wang Y, Zhang GY, Zheng G, Yi S, O'Connell PJ, Harris DC, and Alexander SI**. Regulatory T cells in kidney disease and transplantation. *Kidney Int* 90: 502-514, 2016.

14. **Inagi R**. Endoplasmic reticulum stress as a progression factor for kidney injury. *Curr Opin Pharmacol* 10: 156-165, 2010.

15. **Kammoun HL, Chabanon H, Hainault I, Luquet S, Magnan C, Koike T, Ferre P, and Foufelle F**. GRP78 expression inhibits insulin and ER stress-induced SREBP-1c activation and reduces hepatic steatosis in mice. *J Clin Invest* 119: 1201-1215, 2009.

16. **Kimura K, Jin H, Ogawa M, and Aoe T**. Dysfunction of the ER chaperone BiP accelerates the renal tubular injury. *Biochem Biophys Res Commun* 366: 1048-1053, 2008.

17. **Kirchhoff F, Krebs C, Abdulhag UN, Meyer-Schwesinger C, Maas R, Helmchen U, Hilgers KF, Wolf G, Stahl RA, and Wenzel U**. Rapid development of severe end-organ damage in C57BL/6 mice by combining DOCA salt and angiotensin II. *Kidney Int* 73: 643-650, 2008.

18. **Lindquist AJ, Mertens, P. R.** Translational Nephrology: Taking Aim at Tubular Debris. *Journal of Clinical & Experimental Nephrology* 1: 2016.

19. **Luo S, Mao C, Lee B, and Lee AS**. GRP78/BiP is required for cell proliferation and protecting the inner cell mass from apoptosis during early mouse embryonic development. *Mol Cell Biol* 26: 5688-5697, 2006.

20. **Mimura N, Hamada H, Kashio M, Jin H, Toyama Y, Kimura K, Iida M, Goto S, Saisho H, Toshimori K, Koseki H, and Aoe T**. Aberrant quality control in the endoplasmic reticulum impairs the biosynthesis of pulmonary surfactant in mice expressing mutant BiP. *Cell Death Differ* 14: 1475-1485, 2007.

21. **Mohammed-Ali Z, Cruz GL, and Dickhout JG**. Crosstalk between the unfolded protein response and NF-kappaB-mediated inflammation in the progression of chronic kidney disease. *J Immunol Res* 2015: 428508, 2015.

22. **Park YJ, Yoo SA, and Kim WU**. Role of endoplasmic reticulum stress in rheumatoid arthritis pathogenesis. *J Korean Med Sci* 29: 2-11, 2014.

23. **Pesce JT, Ramalingam TR, Mentink-Kane MM, Wilson MS, El Kasmi KC, Smith AM, Thompson RW, Cheever AW, Murray PJ, and Wynn TA**. Arginase-1-expressing macrophages suppress Th2 cytokine-driven inflammation and fibrosis. *PLoS Pathog* 5: e1000371, 2009.

24. **Ribeiro CM, and O'Neal WK**. Endoplasmic reticulum stress in chronic obstructive lung diseases. *Curr Mol Med* 12: 872-882, 2012.

25. **Ricardo SD, van Goor H, and Eddy AA**. Macrophage diversity in renal injury and repair. *J Clin Invest* 118: 3522-3530, 2008.

26. **Rogers NM, Ferenbach DA, Isenberg JS, Thomson AW, and Hughes J**. Dendritic cells and macrophages in the kidney: a spectrum of good and evil. *Nat Rev Nephrol* 10: 625-643, 2014.

27. **Roszer T**. Understanding the Mysterious M2 Macrophage through Activation Markers and Effector Mechanisms. *Mediators Inflamm* 2015: 816460, 2015.

28. **Sano R, and Reed JC**. ER stress-induced cell death mechanisms. *Biochim Biophys Acta* 1833: 3460-3470, 2013.

29. **Tabas I, and Ron D**. Integrating the mechanisms of apoptosis induced by endoplasmic reticulum stress. *Nat Cell Biol* 13: 184-190, 2011.

30. **Taniguchi M, and Yoshida H**. Endoplasmic reticulum stress in kidney function and disease. *Curr Opin Nephrol Hypertens* 24: 345-350, 2015.

31. **Tian S, and Chen SY**. Macrophage polarization in kidney diseases. *Macrophage (Houst)* 2: 2015.

32. **Wang M, Wey S, Zhang Y, Ye R, and Lee AS**. Role of the unfolded protein response regulator GRP78/BiP in development, cancer, and neurological disorders. *Antioxid Redox Signal* 11: 2307-2316, 2009.

33. **Wang Y, Wang YP, Zheng G, Lee VW, Ouyang L, Chang DH, Mahajan D, Coombs J, Wang YM, Alexander SI, and Harris DC**. Ex vivo programmed macrophages ameliorate experimental chronic inflammatory renal disease. *Kidney Int* 72: 290-299, 2007.

34. **Wang YM, Zhang GY, Wang Y, Hu M, Wu H, Watson D, Hori S, Alexander IE, Harris DC, and Alexander SI**. Foxp3-transduced polyclonal regulatory T cells protect against chronic renal injury from adriamycin. *J Am Soc Nephrol* 17: 697-706, 2006.

35. **Ye R, Jung DY, Jun JY, Li J, Luo S, Ko HJ, Kim JK, and Lee AS**. Grp78 heterozygosity promotes adaptive unfolded protein response and attenuates diet-induced obesity and insulin resistance. *Diabetes* 59: 6-16, 2010.

36. **Ye R, Mareninova OA, Barron E, Wang M, Hinton DR, Pandol SJ, and Lee AS**. Grp78 heterozygosity regulates chaperone balance in exocrine pancreas with differential response to cerulein-induced acute pancreatitis. *Am J Pathol* 177: 2827-2836, 2010.

37. **Yoo SA, You S, Yoon HJ, Kim DH, Kim HS, Lee K, Ahn JH, Hwang D, Lee AS, Kim KJ, Park YJ, Cho CS, and Kim WU**. A novel pathogenic role of the ER chaperone GRP78/BiP in rheumatoid arthritis. *J Exp Med* 209: 871-886, 2012.

38. **Z Mohammed-Ali GLC, C Lu, R E Carlisle, K E Werner, K Ask, J G Dickhout**. Development of a model of Chronic Kidney Disease in the C57BL/6 mouse with Properties of progressive human CKD. *BioMed Research International* 2015: 2015.

Chapter 5

DISCUSSION

In this chapter, the major findings in preceding chapters of this thesis will be discussed in the context of current literature. The significant findings of the studies constituting Chapters 2-4 have been discussed in depth in each individual chapter's discussion. Therefore, the aim in this section is to summarize the key findings in this thesis and elaborate on how they advance the field of nephrology and their implications on future directions in the study of CKD.

Establishing a CKD mouse model

The manuscript in Chapter 2 involves the characterization of a CKD mouse model comprising of a uninephrectomy combined with Ang II and DOCA infusion via subcutaneous implantation of an Ang II containing osmotic mini pump and a DOCA pellet respectively. Additionally, mice were provided with 1% NaCl in the drinking water. Compared to other models described in Chapter 1 such as the SHR and the Dahl salt sensitive rat, this model produces CKD in the C57BL/6 mouse. The C57BL/6 mouse is a background strain for several genetic knockouts, however, these mice are highly resistant to CKD development via Ang II infusion alone (Kirchhoff et al., 2008), albumin overload (Kato et al., 2008) and renal mass reduction (El-Meanawy et al., 2012). Kirchhoff *et al.* first reported this model where it resulted in significant focal and segmental glomerular sclerosis, proteinuria and protein cast formation in Ang II/DOCA salt but not with isolated DOCA or Ang II treatment (Kirchhoff et al., 2008). In addition, Ang II/DOCA salt mice experienced more pronounced increase in systolic blood pressure and cardiac and renal fibrosis

than in mice treated with Ang II or DOCA alone. The experiments discussed in Chapter 2 extended the analysis performed by Kirchhoff *et al.* by showing an increase in both systolic and diastolic blood pressure, lung damage indicative of pulmonary edema as well as renal apoptosis and macrophage infiltration in response to Ang II/DOCA (Z Mohammed-Ali, 2015). The impact of gender on CKD development was also explored and resulted in the finding that although they developed some aspects of CKD, female mice were protected in this model (Z Mohammed-Ali, 2015). This feature resembles what is observed in human CKD where the male gender is associated with faster progression to ESRD (Eriksen & Ingebretsen, 2006; Neugarten, Acharya, & Silbiger, 2000). Female mice on Ang II/DOCA salt had significantly lower proteinuria and albuminuria and their renal histology showed lower protein cast formation, apoptosis and interstitial fibrosis than male mice (Z Mohammed-Ali, 2015). Consequently, female mice were eliminated from further experiments in this thesis to prevent gender from acting as a confounding variable in our studies. Collectively, our data along with that published by Kirchhoff *et al.*, show that Ang II/DOCA salt model is applicable for the study of both hypertensive CKD and CKD that arises from glomerular disease.

Why did we target ER stress to halt CKD progression?

Currently, the main therapeutic approaches to prevent CKD progression include the control of blood pressure and reduction of proteinuria. At the frontline of this strategy is RAAS blockade through the use of Angiotensin-converting enzyme

(ACE) inhibitors and Ang II receptor blockers (ARBs) (Stevens, Levin, & Kidney Disease: Improving Global Outcomes Chronic Kidney Disease Guideline Development Work Group, 2013).

Ang II, the main effector of RAAS, mediates hemodynamic processes that include vasoconstriction, stimulation of aldosterone secretion and positive inotropic effects resulting in water and salt retention and a rise in blood pressure as well as cellular processes such as fibrosis and inflammation mediated by TGF-β and NF-κB respectively (Benigni, Cassis, & Remuzzi, 2010). The vasoconstrictor effect of Ang II also impacts glomerular arterioles where it causes an increase in glomerular hydraulic pressure. This phenomenon leads to a reduction in glomerular barrier selectivity to protein filtration, a feature of all chronic proteinuric renal disease irrespective of their origin (Long, Price, Herrera-Acosta, & Johnson, 2004; Remuzzi & Bertani, 1998). The increase in filtration of plasma proteins results in proteinuria an important marker of CKD progression and GFR decline (Peterson et al., 1995; Ruggenenti, Perna, Mosconi, Pisoni, & Remuzzi, 1998). Clinically, the degree of proteinuria correlates with adverse outcomes and its reduction is associated with improved renal function and the detection of proteinuria is a defining feature of CKD onset (C. H. Chen et al., 2016; Lamb, MacKenzie, & Stevens, 2009). Consequently, ACE inhibitors and ARBs have been used either separately or more commonly as a combination and have shown success in the management of hypertension and proteinuria (Jafar et al., 2003; Nakamura et al., 1999; Wolf & Ritz,

2005; Yanagi et al., 2013). Recently, however, the benefit of the dual use of ARBs and ACE inhibitors has been greatly questioned. Residual proteinuria occurs in patients on these (Brenner et al., 2001; Eijkelkamp et al., 2007; Ruggenenti, Perna, Remuzzi, & Investigators, 2003), which can impact long-term disease progression. Dual therapy has also been associated with adverse side effects such as increased risk of acute kidney injury and life-threatening hyperkalemia (de Zeeuw, 2013; Jafar & Assam, 2015). Further, multiple clinical trials have shown that dual therapy does not impart substantial improvement in cardiovascular or renal outcomes. In fact, two large randomized controlled trials, the Aliskiren Trial in Type 2 diabetes using cardiorenal endpoints (ALTITUDE) and the Veterans Affairs Nephropathy in diabetes trial (VA NEPHRON-D), were terminated prematurely due to safety concerns (Fried et al., 2013; Parving et al., 2009; Parving et al., 2012). Thus, there is currently a significant need in the field of nephrology to identify therapeutic targets for the treatment of CKD.

Accumulating evidence has demonstrated a role for ER stress in the pathogenesis of kidney disease in association with proteinuria (Cybulsky, 2010; El Karoui et al., 2016; Inagi, 2010). Downstream effects of the UPR pathways include apoptosis, autophagy and inflammation and they can thus impact tubular and glomerular pathophysiology. Indeed, an increase in BiP and CHOP expression has been shown in human kidney biopsies of patients with FSGS, membranous nephropathy and membranoproliferative as well as rapidly progressive

glomerulonephritis (Bek et al., 2006; Markan et al., 2009). These studies implicate a role for ER stress in CKD progression and validate the search for therapeutic targets within UPR pathways.

The UPR, Inflammation and Fibrosis in CKD progression

Studies have demonstrated that ER stress inhibition results in the amelioration of renal injury in various animal models (Dickhout & Krepinsky, 2009; Inagi, 2010). However, the precise mechanisms involved in ER stress-induced renal injury in terms of fibrosis and inflammation have yet to be fully elucidated. In Chapter 3, we sought to establish temporal relationships between UPR activation, fibrosis and inflammation by performing a time point analysis of our CKD mouse model. Nanostring analysis was the method of choice for this aim as it allowed the selection of genes that were either established markers of CKD progression or being studied as therapeutic targets in renal disease. Our results showed a significant increase in hypertensive proteinuria within one week of Ang II/DOCA salt treatment. The UPR was also upregulated at the 7-day mark indicating a role for ER stress in the progression of pathology. Thus, Chapter 3 and Chapter 4 largely included experiments where components of the UPR were manipulated to explore the impact of ER stress inhibition on CKD development. The output from Nanostring analysis is highly applicable for future studies on molecular targets for the treatment of CKD as it provides information about the timing and regulation of certain key pathways during the course of the disease. In fact, the group that first

published on the Ang II/DOCA salt model has also published work on potential targets in hypertensive CKD development. This includes studies on IL-17$^{-/-}$, IL-23p19$^{-/-}$ and CCR5$^{-/-}$ mice, where IL17/IL23 deficiency was shown to worsen albuminuria and glomerular injury whereas CCR5 deficiency had no effect on hypertensive-induced decline in renal function (C. Krebs et al., 2012; C. F. Krebs et al., 2014). By using a gene code set based on literature searches of the current pathways targeted for treatment of CKD, our time point analysis sets the foundation for future work. Nanostring data could be directly used in several future projects by focusing on genes that were upregulated early in response to Ang II/DOCA salt to study their impact on CKD development. This strategy was carried out precisely in Chapter 3 and Chapter 4 where we investigated the effect of CHOP deficiency and GRP78 heterozygosity on Ang II/DOCA salt-induced CKD.

Treatment with 4-PBA resulted in diminished TGF-β and canonical and non-canonical Wnt signaling elements at the mRNA level (Chapter 3). Considering that these pathways play a central role in renal fibrosis, it makes sense that renal histology shows decreased α-smooth muscle actin and collagen deposition with 4-PBA treatment. Similarly, 4-PBA lead to diminished levels of NFκB, AP-1, MCP-1 and TLRs—inflammatory mediators shown to play a role in inflammation in renal disease, as well as F4/80^{+} macrophage and CD3^{+} T cell infiltration. Thus, 4-PBA inhibited fibrosis and inflammation in response to Ang II/DOCA salt making it a potential therapeutic in the treatment of CKD. These results are in agreement with

previous experiments where 4-PBA was associated with decreased levels of NFκB and MCP-1 and reduced fibrosis in animal models of diabetic nephropathy (Luo et al., 2010; Qi et al., 2011). However, our analysis provides a comprehensive list of the various potential inflammatory genes that are involved in the protective effect of ER stress inhibition using 4-PBA.

CHOP is one of the UPR genes, which was upregulated after one week on Ang II/DOCA salt and was significantly decreased with 4-PBA treatment that conferred renoprotection. Various experimental models of kidney disease have investigated the role of CHOP. As indicated in Chapter 3, CHOP deficiency has been shown to ameliorate fibrosis and reduce inflammation in UUO models and animal models of AKI (Carlisle et al., 2014; B. L. Chen et al., 2015; Chiang et al., 2011; Zhang et al., 2015). In the Ang II/DOCA salt model, CHOP deficient animals showed an overall lower level of fibrosis and inflammatory gene regulation as well as decreased macrophage infiltration and ECM deposition. Interestingly, applying the Ang II/DOCA salt model to GRP78$^{+/-}$ mice also resulted in decreased fibrosis and macrophage infiltration. The GRP78$^{+/-}$ mice also showed significantly lower albuminuria and protein cast formation and thus GRP78 heterozygosity had ameliorated CKD induced by Ang II/DOCA salt. In Chapter 4, this finding was discussed from the perspective of a study by Ayaub *et al.*, which showed that GRP78$^{+/-}$ mice were protected in a model of bleomycin-induced pulmonary fibrosis

due to increased CHOP-induced apoptosis in M2 macrophages (Ayaub et al., 2016). The decrease in fibrosis was attributed to lower M2 macrophage numbers.

Our work builds on studies by Harrison, Mattson and Remuzzi that compiled evidence implicating a role for T cells and macrophages in the development of hypertensive kidney disease in several animal models (Benigni et al., 2010; Harrison, 2014; Mattson, 2014). Gene expression data from our Nanostring analysis could therefore be used to further study the various immune cell subsets that are involved in the pathogenesis of CKD.

ER stress inhibition and proteinuria

Chapter 3 demonstrated that inhibiting ER stress using 4-PBA attenuated hypertension, albuminuria and protein cast formation. CHOP deficiency, however, significantly lowered albuminuria and protein cast formation without affecting the development of hypertension due to Ang II/DOCA salt treatment. This finding shows that ER stress inhibition can protect the kidney against proteinuric damage regardless of its effect on hypertension in experimental CKD. The blood pressure lowering effect of 4-PBA has also been observed in the SHR model. In a recent study published by our laboratory, 4-PBA restored vasodilatory responses in SHR resistant vessels and reduced the the media-to-lumen ratio in maximally relaxed renal arcuate arteries and mesenteric vessels (Carlisle et al., 2016). However, an added control for the blood pressure lowering effect of 4-PBA in response to Ang

II/DOCA salt seen in Chapter 3 can include the use of Hydralazine. Hydralazine is a blood pressure-lowering drug that exerts its hypotensive effect by direct relaxation of arteriolar smooth muscle and can be administered in the drinking water in animal studies (Hartono, Knudsen, Lerman, Textor, & Grande, 2014; Jacobs, 1984; Leelahavanichkul et al., 2010). Interestingly, experiments using a diabetic db/db mouse model (Hartono et al., 2014) and a model of renal mass reduction (Leelahavanichkul et al., 2010) showed that while hydralazine was able to significantly lower blood pressure comparable to treatment with ARBs, it had no effect on urinary protein excretion. Therefore, theoretically, if hydralazine was given to mice on the Ang II/DOCA salt model, one would expect reduced hypertension but unchanged proteinuria and thus a different outcome than with 4-PBA treatment. Such an experiment would further establish the protective effect of 4-PBA as a result of its ER stress inhibiting property (i.e. its actions as a small molecular weight chaperone) as opposed to being attributed to its blood pressure lowering effect.

In the experiments in Chapter 3, 4-PBA is shown to upregulate cubilin, a peripheral membrane protein expressed on the apical plasma membrane of renal proximal tubule cells that is responsible for the reabsorption of proteins (Verroust & Christensen, 2002). We speculate that during Ang II/DOCA salt-induced CKD, the hyperfiltration of proteins results in an increased demand for cubilin thereby causing ER stress. As a chaperone molecule, 4-PBA is able to aid in protein folding in the ER thus alleviating ER stress. This may have made more cubilin available

for reabsorption of filtered proteins such as albumin. The question then arises as to whether this is the mechanism by which 4-PBA attenuates albuminuria in our model. Based on glomerular scoring, we show in Chapter 3 that 4-PBA treatment also results in decreased glomerulosclerosis in response to Ang II/DOCA salt. Therefore, although we have shown that 4-PBA acts to increase cubilin, the decrease in urinary albumin excretion could also be attributed to the preservation of glomerular structure in 4-PBA treated animals. Interestingly, an in vitro study by Liu et al. on human embryonic kidney 293 cells that stably express either wild type or missense nephrin mutants retained in the ER showed that treatment with 4-PBA rescued some of the nephrin mutants to the cell surface where they were able to function in the same manner as wild type (Liu et al., 2004). This data suggests that 4-PBA may be improving urinary albumin excretion by alleviating ER stress in both glomerular and tubular cells; however, further experiments are required to determine the relative contribution of glomerular and tubular effects in reducing albuminuria.

ER stress inhibition through CHOP deficiency, however, resulted in an increase in nephrin mRNA and protein levels in the kidney demonstrating a direct link between ER stress inhibition and maintenance of glomerular integrity. These results are built on previous work by Cybulsky *et al.* which established that nephrin had a short open reading frame similar to ATF4 and was preferentially translated during global translation attenuation induced by eIF2α phosphorylation during ER

stress (Cybulsky, Takano, Papillon, & Bijian, 2005). The recovery of protein translation occurs through the activation of GADD34 by CHOP upregulation under ER stress conditions (Marciniak et al., 2004). CHOP deficient mice have lower GADD34 activity thus prolonging the global translation attenuation phase thereby allowing the translation of more proteins with short open reading frames such as nephrin leading to the preservation of glomerular structure. To further galvanise this theory, in vitro experiments could be performed using a similar setup as Cybulsky et al. where COS cells were used since cultured glomerular epithelial cells do not typically express nephrin. This group showed an increase in eIF2α phosphorylation in an in vitro model of anoxia/recovery (Cybulsky et al., 2005). Transfection with a DNA construct containing a CMV promoter linked to a GFP reporter and the 391-nucleotide fragment of nephrin 5'-flanking region from the nephrin transcription start site to the initiation ATG codon lead to an increase in GRP expression during anoxia/recovery meaning that nephrin was preferentially translated during eIF2α phosphorylation (Cybulsky et al., 2005). To validate the increase in nephrin in CHOP$^{-/-}$ mice with CKD, mouse embryonic fibroblasts from CHOP$^{-/-}$ mice could be transfected with the DNA constructs and then treated with ER stress-inducing agents TM and/or TG (both discussed in Chapter 1). Another interesting experiment would involve the use of GSK2606414, a selective PERK inhibitor, or Salbubrinal, a phosphatase inhibitor of eIF2α activation (both described in Chapter 1), to inhibit the molecular steps upstream of CHOP. These pharmacological interventions could be administered to mice undergoing CKD

through the Ang II/DOCA salt model to investigate their impact on CKD development by preserving glomerular integrity. However, preliminary in vitro experiments would be required first to assess the efficacy of these drugs in CHOP inhibition.

Summary and concluding thoughts

The research presented in Chapters 2-4 has included: 1) a characterization of a CKD mouse model in the C57BL/6 mouse, 2) a time point analysis demonstrating the genes regulated during CKD progression in this model, 3) A pharmacological intervention using 4-PBA and 4) Genetic manipulation of UPR genes, CHOP and GRP78 to investigate the effect of UPR modulation on CKD development.

The model of CKD characterized in Chapter 2 of this thesis is highly applicable to basic science research in nephrology. Primarily, the induction of CKD by Ang II/DOCA showed key features of human CKD such as proteinuria, glomeruloscleoris, fibrosis, inflammation and apoptosis. Moreover, the increased RAAS activity observed in the kidneys of CKD patients makes this model increasingly clinically relevant. Establishing this model in the C57BL/6 mouse, a background strain for many genetic knockouts that is generally resistant to CKD induction by renal mass reduction or albumin overload widens the scope of its application to different studies. Next, in Chapter 3, regulation of UPR, inflammation and fibrosis genes was studied in the context of CKD progression. The UPR was

shown to be regulated early in Ang II/DOCA salt induced CKD. Thus, the UPR was modulated pharmacologically using 4-PBA (Chapter 3) and genetically using $CHOP^{-/-}$ mice (Chapter 3) and $GRP78^{+/-}$ mice (Chapter 4). Treatment with 4-PBA and CHOP deficiency resulted in attenuated disease that was associated with the effects of ER stress inhibition on maintaining glomerular structure and tubular reabsorption of hyperfiltered albumin. GRP78 heterozygosity also resulted in protection from proteinuria, albuminuria and protein cast formation. The decrease in macrophages observed in $GRP78^{+/-}$ mice treated with Ang II/DOCA salt is a future avenue to explore the mechanism behind the renoprotection imparted by GRP78 heterozygosity.

Overall, this project has established CHOP as a potential therapeutic target and provided data on its action on the glomerular compartment. The therapeutic benefits of 4-PBA, an FDA-approved drug already prescribed to treat urea cycle disorders was also demonstrated. The value of the experiments in this thesis lies in the foundation they have assembled for future work on the treatment of hypertensive, proteinuric CKD.

References for Chapters 1 & 5

Agarwal, R., Campbell, R. C., & Warnock, D. G. (2004). Oxidative stress in hypertension and chronic kidney disease: role of angiotensin II. *Semin Nephrol, 24*(2), 101-114.

Al Banchaabouchi, M., Marescau, B., D'Hooge, R., Van Marck, E., Van Daele, A., Levillain, O., & De Deyn, P. P. (1998). Biochemical and histopathological changes in nephrectomized mice. *Metabolism, 47*(3), 355-361.

Anand, S., Bitton, A., & Gaziano, T. (2013). The gap between estimated incidence of end-stage renal disease and use of therapy. *PLoS One, 8*(8), e72860. doi:10.1371/journal.pone.0072860

Arendshorst, W. J., & Beierwaltes, W. H. (1979). Renal and nephron hemodynamics in spontaneously hypertensive rats. *Am J Physiol, 236*(3), F246-251.

Axten, J. M., Medina, J. R., Feng, Y., Shu, A., Romeril, S. P., Grant, S. W., . . . Gampe, R. T. (2012). Discovery of 7-methyl-5-(1-{[3-(trifluoromethyl)phenyl]acetyl}-2,3-dihydro-1H-indol-5-yl)-7H-p yrrolo[2,3-d]pyrimidin-4-amine (GSK2606414), a potent and selective first-in-class inhibitor of protein kinase R (PKR)-like endoplasmic reticulum kinase (PERK). *J Med Chem, 55*(16), 7193-7207. doi:10.1021/jm300713s

Ayaub, E. A., Kolb, P. S., Mohammed-Ali, Z., Tat, V., Murphy, J., Bellaye, P. S., . . . Ask, K. (2016). GRP78 and CHOP modulate macrophage apoptosis and the development of bleomycin-induced pulmonary fibrosis. *J Pathol, 239*(4), 411-425. doi:10.1002/path.4738

Bakris, G. L., Weir, M. R., Shanifar, S., Zhang, Z., Douglas, J., van Dijk, D. J., . . . Group, R. S. (2003). Effects of blood pressure level on progression of diabetic nephropathy: results from the RENAAL study. *Arch Intern Med, 163*(13), 1555-1565. doi:10.1001/archinte.163.13.1555

Baldwin, A. S., Jr. (1996). The NF-kappa B and I kappa B proteins: new discoveries and insights. *Annu Rev Immunol, 14*, 649-683. doi:10.1146/annurev.immunol.14.1.649

Barreto, F. C., Barreto, D. V., Liabeuf, S., Meert, N., Glorieux, G., Temmar, M., . . . European Uremic Toxin Work, G. (2009). Serum indoxyl sulfate is associated with vascular disease and mortality in chronic kidney disease patients. *Clin J Am Soc Nephrol, 4*(10), 1551-1558. doi:10.2215/CJN.03980609

Barri, Y. M. (2008). Hypertension and kidney disease: a deadly connection. *Curr Hypertens Rep, 10*(1), 39-45.

Basseri, S., Lhotak, S., Sharma, A. M., & Austin, R. C. (2009). The chemical chaperone 4-phenylbutyrate inhibits adipogenesis by modulating the unfolded protein response. *J Lipid Res, 50*(12), 2486-2501. doi:10.1194/jlr.M900216-JLR200

Baum, J., & Duffy, H. S. (2011). Fibroblasts and myofibroblasts: what are we talking about? *J Cardiovasc Pharmacol, 57*(4), 376-379. doi:10.1097/FJC.0b013e3182116e39

Beg, A. A., Ruben, S. M., Scheinman, R. I., Haskill, S., Rosen, C. A., & Baldwin, A. S., Jr. (1992). I kappa B interacts with the nuclear localization sequences of the subunits of NF-kappa B: a mechanism for cytoplasmic retention. *Genes Dev, 6*(10), 1899-1913.

Bek, M. F., Bayer, M., Muller, B., Greiber, S., Lang, D., Schwab, A., . . . Pavenstadt, H. (2006). Expression and function of C/EBP homology protein (GADD153) in podocytes. *Am J Pathol, 168*(1), 20-32. doi:10.2353/ajpath.2006.040774

Benigni, A., Cassis, P., & Remuzzi, G. (2010). Angiotensin II revisited: new roles in inflammation, immunology and aging. *EMBO Mol Med, 2*(7), 247-257. doi:10.1002/emmm.201000080

Berger, E., & Haller, D. (2011). Structure-function analysis of the tertiary bile acid TUDCA for the resolution of endoplasmic reticulum stress in intestinal epithelial cells. *Biochem Biophys Res Commun, 409*(4), 610-615. doi:10.1016/j.bbrc.2011.05.043

Biswas, S. K., & de Faria, J. B. (2007). Which comes first: renal inflammation or oxidative stress in spontaneously hypertensive rats? *Free Radic Res, 41*(2), 216-224. doi:10.1080/10715760601059672

Blizard, D. A., Peterson, W. N., Iskandar, S. S., Shihabi, Z. K., & Adams, N. (1991). The effect of a high salt diet and gender on blood pressure, urinary protein excretion and renal pathology in SHR rats. *Clin Exp Hypertens A, 13*(5), 687-697.

Bouvier, N., Flinois, J. P., Gilleron, J., Sauvage, F. L., Legendre, C., Beaune, P., . . . Pallet, N. (2009). Cyclosporine triggers endoplasmic reticulum stress in endothelial cells: a role for endothelial phenotypic changes and death. *Am J Physiol Renal Physiol, 296*(1), F160-169. doi:10.1152/ajprenal.90567.2008

Boyce, M., Bryant, K. F., Jousse, C., Long, K., Harding, H. P., Scheuner, D., . . . Yuan, J. (2005). A selective inhibitor of eIF2alpha dephosphorylation protects cells from ER stress. *Science, 307*(5711), 935-939. doi:10.1126/science.1101902

Brenner, B. M., Cooper, M. E., de Zeeuw, D., Keane, W. F., Mitch, W. E., Parving, H. H., . . . Investigators, R. S. (2001). Effects of losartan on renal and cardiovascular outcomes in patients with type 2 diabetes and nephropathy. *N Engl J Med, 345*(12), 861-869. doi:10.1056/NEJMoa011161

Bubb, K. J., Khambata, R. S., & Ahluwalia, A. (2012). Sexual dimorphism in rodent models of hypertension and atherosclerosis. *Br J Pharmacol, 167*(2), 298-312. doi:10.1111/j.1476-5381.2012.02036.x

Buitrago-Rey, R., Olarte, J., & Gomez-Marin, J. E. (2002). Evaluation of two inhibitors of invasion: LY311727 [3-(3-acetamide-1-benzyl-2-ethyl-indolyl-5-oxy)propane phosphonic acid] and AEBSF [4-(2-aminoethyl)-benzenesulphonyl fluoride] in acute murine toxoplasmosis. *J Antimicrob Chemother, 49*(5), 871-874.

Campese, V. M. (1994). Salt sensitivity in hypertension. Renal and cardiovascular implications. *Hypertension, 23*(4), 531-550.

Carlisle, R. E., Brimble, E., Werner, K. E., Cruz, G. L., Ask, K., Ingram, A. J., & Dickhout, J. G. (2014). 4-Phenylbutyrate inhibits tunicamycin-induced acute kidney injury via CHOP/GADD153 repression. *PLoS One, 9*(1), e84663. doi:10.1371/journal.pone.0084663

Carlisle, R. E., Heffernan, A., Brimble, E., Liu, L., Jerome, D., Collins, C. A., . . . Dickhout, J. G. (2012). TDAG51 mediates epithelial-to-mesenchymal transition in human proximal tubular epithelium. *Am J Physiol Renal Physiol, 303*(3), F467-481. doi:10.1152/ajprenal.00481.2011

Carlisle, R. E., Werner, K. E., Yum, V., Lu, C., Tat, V., Memon, M., . . . Dickhout, J. G. (2016). Endoplasmic reticulum stress inhibition reduces hypertension through the preservation of resistance blood vessel structure and function. *J Hypertens, 34*(8), 1556-1569. doi:10.1097/HJH.0000000000000943

Chen, B. L., Sheu, M. L., Tsai, K. S., Lan, K. C., Guan, S. S., Wu, C. T., . . . Liu, S. H. (2015). CCAAT-Enhancer-Binding Protein Homologous Protein Deficiency Attenuates Oxidative Stress and Renal Ischemia-Reperfusion Injury. *Antioxid Redox Signal, 23*(15), 1233-1245. doi:10.1089/ars.2013.5768

Chen, C. H., Wu, H. Y., Wang, C. L., Yang, F. J., Wu, P. C., Hung, S. C., . . . Hung, K. Y. (2016). Proteinuria as a Therapeutic Target in Advanced Chronic Kidney Disease: a Retrospective Multicenter Cohort Study. *Sci Rep, 6*, 26539. doi:10.1038/srep26539

Chen, Y., & Brandizzi, F. (2013). IRE1: ER stress sensor and cell fate executor. *Trends Cell Biol, 23*(11), 547-555. doi:10.1016/j.tcb.2013.06.005

Chiang, C. K., Hsu, S. P., Wu, C. T., Huang, J. W., Cheng, H. T., Chang, Y. W., . . . Liu, S. H. (2011). Endoplasmic reticulum stress implicated in the development of renal fibrosis. *Mol Med, 17*(11-12), 1295-1305. doi:10.2119/molmed.2011.00131

Colgan, S. M., Tang, D., Werstuck, G. H., & Austin, R. C. (2007). Endoplasmic reticulum stress causes the activation of sterol regulatory element binding protein-2. *Int J Biochem Cell Biol, 39*(10), 1843-1851. doi:10.1016/j.biocel.2007.05.002

Conrad, C. H., Brooks, W. W., Hayes, J. A., Sen, S., Robinson, K. G., & Bing, O. H. (1995). Myocardial fibrosis and stiffness with hypertrophy and heart failure in the spontaneously hypertensive rat. *Circulation, 91*(1), 161-170.

Cordellini, S. (1999). Endothelial dysfunction in DOCA-salt hypertension: possible involvement of prostaglandin endoperoxides. *Gen Pharmacol, 32*(3), 315-320.

Cowley, A. W., Jr., & Roman, R. J. (1996). The role of the kidney in hypertension. *JAMA, 275*(20), 1581-1589.

Cowley, A. W., Jr., Roman, R. J., Kaldunski, M. L., Dumas, P., Dickhout, J. G., Greene, A. S., & Jacob, H. J. (2001). Brown Norway chromosome 13

confers protection from high salt to consomic Dahl S rat. *Hypertension, 37*(2 Pt 2), 456-461.
Cybulsky, A. V. (2010). Endoplasmic reticulum stress in proteinuric kidney disease. *Kidney Int, 77*(3), 187-193. doi:10.1038/ki.2009.389
Cybulsky, A. V., Takano, T., Papillon, J., & Bijian, K. (2005). Role of the endoplasmic reticulum unfolded protein response in glomerular epithelial cell injury. *J Biol Chem, 280*(26), 24396-24403. doi:10.1074/jbc.M500729200
Dahl, L. K., Heine, M., & Tassinari, L. (1962). Role of genetic factors in susceptibility to experimental hypertension due to chronic excess salt ingestion. *Nature, 194*, 480-482.
Dahl, L. K., Heine, M., & Tassinari, L. (1963). Effects of Chronic Excess Salt Ingestion. Role of Genetic Factors in Both Doca-Salt and Renal Hypertension. *J Exp Med, 118*, 605-617.
Davis, R. J. (2000). Signal transduction by the JNK group of MAP kinases. *Cell, 103*(2), 239-252.
De Miguel, C., Das, S., Lund, H., & Mattson, D. L. (2010). T lymphocytes mediate hypertension and kidney damage in Dahl salt-sensitive rats. *Am J Physiol Regul Integr Comp Physiol, 298*(4), R1136-1142. doi:10.1152/ajpregu.00298.2009
de Zeeuw, D. (2013). The end of dual therapy with renin-angiotensin-aldosterone system blockade? *N Engl J Med, 369*(20), 1960-1962. doi:10.1056/NEJMe1312286
Deng, J., Lu, P. D., Zhang, Y., Scheuner, D., Kaufman, R. J., Sonenberg, N., . . . Ron, D. (2004). Translational repression mediates activation of nuclear factor kappa B by phosphorylated translation initiation factor 2. *Mol Cell Biol, 24*(23), 10161-10168. doi:10.1128/MCB.24.23.10161-10168.2004
Deng, L. Y., & Schiffrin, E. L. (1992). Effects of endothelin on resistance arteries of DOCA-salt hypertensive rats. *Am J Physiol, 262*(6 Pt 2), H1782-1787.
Dickhout, J. G., Carlisle, R. E., Jerome, D. E., Mohammed-Ali, Z., Jiang, H., Yang, G., . . . Austin, R. C. (2012). Integrated stress response modulates cellular redox state via induction of cystathionine gamma-lyase: cross-talk between integrated stress response and thiol metabolism. *J Biol Chem, 287*(10), 7603-7614. doi:10.1074/jbc.M111.304576
Dickhout, J. G., & Krepinsky, J. C. (2009). Endoplasmic reticulum stress and renal disease. *Antioxid Redox Signal, 11*(9), 2341-2352. doi:10.1089/ARS.2009.2705
Dickhout, J. G., & Lee, R. M. (1997). Structural and functional analysis of small arteries from young spontaneously hypertensive rats. *Hypertension, 29*(3), 781-789.
Ding, W., Wang, B., Zhang, M., & Gu, Y. (2016). Involvement of Endoplasmic Reticulum Stress in Uremic Cardiomyopathy: Protective Effects of Tauroursodeoxycholic Acid. *Cell Physiol Biochem, 38*(1), 141-152. doi:10.1159/000438616

Dobrzynski, E., Wang, C., Chao, J., & Chao, L. (2000). Adrenomedullin gene delivery attenuates hypertension, cardiac remodeling, and renal injury in deoxycorticosterone acetate-salt hypertensive rats. *Hypertension, 36*(6), 995-1001.

Drenjancevic-Peric, I., Jelakovic, B., Lombard, J. H., Kunert, M. P., Kibel, A., & Gros, M. (2011). High-salt diet and hypertension: focus on the renin-angiotensin system. *Kidney Blood Press Res, 34*(1), 1-11. doi:10.1159/000320387

Dworkin, L. D., & Feiner, H. D. (1986). Glomerular injury in uninephrectomized spontaneously hypertensive rats. A consequence of glomerular capillary hypertension. *J Clin Invest, 77*(3), 797-809. doi:10.1172/JCI112377

Eijkelkamp, W. B., Zhang, Z., Remuzzi, G., Parving, H. H., Cooper, M. E., Keane, W. F., . . . de Zeeuw, D. (2007). Albuminuria is a target for renoprotective therapy independent from blood pressure in patients with type 2 diabetic nephropathy: post hoc analysis from the Reduction of Endpoints in NIDDM with the Angiotensin II Antagonist Losartan (RENAAL) trial. *J Am Soc Nephrol, 18*(5), 1540-1546. doi:10.1681/ASN.2006050445

El Karoui, K., Viau, A., Dellis, O., Bagattin, A., Nguyen, C., Baron, W., . . . Terzi, F. (2016). Endoplasmic reticulum stress drives proteinuria-induced kidney lesions via Lipocalin 2. *Nat Commun, 7*, 10330. doi:10.1038/ncomms10330

El-Meanawy, A., Schelling, J. R., Iyengar, S. K., Hayden, P., Barathan, S., Goddard, K., . . . Sedor, J. R. (2012). Identification of nephropathy candidate genes by comparing sclerosis-prone and sclerosis-resistant mouse strain kidney transcriptomes. *BMC Nephrol, 13*, 61. doi:10.1186/1471-2369-13-61

Elmarakby, A. A., Quigley, J. E., Imig, J. D., Pollock, J. S., & Pollock, D. M. (2008). TNF-alpha inhibition reduces renal injury in DOCA-salt hypertensive rats. *Am J Physiol Regul Integr Comp Physiol, 294*(1), R76-83. doi:10.1152/ajpregu.00466.2007

Enomoto, A., Takeda, M., Tojo, A., Sekine, T., Cha, S. H., Khamdang, S., . . . Niwa, T. (2002). Role of organic anion transporters in the tubular transport of indoxyl sulfate and the induction of its nephrotoxicity. *J Am Soc Nephrol, 13*(7), 1711-1720.

Eriksen, B. O., & Ingebretsen, O. C. (2006). The progression of chronic kidney disease: a 10-year population-based study of the effects of gender and age. *Kidney Int, 69*(2), 375-382. doi:10.1038/sj.ki.5000058

Feld, L. G., Van Liew, J. B., Brentjens, J. R., & Boylan, J. W. (1981). Renal lesions and proteinuria in the spontaneously hypertensive rat made normotensive by treatment. *Kidney Int, 20*(5), 606-614.

Feldman, D., & Koong, A. C. (2007). Irestatin, a potent inhibitor of IRE1{alpha} and the unfolded protein response, is a hypoxia-selective cytotoxin and impairs tumor growth. *J Clin Oncol, 25*(18S).

Fleck, C., Appenroth, D., Jonas, P., Koch, M., Kundt, G., Nizze, H., & Stein, G. (2006). Suitability of 5/6 nephrectomy (5/6NX) for the induction of interstitial renal fibrosis in rats--influence of sex, strain, and surgical procedure. *Exp Toxicol Pathol, 57*(3), 195-205. doi:10.1016/j.etp.2005.09.005

Fried, L. F., Emanuele, N., Zhang, J. H., Brophy, M., Conner, T. A., Duckworth, W., . . . Investigators, V. N.-D. (2013). Combined angiotensin inhibition for the treatment of diabetic nephropathy. *N Engl J Med, 369*(20), 1892-1903. doi:10.1056/NEJMoa1303154

Garg, A. D., Kaczmarek, A., Krysko, O., Vandenabeele, P., Krysko, D. V., & Agostinis, P. (2012). ER stress-induced inflammation: does it aid or impede disease progression? *Trends Mol Med, 18*(10), 589-598. doi:10.1016/j.molmed.2012.06.010

Ghosh, S. S., Massey, H. D., Krieg, R., Fazelbhoy, Z. A., Ghosh, S., Sica, D. A., . . . Gehr, T. W. (2009). Curcumin ameliorates renal failure in 5/6 nephrectomized rats: role of inflammation. *Am J Physiol Renal Physiol, 296*(5), F1146-1157. doi:10.1152/ajprenal.90732.2008

Greene, A. S., Yu, Z. Y., Roman, R. J., & Cowley, A. W., Jr. (1990). Role of blood volume expansion in Dahl rat model of hypertension. *Am J Physiol, 258*(2 Pt 2), H508-514.

Griffin, K. A., & Bidani, A. K. (2009). Angiotensin II type 2 receptor in chronic kidney disease: the good side of angiotensin II? *Kidney Int, 75*(10), 1006-1008. doi:10.1038/ki.2009.59

Guo, X. F., & Yang, X. J. (2015). Endoplasmic reticulum stress response in spontaneously hypertensive rats is affected by myocardial ischemia reperfusion injury. *Exp Ther Med, 9*(2), 319-326. doi:10.3892/etm.2014.2094

Han, S. W., Li, C., Ahn, K. O., Lim, S. W., Song, H. G., Jang, Y. S., . . . Yang, C. W. (2008). Prolonged endoplasmic reticulum stress induces apoptotic cell death in an experimental model of chronic cyclosporine nephropathy. *Am J Nephrol, 28*(5), 707-714. doi:10.1159/000127432

Harrison, D. G. (2014). The immune system in hypertension. *Trans Am Clin Climatol Assoc, 125*, 130-138; discussion 138-140.

Hartner, A., Cordasic, N., Klanke, B., Veelken, R., & Hilgers, K. F. (2003). Strain differences in the development of hypertension and glomerular lesions induced by deoxycorticosterone acetate salt in mice. *Nephrol Dial Transplant, 18*(10), 1999-2004. doi:10.1093/ndt/gfg299

Hartono, S. P., Knudsen, B. E., Lerman, L. O., Textor, S. C., & Grande, J. P. (2014). Combined effect of hyperfiltration and renin angiotensin system activation on development of chronic kidney disease in diabetic db/db mice. *BMC Nephrol, 15*, 58. doi:10.1186/1471-2369-15-58

Hasenfuss, G. (1998). Animal models of human cardiovascular disease, heart failure and hypertrophy. *Cardiovasc Res, 39*(1), 60-76.

Hasnain, S. Z., Lourie, R., Das, I., Chen, A. C., & McGuckin, M. A. (2012). The interplay between endoplasmic reticulum stress and inflammation. *Immunol Cell Biol, 90*(3), 260-270. doi:10.1038/icb.2011.112

Hayakawa, H., Coffee, K., & Raij, L. (1997). Endothelial dysfunction and cardiorenal injury in experimental salt-sensitive hypertension: effects of antihypertensive therapy. *Circulation, 96*(7), 2407-2413.

Hetz, C., Martinon, F., Rodriguez, D., & Glimcher, L. H. (2011). The unfolded protein response: integrating stress signals through the stress sensor IRE1alpha. *Physiol Rev, 91*(4), 1219-1243. doi:10.1152/physrev.00001.2011

Hoagland, K. M., Flasch, A. K., Dahly-Vernon, A. J., dos Santos, E. A., Knepper, M. A., & Roman, R. J. (2004). Elevated BSC-1 and ROMK expression in Dahl salt-sensitive rat kidneys. *Hypertension, 43*(4), 860-865. doi:10.1161/01.HYP.0000120123.44945.47

Hotamisligil, G. S. (2010). Endoplasmic reticulum stress and the inflammatory basis of metabolic disease. *Cell, 140*(6), 900-917. doi:10.1016/j.cell.2010.02.034

Hsu, C. Y., Lin, F., Vittinghoff, E., & Shlipak, M. G. (2003). Racial differences in the progression from chronic renal insufficiency to end-stage renal disease in the United States. *J Am Soc Nephrol, 14*(11), 2902-2907.

Hu, P., Han, Z., Couvillon, A. D., Kaufman, R. J., & Exton, J. H. (2006). Autocrine tumor necrosis factor alpha links endoplasmic reticulum stress to the membrane death receptor pathway through IRE1alpha-mediated NF-kappaB activation and down-regulation of TRAF2 expression. *Mol Cell Biol, 26*(8), 3071-3084. doi:10.1128/MCB.26.8.3071-3084.2006

Hye Khan, M. A., Neckar, J., Manthati, V., Errabelli, R., Pavlov, T. S., Staruschenko, A., . . . Imig, J. D. (2013). Orally active epoxyeicosatrienoic acid analog attenuates kidney injury in hypertensive Dahl salt-sensitive rat. *Hypertension, 62*(5), 905-913. doi:10.1161/HYPERTENSIONAHA.113.01949

Inagi, R. (2009). Endoplasmic reticulum stress in the kidney as a novel mediator of kidney injury. *Nephron Exp Nephrol, 112*(1), e1-9. doi:000210573 [pii]
10.1159/000210573

Inagi, R. (2010). Endoplasmic reticulum stress as a progression factor for kidney injury. *Curr Opin Pharmacol, 10*(2), 156-165. doi:10.1016/j.coph.2009.11.006

Iyer, A., Chan, V., & Brown, L. (2010). The DOCA-Salt Hypertensive Rat as a Model of Cardiovascular Oxidative and Inflammatory Stress. *Curr Cardiol Rev, 6*(4), 291-297. doi:10.2174/157340310793566109

Jacobs, M. (1984). Mechanism of action of hydralazine on vascular smooth muscle. *Biochem Pharmacol, 33*(18), 2915-2919.

Jadhav, A., Torlakovic, E., & Ndisang, J. F. (2009). Hemin therapy attenuates kidney injury in deoxycorticosterone acetate-salt hypertensive rats. *Am J Physiol Renal Physiol, 296*(3), F521-534. doi:10.1152/ajprenal.00510.2007

Jafar, T. H., & Assam, P. N. (2015). Dual RAAS blockade for kidney failure: hope for the future. *Lancet, 385*(9982), 2018-2020. doi:10.1016/S0140-6736(15)60132-5

Jafar, T. H., Stark, P. C., Schmid, C. H., Landa, M., Maschio, G., de Jong, P. E., . . . Group, A. S. (2003). Progression of chronic kidney disease: the role of blood pressure control, proteinuria, and angiotensin-converting enzyme inhibition: a patient-level meta-analysis. *Ann Intern Med, 139*(4), 244-252.

Jager, R., Bertrand, M. J., Gorman, A. M., Vandenabeele, P., & Samali, A. (2012). The unfolded protein response at the crossroads of cellular life and death during endoplasmic reticulum stress. *Biol Cell, 104*(5), 259-270. doi:10.1111/boc.201100055

Jha, V., Garcia-Garcia, G., Iseki, K., Li, Z., Naicker, S., Plattner, B., . . . Yang, C. W. (2013). Chronic kidney disease: global dimension and perspectives. *Lancet, 382*(9888), 260-272. doi:10.1016/S0140-6736(13)60687-X

Jiang, H. Y., Wek, S. A., McGrath, B. C., Scheuner, D., Kaufman, R. J., Cavener, D. R., & Wek, R. C. (2003). Phosphorylation of the alpha subunit of eukaryotic initiation factor 2 is required for activation of NF-kappaB in response to diverse cellular stresses. *Mol Cell Biol, 23*(16), 5651-5663.

Kaneko, M., Niinuma, Y., & Nomura, Y. (2003). Activation signal of nuclear factor-kappa B in response to endoplasmic reticulum stress is transduced via IRE1 and tumor necrosis factor receptor-associated factor 2. *Biol Pharm Bull, 26*(7), 931-935.

Karatas, A., Hegner, B., de Windt, L. J., Luft, F. C., Schubert, C., Gross, V., . . . Dragun, D. (2008). Deoxycorticosterone acetate-salt mice exhibit blood pressure-independent sexual dimorphism. *Hypertension, 51*(4), 1177-1183. doi:10.1161/HYPERTENSIONAHA.107.107938

Kassan, M., Galan, M., Partyka, M., Saifudeen, Z., Henrion, D., Trebak, M., & Matrougui, K. (2012). Endoplasmic reticulum stress is involved in cardiac damage and vascular endothelial dysfunction in hypertensive mice. *Arterioscler Thromb Vasc Biol, 32*(7), 1652-1661. doi:10.1161/ATVBAHA.112.249318

Kato, N., Watanabe, Y., Ohno, Y., Inoue, T., Kanno, Y., Suzuki, H., & Okada, H. (2008). Mapping quantitative trait loci for proteinuria-induced renal collagen deposition. *Kidney Int, 73*(9), 1017-1023. doi:10.1038/KI.2008.7

Kaufman, R. J. (2004). Regulation of mRNA translation by protein folding in the endoplasmic reticulum. *Trends Biochem Sci, 29*(3), 152-158. doi:10.1016/j.tibs.2004.01.004

Kawakami, T., Inagi, R., Wada, T., Tanaka, T., Fujita, T., & Nangaku, M. (2010). Indoxyl sulfate inhibits proliferation of human proximal tubular cells via endoplasmic reticulum stress. *Am J Physiol Renal Physiol, 299*(3), F568-576. doi:10.1152/ajprenal.00659.2009

Kim, H. J., & Vaziri, N. D. (2010). Contribution of impaired Nrf2-Keap1 pathway to oxidative stress and inflammation in chronic renal failure. *Am J Physiol Renal Physiol, 298*(3), F662-671. doi:10.1152/ajprenal.00421.2009

Kim, M. K., Maeng, Y. I., Sung, W. J., Oh, H. K., Park, J. B., Yoon, G. S., . . . Park, K. K. (2013). The differential expression of TGF-beta1, ILK and wnt signaling inducing epithelial to mesenchymal transition in human renal fibrogenesis: an immunohistochemical study. *Int J Clin Exp Pathol, 6*(9), 1747-1758.

Kimura, G., & Brenner, B. M. (1997). Implications of the linear pressure-natriuresis relationship and importance of sodium sensitivity in hypertension. *J Hypertens, 15*(10), 1055-1061.

Kimura, K., Jin, H., Ogawa, M., & Aoe, T. (2008). Dysfunction of the ER chaperone BiP accelerates the renal tubular injury. *Biochem Biophys Res Commun, 366*(4), 1048-1053. doi:10.1016/j.bbrc.2007.12.098

Kinuno, H., Tomoda, F., Koike, T., Takata, M., & Inoue, H. (2005). Effects of uninephrectomy on renal structural properties in spontaneously hypertensive rats. *Clin Exp Pharmacol Physiol, 32*(3), 173-178. doi:10.1111/j.1440-1681.2005.04167.x

Kirchhoff, F., Krebs, C., Abdulhag, U. N., Meyer-Schwesinger, C., Maas, R., Helmchen, U., . . . Wenzel, U. (2008). Rapid development of severe end-organ damage in C57BL/6 mice by combining DOCA salt and angiotensin II. *Kidney Int, 73*(5), 643-650. doi:10.1038/sj.ki.5002689

Krebs, C., Fraune, C., Schmidt-Haupt, R., Turner, J. E., Panzer, U., Quang, M. N., . . . Wenzel, U. O. (2012). CCR5 deficiency does not reduce hypertensive end-organ damage in mice. *Am J Hypertens, 25*(4), 479-486. doi:10.1038/ajh.2011.243

Krebs, C. F., Lange, S., Niemann, G., Rosendahl, A., Lehners, A., Meyer-Schwesinger, C., . . . Wenzel, U. O. (2014). Deficiency of the interleukin 17/23 axis accelerates renal injury in mice with deoxycorticosterone acetate+angiotensin ii-induced hypertension. *Hypertension, 63*(3), 565-571. doi:10.1161/HYPERTENSIONAHA.113.02620

Kren, S., & Hostetter, T. H. (1999). The course of the remnant kidney model in mice. *Kidney Int, 56*(1), 333-337. doi:10.1046/j.1523-1755.1999.00527.x

Kumar, D., Robertson, S., & Burns, K. D. (2004). Evidence of apoptosis in human diabetic kidney. *Mol Cell Biochem, 259*(1-2), 67-70.

Lamb, E. J., MacKenzie, F., & Stevens, P. E. (2009). How should proteinuria be detected and measured? *Ann Clin Biochem, 46*(Pt 3), 205-217. doi:10.1258/acb.2009.009007

LeBleu, V. S., Taduri, G., O'Connell, J., Teng, Y., Cooke, V. G., Woda, C., . . . Kalluri, R. (2013). Origin and function of myofibroblasts in kidney fibrosis. *Nat Med, 19*(8), 1047-1053. doi:10.1038/nm.3218

Leelahavanichkul, A., Yan, Q., Hu, X., Eisner, C., Huang, Y., Chen, R., . . . Star, R. A. (2010). Angiotensin II overcomes strain-dependent resistance of rapid CKD progression in a new remnant kidney mouse model. *Kidney Int, 78*(11), 1136-1153. doi:10.1038/ki.2010.287

Lhotak, S., Sood, S., Brimble, E., Carlisle, R. E., Colgan, S. M., Mazzetti, A., . . . Austin, R. C. (2012). ER stress contributes to renal proximal tubule injury

by increasing SREBP-2-mediated lipid accumulation and apoptotic cell death. *Am J Physiol Renal Physiol, 303*(2), F266-278. doi:10.1152/ajprenal.00482.2011

Li, P., Ma, L. L., Xie, R. J., Xie, Y. S., Wei, R. B., Yin, M., . . . Chen, X. M. (2012). Treatment of 5/6 nephrectomy rats with sulodexide: a novel therapy for chronic renal failure. *Acta Pharmacol Sin, 33*(5), 644-651. doi:10.1038/aps.2012.2

Liu, G., Sun, Y., Li, Z., Song, T., Wang, H., Zhang, Y., & Ge, Z. (2008). Apoptosis induced by endoplasmic reticulum stress involved in diabetic kidney disease. *Biochem Biophys Res Commun, 370*(4), 651-656. doi:10.1016/j.bbrc.2008.04.031

Liu, X. L., Done, S. C., Yan, K., Kilpelainen, P., Pikkarainen, T., & Tryggvason, K. (2004). Defective trafficking of nephrin missense mutants rescued by a chemical chaperone. *J Am Soc Nephrol, 15*(7), 1731-1738.

Liu, Y. (2010). New insights into epithelial-mesenchymal transition in kidney fibrosis. *J Am Soc Nephrol, 21*(2), 212-222. doi:10.1681/ASN.2008121226

Loch, D., Hoey, A., & Brown, L. (2006). Attenuation of cardiovascular remodeling in DOCA-salt rats by the vasopeptidase inhibitor, omapatrilat. *Clin Exp Hypertens, 28*(5), 475-488. doi:10.1080/10641960600798754

Long, D. A., Price, K. L., Herrera-Acosta, J., & Johnson, R. J. (2004). How does angiotensin II cause renal injury? *Hypertension, 43*(4), 722-723. doi:10.1161/01.HYP.0000120964.22281.3e

Luo, Z. F., Feng, B., Mu, J., Qi, W., Zeng, W., Guo, Y. H., . . . Yuan, F. H. (2010). Effects of 4-phenylbutyric acid on the process and development of diabetic nephropathy induced in rats by streptozotocin: regulation of endoplasmic reticulum stress-oxidative activation. *Toxicol Appl Pharmacol, 246*(1-2), 49-57. doi:10.1016/j.taap.2010.04.005

Lytton, J., Westlin, M., & Hanley, M. R. (1991). Thapsigargin inhibits the sarcoplasmic or endoplasmic reticulum Ca-ATPase family of calcium pumps. *J Biol Chem, 266*(26), 17067-17071.

Ma, L. J., & Fogo, A. B. (2003). Model of robust induction of glomerulosclerosis in mice: importance of genetic background. *Kidney Int, 64*(1), 350-355. doi:10.1046/j.1523-1755.2003.00058.x

Ma, L. J., Nakamura, S., Aldigier, J. C., Rossini, M., Yang, H., Liang, X., . . . Fogo, A. B. (2005). Regression of glomerulosclerosis with high-dose angiotensin inhibition is linked to decreased plasminogen activator inhibitor-1. *J Am Soc Nephrol, 16*(4), 966-976. doi:10.1681/ASN.2004060492

Marciniak, S. J., Yun, C. Y., Oyadomari, S., Novoa, I., Zhang, Y., Jungreis, R., . . . Ron, D. (2004). CHOP induces death by promoting protein synthesis and oxidation in the stressed endoplasmic reticulum. *Genes Dev, 18*(24), 3066-3077. doi:10.1101/gad.1250704

Markan, S., Kohli, H. S., Joshi, K., Minz, R. W., Sud, K., Ahuja, M., . . . Khullar, M. (2009). Up regulation of the GRP-78 and GADD-153 and down

regulation of Bcl-2 proteins in primary glomerular diseases: a possible involvement of the ER stress pathway in glomerulonephritis. *Mol Cell Biochem, 324*(1-2), 131-138. doi:10.1007/s11010-008-9991-2

Mattson, D. L. (2014). Infiltrating immune cells in the kidney in salt-sensitive hypertension and renal injury. *Am J Physiol Renal Physiol, 307*(5), F499-508. doi:10.1152/ajprenal.00258.2014

Mattson, D. L., James, L., Berdan, E. A., & Meister, C. J. (2006). Immune suppression attenuates hypertension and renal disease in the Dahl salt-sensitive rat. *Hypertension, 48*(1), 149-156. doi:10.1161/01.HYP.0000228320.23697.29

Miguel-Carrasco, J. L., Zambrano, S., Blanca, A. J., Mate, A., & Vazquez, C. M. (2010). Captopril reduces cardiac inflammatory markers in spontaneously hypertensive rats by inactivation of NF-kB. *J Inflamm (Lond), 7*, 21. doi:10.1186/1476-9255-7-21

Moreno, J. A., Halliday, M., Molloy, C., Radford, H., Verity, N., Axten, J. M., . . . Mallucci, G. R. (2013). Oral treatment targeting the unfolded protein response prevents neurodegeneration and clinical disease in prion-infected mice. *Sci Transl Med, 5*(206), 206ra138. doi:10.1126/scitranslmed.3006767

Mortality, G. B. D., & Causes of Death, C. (2015). Global, regional, and national age-sex specific all-cause and cause-specific mortality for 240 causes of death, 1990-2013: a systematic analysis for the Global Burden of Disease Study 2013. *Lancet, 385*(9963), 117-171. doi:10.1016/S0140-6736(14)61682-2

Muller, D. N., Dechend, R., Mervaala, E. M., Park, J. K., Schmidt, F., Fiebeler, A., . . . Luft, F. C. (2000). NF-kappaB inhibition ameliorates angiotensin II-induced inflammatory damage in rats. *Hypertension, 35*(1 Pt 2), 193-201.

Nakamura, T., Obata, J., Kimura, H., Ohno, S., Yoshida, Y., Kawachi, H., & Shimizu, F. (1999). Blocking angiotensin II ameliorates proteinuria and glomerular lesions in progressive mesangioproliferative glomerulonephritis. *Kidney Int, 55*(3), 877-889. doi:10.1046/j.1523-1755.1999.055003877.x

Namba, S., Okuda, Y., Morimoto, A., Kojima, T., & Morita, T. (2010). [Serum indoxyl sulfate is a useful predictor for progression of chronic kidney disease]. *Rinsho Byori, 58*(5), 448-453.

Nelson, C. M., Khauv, D., Bissell, M. J., & Radisky, D. C. (2008). Change in cell shape is required for matrix metalloproteinase-induced epithelial-mesenchymal transition of mammary epithelial cells. *J Cell Biochem, 105*(1), 25-33. doi:10.1002/jcb.21821

Neugarten, J., Acharya, A., & Silbiger, S. R. (2000). Effect of gender on the progression of nondiabetic renal disease: a meta-analysis. *J Am Soc Nephrol, 11*(2), 319-329.

Norris, K. C., Greene, T., Kopple, J., Lea, J., Lewis, J., Lipkowitz, M., . . . Appel, L. J. (2006). Baseline predictors of renal disease progression in the African

American Study of Hypertension and Kidney Disease. *J Am Soc Nephrol, 17*(10), 2928-2936. doi:10.1681/ASN.2005101101

O'Bryan, G. T., & Hostetter, T. H. (1997). The renal hemodynamic basis of diabetic nephropathy. *Semin Nephrol, 17*(2), 93-100.

Oeckinghaus, A., Hayden, M. S., & Ghosh, S. (2011). Crosstalk in NF-kappaB signaling pathways. *Nat Immunol, 12*(8), 695-708. doi:10.1038/ni.2065

Ofstad, J., & Iversen, B. M. (2005). Glomerular and tubular damage in normotensive and hypertensive rats. *Am J Physiol Renal Physiol, 288*(4), F665-672. doi:10.1152/ajprenal.00226.2004

Okada, T., Haze, K., Nadanaka, S., Yoshida, H., Seidah, N. G., Hirano, Y., . . . Mori, K. (2003). A serine protease inhibitor prevents endoplasmic reticulum stress-induced cleavage but not transport of the membrane-bound transcription factor ATF6. *J Biol Chem, 278*(33), 31024-31032. doi:10.1074/jbc.M300923200

Okamoto, K., & Aoki, K. (1963). Development of a strain of spontaneously hypertensive rats. *Jpn Circ J, 27*, 282-293.

Ortiz, A., Sanchez-Nino, M. D., Izquierdo, M. C., Martin-Cleary, C., Garcia-Bermejo, L., Moreno, J. A., . . . Consorcio Madrileno para investigacion del fracaso renal, a. (2015). Translational value of animal models of kidney failure. *Eur J Pharmacol, 759*, 205-220. doi:10.1016/j.ejphar.2015.03.026

Ozawa, Y., Kobori, H., Suzaki, Y., & Navar, L. G. (2007). Sustained renal interstitial macrophage infiltration following chronic angiotensin II infusions. *Am J Physiol Renal Physiol, 292*(1), F330-339. doi:10.1152/ajprenal.00059.2006

Ozcan, U., Yilmaz, E., Ozcan, L., Furuhashi, M., Vaillancourt, E., Smith, R. O., . . . Hotamisligil, G. S. (2006). Chemical chaperones reduce ER stress and restore glucose homeostasis in a mouse model of type 2 diabetes. *Science, 313*(5790), 1137-1140.

Pallet, N., Bouvier, N., Bendjallabah, A., Rabant, M., Flinois, J. P., Hertig, A., . . . Anglicheau, D. (2008a). Cyclosporine-induced endoplasmic reticulum stress triggers tubular phenotypic changes and death. *Am J Transplant, 8*(11), 2283-2296. doi:10.1111/j.1600-6143.2008.02396.x

Pallet, N., Bouvier, N., Bendjallabah, A., Rabant, M., Flinois, J. P., Hertig, A., . . . Anglicheau, D. (2008b). Cyclosporine-induced endoplasmic reticulum stress triggers tubular phenotypic changes and death. *American Journal of Transplantation, 8*(11), 2283-2296.

Papandreou, I., Denko, N. C., Olson, M., Van Melckebeke, H., Lust, S., Tam, A., . . . Koong, A. C. (2011). Identification of an Ire1alpha endonuclease specific inhibitor with cytotoxic activity against human multiple myeloma. *Blood, 117*(4), 1311-1314. doi:10.1182/blood-2010-08-303099

Parving, H. H., Brenner, B. M., McMurray, J. J., de Zeeuw, D., Haffner, S. M., Solomon, S. D., . . . Pfeffer, M. A. (2009). Aliskiren Trial in Type 2 Diabetes Using Cardio-Renal Endpoints (ALTITUDE): rationale and study design. *Nephrol Dial Transplant, 24*(5), 1663-1671. doi:10.1093/ndt/gfn721

Parving, H. H., Brenner, B. M., McMurray, J. J., de Zeeuw, D., Haffner, S. M., Solomon, S. D., . . . Investigators, A. (2012). Cardiorenal end points in a trial of aliskiren for type 2 diabetes. *N Engl J Med, 367*(23), 2204-2213. doi:10.1056/NEJMoa1208799

Perlmutter, D. H. (2002). Chemical chaperones: a pharmacological strategy for disorders of protein folding and trafficking. *Pediatr Res, 52*(6), 832-836. doi:10.1203/00006450-200212000-00004

Peterson, J. C., Adler, S., Burkart, J. M., Greene, T., Hebert, L. A., Hunsicker, L. G., . . . Seifter, J. L. (1995). Blood pressure control, proteinuria, and the progression of renal disease. The Modification of Diet in Renal Disease Study. *Ann Intern Med, 123*(10), 754-762.

Qi, W., Mu, J., Luo, Z. F., Zeng, W., Guo, Y. H., Pang, Q., . . . Feng, B. (2011). Attenuation of diabetic nephropathy in diabetes rats induced by streptozotocin by regulating the endoplasmic reticulum stress inflammatory response. *Metabolism, 60*(5), 594-603. doi:10.1016/j.metabol.2010.07.021

Qi, X., Hosoi, T., Okuma, Y., Kaneko, M., & Nomura, Y. (2004). Sodium 4-phenylbutyrate protects against cerebral ischemic injury. *Mol Pharmacol, 66*(4), 899-908. doi:10.1124/mol.104.001339

Raij, L., Azar, S., & Keane, W. (1984). Mesangial immune injury, hypertension, and progressive glomerular damage in Dahl rats. *Kidney Int, 26*(2), 137-143.

Rao, M. V., Qiu, Y., Wang, C., & Bakris, G. (2008). Hypertension and CKD: Kidney Early Evaluation Program (KEEP) and National Health and Nutrition Examination Survey (NHANES), 1999-2004. *Am J Kidney Dis, 51*(4 Suppl 2), S30-37. doi:10.1053/j.ajkd.2007.12.012

Rapp, J. P., & Dene, H. (1985). Development and characteristics of inbred strains of Dahl salt-sensitive and salt-resistant rats. *Hypertension, 7*(3 Pt 1), 340-349.

Reckelhoff, J. F., Zhang, H., & Granger, J. P. (1997). Decline in renal hemodynamic function in aging SHR: role of androgens. *Hypertension, 30*(3 Pt 2), 677-681.

Remuzzi, G., & Bertani, T. (1998). Pathophysiology of progressive nephropathies. *N Engl J Med, 339*(20), 1448-1456. doi:10.1056/NEJM199811123392007

Ritz, E., & Orth, S. R. (1999). Nephropathy in patients with type 2 diabetes mellitus. *N Engl J Med, 341*(15), 1127-1133. doi:10.1056/NEJM199910073411506

Rodriguez-Iturbe, B., Ferrebuz, A., Vanegas, V., Quiroz, Y., Mezzano, S., & Vaziri, N. D. (2005). Early and sustained inhibition of nuclear factor-kappaB prevents hypertension in spontaneously hypertensive rats. *J Pharmacol Exp Ther, 315*(1), 51-57. doi:10.1124/jpet.105.088062

Rodriguez-Iturbe, B., Quiroz, Y., Ferrebuz, A., Parra, G., & Vaziri, N. D. (2004). Evolution of renal interstitial inflammation and NF-kappaB activation in

spontaneously hypertensive rats. *Am J Nephrol, 24*(6), 587-594. doi:10.1159/000082313

Rodriguez-Iturbe, B., Quiroz, Y., Nava, M., Bonet, L., Chavez, M., Herrera-Acosta, J., . . . Pons, H. A. (2002). Reduction of renal immune cell infiltration results in blood pressure control in genetically hypertensive rats. *Am J Physiol Renal Physiol, 282*(2), F191-201. doi:10.1152/ajprenal.0197.2001

Romero, F., Rodriguez-Iturbe, B., Parra, G., Gonzalez, L., Herrera-Acosta, J., & Tapia, E. (1999). Mycophenolate mofetil prevents the progressive renal failure induced by 5/6 renal ablation in rats. *Kidney Int, 55*(3), 945-955. doi:10.1046/j.1523-1755.1999.055003945.x

Ruggenenti, P., Perna, A., Mosconi, L., Pisoni, R., & Remuzzi, G. (1998). Urinary protein excretion rate is the best independent predictor of ESRF in non-diabetic proteinuric chronic nephropathies. "Gruppo Italiano di Studi Epidemiologici in Nefrologia" (GISEN). *Kidney Int, 53*(5), 1209-1216. doi:10.1046/j.1523-1755.1998.00874.x

Ruggenenti, P., Perna, A., Remuzzi, G., & Investigators, G. G. (2003). Retarding progression of chronic renal disease: the neglected issue of residual proteinuria. *Kidney Int, 63*(6), 2254-2261. doi:10.1046/j.1523-1755.2003.00033.x

Ruiz-Ortega, M., Ruperez, M., Esteban, V., Rodriguez-Vita, J., Sanchez-Lopez, E., Carvajal, G., & Egido, J. (2006). Angiotensin II: a key factor in the inflammatory and fibrotic response in kidney diseases. *Nephrol Dial Transplant, 21*(1), 16-20. doi:10.1093/ndt/gfi265

Sanz, A. B., Sanchez-Nino, M. D., Ramos, A. M., Moreno, J. A., Santamaria, B., Ruiz-Ortega, M., . . . Ortiz, A. (2010). NF-kappaB in renal inflammation. *J Am Soc Nephrol, 21*(8), 1254-1262. doi:10.1681/ASN.2010020218

Sanz, A. B., Santamaria, B., Ruiz-Ortega, M., Egido, J., & Ortiz, A. (2008). Mechanisms of renal apoptosis in health and disease. *J Am Soc Nephrol, 19*(9), 1634-1642. doi:10.1681/ASN.2007121336

Sanz-Rosa, D., Oubina, M. P., Cediel, E., de Las Heras, N., Vegazo, O., Jimenez, J., . . . Cachofeiro, V. (2005). Effect of AT1 receptor antagonism on vascular and circulating inflammatory mediators in SHR: role of NF-kappaB/IkappaB system. *Am J Physiol Heart Circ Physiol, 288*(1), H111-115. doi:10.1152/ajpheart.01061.2003

Silverstein, D. M. (2009). Inflammation in chronic kidney disease: role in the progression of renal and cardiovascular disease. *Pediatr Nephrol, 24*(8), 1445-1452. doi:10.1007/s00467-008-1046-0

Smith, T. L., & Hutchins, P. M. (1979). Central hemodynamics in the developmental stage of spontaneous hypertension in the unanesthetized rat. *Hypertension, 1*(5), 508-517.

Spitler, K. M., Matsumoto, T., & Webb, R. C. (2013). Suppression of endoplasmic reticulum stress improves endothelium-dependent contractile responses in

aorta of the spontaneously hypertensive rat. *Am J Physiol Heart Circ Physiol, 305*(3), H344-353. doi:10.1152/ajpheart.00952.2012
Stevens, P. E., Levin, A., & Kidney Disease: Improving Global Outcomes Chronic Kidney Disease Guideline Development Work Group, M. (2013). Evaluation and management of chronic kidney disease: synopsis of the kidney disease: improving global outcomes 2012 clinical practice guideline. *Ann Intern Med, 158*(11), 825-830. doi:10.7326/0003-4819-158-11-201306040-00007
Sun, Y., Zhang, T., Li, L., & Wang, J. (2015). Induction of apoptosis by hypertension via endoplasmic reticulum stress. *Kidney Blood Press Res, 40*(1), 41-51. doi:10.1159/000368481
Szegezdi, E., Logue, S. E., Gorman, A. M., & Samali, A. (2006). Mediators of endoplasmic reticulum stress-induced apoptosis. *EMBO Rep, 7*(9), 880-885. doi:10.1038/sj.embor.7400779
Tabas, I., & Ron, D. (2011). Integrating the mechanisms of apoptosis induced by endoplasmic reticulum stress. *Nat Cell Biol, 13*(3), 184-190. doi:10.1038/ncb0311-184
Tanase, H., Yamori, Y., Hansen, C. T., & Lovenberg, W. (1982). Heart size in inbred strains of rats. Part 1. Genetic determination of the development of cardiovascular enlargement in rats. *Hypertension, 4*(6), 864-872.
Tobian, L., Lange, J., Iwai, J., Hiller, K., Johnson, M. A., & Goossens, P. (1979). Prevention with thiazide of NaCl-induced hypertension in Dahl "S" rats. Evidence for a Na-retaining humoral agent in "S" rats. *Hypertension, 1*(3), 316-323.
Tomaschitz, A., Pilz, S., Ritz, E., Obermayer-Pietsch, B., & Pieber, T. R. (2010). Aldosterone and arterial hypertension. *Nat Rev Endocrinol, 6*(2), 83-93. doi:10.1038/nrendo.2009.263
Uchida, A., Yamada, T., Hayakawa, T., & Hoshino, M. (1997). Taurochenodeoxycholic acid ameliorates and ursodeoxycholic acid exacerbates small intestinal inflammation. *Am J Physiol, 272*(5 Pt 1), G1249-1257.
Urano, F., Wang, X., Bertolotti, A., Zhang, Y., Chung, P., Harding, H. P., & Ron, D. (2000). Coupling of stress in the ER to activation of JNK protein kinases by transmembrane protein kinase IRE1. *Science, 287*(5453), 664-666.
Verroust, P. J., & Christensen, E. I. (2002). Megalin and cubilin--the story of two multipurpose receptors unfolds. *Nephrol Dial Transplant, 17*(11), 1867-1871.
Wang, S., & Kaufman, R. J. (2012). The impact of the unfolded protein response on human disease. *J Cell Biol, 197*(7), 857-867. doi:10.1083/jcb.201110131
Wang, T. N., Chen, X., Li, R., Gao, B., Mohammed-Ali, Z., Lu, C., . . . Krepinsky, J. C. (2015). SREBP-1 Mediates Angiotensin II-Induced TGF-beta1 Upregulation and Glomerular Fibrosis. *J Am Soc Nephrol, 26*(8), 1839-1854. doi:10.1681/ASN.2013121332

Westphal, D., Dewson, G., Czabotar, P. E., & Kluck, R. M. (2011). Molecular biology of Bax and Bak activation and action. *Biochim Biophys Acta, 1813*(4), 521-531. doi:10.1016/j.bbamcr.2010.12.019

Wolf, G., & Ritz, E. (2005). Combination therapy with ACE inhibitors and angiotensin II receptor blockers to halt progression of chronic renal disease: pathophysiology and indications. *Kidney Int, 67*(3), 799-812. doi:10.1111/j.1523-1755.2005.00145.x

Woo, D. (1995). Apoptosis and loss of renal tissue in polycystic kidney diseases. *N Engl J Med, 333*(1), 18-25. doi:10.1056/NEJM199507063330104

Wu, X., He, Y., Jing, Y., Li, K., & Zhang, J. (2010). Albumin overload induces apoptosis in renal tubular epithelial cells through a CHOP-dependent pathway. *OMICS, 14*(1), 61-73. doi:10.1089/omi.2009.0073

Xia, C. F., Bledsoe, G., Chao, L., & Chao, J. (2005). Kallikrein gene transfer reduces renal fibrosis, hypertrophy, and proliferation in DOCA-salt hypertensive rats. *Am J Physiol Renal Physiol, 289*(3), F622-631. doi:10.1152/ajprenal.00427.2004

Xu, C., Bailly-Maitre, B., & Reed, J. C. (2005). Endoplasmic reticulum stress: cell life and death decisions. *J Clin Invest, 115*(10), 2656-2664. doi:10.1172/JCI26373

Yamazaki, H., Hiramatsu, N., Hayakawa, K., Tagawa, Y., Okamura, M., Ogata, R., . . . Kitamura, M. (2009). Activation of the Akt-NF-kappaB pathway by subtilase cytotoxin through the ATF6 branch of the unfolded protein response. *J Immunol, 183*(2), 1480-1487. doi:10.4049/jimmunol.0900017

Yanagi, M., Tamura, K., Fujikawa, T., Wakui, H., Kanaoka, T., Ohsawa, M., . . . Umemura, S. (2013). The angiotensin II type 1 receptor blocker olmesartan preferentially improves nocturnal hypertension and proteinuria in chronic kidney disease. *Hypertens Res, 36*(3), 262-269. doi:10.1038/hr.2012.184

Yang, H. C., Zuo, Y., & Fogo, A. B. (2010). Models of chronic kidney disease. *Drug Discov Today Dis Models, 7*(1-2), 13-19. doi:10.1016/j.ddmod.2010.08.002

Ye, J., Rawson, R. B., Komuro, R., Chen, X., Dave, U. P., Prywes, R., . . . Goldstein, J. L. (2000). ER stress induces cleavage of membrane-bound ATF6 by the same proteases that process SREBPs. *Mol Cell, 6*(6), 1355-1364.

Yoon, H. E., & Yang, C. W. (2009). Established and newly proposed mechanisms of chronic cyclosporine nephropathy. *Korean J Intern Med, 24*(2), 81-92. doi:10.3904/kjim.2009.24.2.81

Yoshida, H. (2007). ER stress and diseases. *FEBS J, 274*(3), 630-658. doi:10.1111/j.1742-4658.2007.05639.x

Yu, H. C., Burrell, L. M., Black, M. J., Wu, L. L., Dilley, R. J., Cooper, M. E., & Johnston, C. I. (1998). Salt induces myocardial and renal fibrosis in normotensive and hypertensive rats. *Circulation, 98*(23), 2621-2628.

Yu, M., Moreno, C., Hoagland, K. M., Dahly, A., Ditter, K., Mistry, M., & Roman, R. J. (2003). Antihypertensive effect of glucagon-like peptide 1 in Dahl salt-sensitive rats. *J Hypertens, 21*(6), 1125-1135. doi:10.1097/01.hjh.0000059046.65882.49

Z Mohammed-Ali, G. L. C., C Lu, R E Carlisle, K E Werner, K Ask, J G Dickhout. (2015). Development of a model of Chronic Kidney Disease in the C57BL/6 mouse with Properties of progressive human CKD. *BioMed Research International, 2015*.

Zen, K., Guo, Y. L., Li, L. M., Bian, Z., Zhang, C. Y., & Liu, Y. (2011). Cleavage of the CD11b extracellular domain by the leukocyte serprocidins is critical for neutrophil detachment during chemotaxis. *Blood, 117*(18), 4885-4894. doi:10.1182/blood-2010-05-287722

Zhang, K., & Kaufman, R. J. (2006). The unfolded protein response: a stress signaling pathway critical for health and disease. *Neurology, 66*(2 Suppl 1), S102-109. doi:10.1212/01.wnl.0000192306.98198.ec

Zhang, K., & Kaufman, R. J. (2008). From endoplasmic-reticulum stress to the inflammatory response. *Nature, 454*(7203), 455-462. doi:10.1038/nature07203

Zhang, K., Shen, X., Wu, J., Sakaki, K., Saunders, T., Rutkowski, D. T., . . . Kaufman, R. J. (2006). Endoplasmic reticulum stress activates cleavage of CREBH to induce a systemic inflammatory response. *Cell, 124*(3), 587-599. doi:10.1016/j.cell.2005.11.040

Zhang, M., Guo, Y., Fu, H., Hu, S., Pan, J., Wang, Y., . . . Wang, C. Y. (2015). Chop deficiency prevents UUO-induced renal fibrosis by attenuating fibrotic signals originated from Hmgb1/TLR4/NFkappaB/IL-1beta signaling. *Cell Death Dis, 6*, e1847. doi:10.1038/cddis.2015.206

Zhao, G., Tu, L., Li, X., Yang, S., Chen, C., Xu, X., . . . Wang, D. W. (2012). Delivery of AAV2-CYP2J2 protects remnant kidney in the 5/6-nephrectomized rat via inhibition of apoptosis and fibrosis. *Hum Gene Ther, 23*(7), 688-699. doi:10.1089/hum.2011.135

Appendix

COPYRIGHT INFORMATION

Parts of the thesis consists of reprints of previously published work; this includes:

1) Chapter 1: Introduction

   Publication 1 (Review Article): Crosstalk between the unfolded protein response and NF-κB-mediated inflammation in the progression of chronic kidney disease. *Journal of Immunology Research.* 2015. doi: 10.1155/2015/428508. **Authors:** Zahraa Mohammed-Ali, Gaile L. Cruz and Jeffrey G. Dickhout.

   Copyright information:
   https://www.hindawi.com/journals/jir/guidelines/

   Journal of Immunology Research is an open access journal where articles are distributed under the terms of the Creative Commons Attributions License. This license permits the unrestricted use, distribution and reproduction in any medium, provided the original work is properly cited.

   Publication 2 (Book Chapter): Animal Models of Kidney Disease (submitted). Authors: Zahraa Mohammed-Ali, Rachel E. Carlisle, Samera Nademi and Jeffrey G. Dickhout. In "Animal Models for the Study of Human Disease 2nd Edition" to be published in June 2017 (Elsevier publishing group, Academic Press).

   Copyright information: https://www.elsevier.com/about/company-information/policies/copyright/permissions

   Authors can include their articles in full or in part in a thesis or dissertation for non-commercial purposes.

2) Chapter 2: **Development of a Model of Chronic Kidney Disease in the C57BL/6 Mouse with Properties of Progressive Human CKD.** *BioMed Research International.* 2015. http://dx.doi.org/10.1155/2015/172302. **Authors:** Zahraa Mohammed-Ali, Gaile L. Cruz, Rachel E. Carlisle, Kaitlyn E. Werner, Kjetil Ask and Jeffrey G. Dickhout.

   Copyright information:
   https://www.hindawi.com/journals/bmri/guidelines/

   BioMed Research International is an open access journal where articles are distributed under the terms of the Creative Commons Attributions License. This license permits the unrestricted use, distribution and reproduction in any medium, provided the original work is properly cited.

3) Chapter 3: **ER stress inhibition attenuates chronic kidney disease progression by preserving glomerular filtration barrier integrity and endocytic receptor-mediated albumin scavenging.** *Nature Scientific Reports,* 2016 (submitted). **Authors:** Zahraa Mohammed-Ali, Chao Lu, Mandeep K. Marway, Rachel E. Carlisle, Kjetil Ask, Dusan Lukic, Joan K. Krepinsky, Jeffrey G. Dickhout.